การศึกษากลุ่มเอนไซม์ที่ย่อยไคตินจากเชื้อ *Vibrio harveyi*: การเกิดปฏิกิริยาทรานส์ไกลโคซิเลชันและการยับยั้งทางจลนพลศาสตร์ของเกลือโซเดียม

นางสาวพักตร์นิศา ศิริมนตรี

STUDIES ON CHITINOLYTIC ENZYMES FROM *VIBRIO HARVEYI*: TRANSGLYCOSYLATION REACTION AND INHIBITION KINETICS OF SODIUM SALTS

Paknisa Sirimontree

A Thesis Submitted in Partial Fulfillment of the Requirements for the

Degree of Doctor of Philosophy in Biochemistry

Suranaree University of Technology

Academic Year 2014

STUDIES ON CHITINOLYTIC ENZYMES FROM *VIBRIO HARVEYI*: TRANSGLYCOSYLATION REACTION AND INHIBITION KINETICS OF SODIUM SALTS

Suranaree University of Technology has approved this thesis submitted in partial fulfillment of the requirements for the Degree of Doctor of Philosophy.

Thesis Examining Committee

_____

(Assoc. Prof. Dr. Jatuporn Wittayakun)

Chairperson

_____

(Assoc. Prof. Dr. Wipa Suginta)

Member (Thesis Advisor)

_____

(Prof. Dr. Tamo Fukamizo)

Member

_____

(Asst. Prof. Dr. Jeerus Sucharitakul)

Member

_____

(Assoc. Prof. Dr. Jaruwan Siritapetawee)

Member

_____   _____

(Prof. Dr. Sukit Limpijumnong)   (Assoc. Prof. Dr. Prapun Manyum)

Vice Rector for Academic Affairs   Dean of Institute of Science

and Innovation

พักตร์นิศา ศิริมนตรี : การศึกษากลุ่มเอนไซม์ที่ย่อยไคตินจากเชื้อ *Vibrio harveyi*:
การเกิดปฏิกิริยาทรานสไกลโคซิเลชันและการยับยั้งทางจลนพลศาสตร์ของเกลือโซเดียม
(STUDIES ON CHITINOLYTIC ENZYMES FROM *VIBRIO HARVEYI*:
TRANSGLYCOSYLATION REACTION AND INHIBITION KINETICS OF SODIUM
SALTS) อาจารย์ที่ปรึกษา : รองศาสตราจารย์ ดร.วิภา สุจินต์, 137 หน้า

การเพิ่มปฏิกิริยาทรานสไกลโคซิเลชันของเอนไซม์ในกลุ่มไกลโคไซด์ ไฮโดรเลส ไม่ได้ทำให้
ผลิตน้ำตาลโอลิโกแซคคาไรด์สายยาวได้เสมอไป เพราะว่าผลิตภัณฑ์จากทรานสไกลโคซิเลชันมักจะถูก
ย่อยสลายกลายเป็นน้ำตาลโอลิโกแซคคาไรด์สายสั้น ในครั้งนี้ เราได้ทำการตรวจสอบถึงกลยุทธ์การ
กลายพันธุ์ เพื่อให้ได้น้ำตาลโอลิโกแซคคาไรด์สายยาวด้วยวิธีของปฏิกิริยาทรานสไกลโคซิเลชัน โดยใช้
เอนไซม์ไคติเนส เอ ที่อยู่ในกลุ่มแฟมิลีไกลโคไซด์ ไฮโดรเลส 18 จากเชื้อ *Vibrio harveyi* (*Vh*ChiA)
ผลการวิเคราะห์ผลิตภัณฑ์จากปฏิกิริยาทรานสไกลโคซิเลชันโดยใช้เครื่อง HPLC หลังจากทำการบ่ม
น้ำตาลโอลิโกแซคคาไรด์ ($GlcNAc_n$) กับเอนไซม์หลายตัวที่กลายพันธุ์ ได้ชี้ให้เห็นว่าเอนไซม์กลายพันธุ์
W570G (การกลายพันธุ์ที่ตำแหน่งกรดอะมิโน Trp570 ไปเป็น Gly) และเอนไซม์กลายพันธุ์ D392N (การ
กลายพันธุ์ที่ตำแหน่งกรดอะมิโน Asp392 ไปเป็น Asn) ช่วยเพิ่มปฏิกิริยาการเกิดทรานสไกลโคซิเลชัน
แต่ผลิตภัณฑ์ที่ได้ ได้ถูกย่อยสลายต่อเป็นน้ำตาลโอลิโกแซคคาไรด์สายสั้นในทันที ในทางตรงกันข้าม
ผลิตภัณฑ์จากปฏิกิริยาทรานสไกลโคซิเลชัน ที่ได้รับจากเอนไซม์กลายพันธุ์ D313A และ D313N (การ
กลายพันธุ์ที่ตำแหน่งกรดอะมิโน Asp313 ไปเป็น Ala และ Asn ตามลำดับ) ไม่ได้ถูกย่อยสลายต่อ ทำให้
เกิดการสะสมของน้ำตาลโอลิโกแซคคาไรด์สายยาว โดยข้อมูลที่ได้จากเอนไซม์ไคติเนส เอ กลายพันธุ์
แสดงให้เห็นว่า การกลายพันธุ์ของกรดอะมิโนที่ตำแหน่ง Asp313 ซึ่งเป็นตำแหน่งตรงกลางของ DxDxE
catalytic motif ไปเป็น Ala และ Asn มีประสิทธิภาพมากที่สุดสำหรับการผลิตน้ำตาลโอลิโกแซคคาไรด์
สายยาว

เอนไซม์ไคติเนส เอ จาก เชื้อ *Vibrio harveyi* (*Vh*ChiA) ทำหน้าที่ย่อยไคตินผ่านกลไกที่เรียกว่า
substrate assisted-retaining ในการศึกษาครั้งนี้มีเป้าหมายเพื่อตรวจสอบถึงผลกระทบของเกลือโซเดียม
ต่อปฏิกิริยาการย่อยสลายของเอนไซม์ไคติเนส โดยการหาค่า IC_{50} และ TLC ได้ชี้ให้เห็นว่า โซเดียม
เอไซด์ มีผลต่อการยับยั้งการทำงานของเอนไซม์ที่เป็น wild-type มากที่สุด และจากการหาค่าคงที่ทาง
จลนพลศาสน์ของกราฟ Michaelis-Menten พบว่าค่า K_m และ k_{cat} ลดลงเมื่อความเข้มข้นโซเดียม เอไซด์
เพิ่มขึ้น แสดงให้เห็นว่า โซเดียม เอไซด์ แสดงการยับยั้งแบบผสมต่อ pNP-$GlcNAc_2$ โดยการยับยั้งนี้ได้ถูก
ยืนยันด้วยกราฟจาก Lineweaver-Burk plots ซึ่งเป็นกราฟส่วนกลับระหว่าง $1/v_0$ ต่อ $1/[S]$ ที่ความเข้มข้น
ต่างๆ ของโซเดียม เอไซด์ โดยค่า K_i ของ EI complex มีค่าเท่ากับ 1.50$\pm$ 0.10 M และ ค่า αK_i ของ ESI

complex มีค่าเท่ากับ 0.40 ± 0.02 M ซึ่งค่าที่ได้แสดงให้เห็นว่า โซเดียม เอไซด์จับกับเอนไซม์ในรูป ES complex ได้ดีกว่าในรูปเอนไซม์อิสระ และข้อมูลที่ได้ในการศึกครั้งนี้ สามารถนำเสนอได้ว่า เอไซด์ แอนไอออน จะเข้าไปแย่งโปรตอนจากหมู่คาร์บอกซิลของ Glu315 ซึ่งเป็นกรดอะมิโนที่ทำหน้าที่ในการให้โปรตอนกับสับสเตรตเพื่อย่อยสลายพันธะไกลโคซิดิคเกิดเป็นผลิตภัณฑ์ ดังนั้นเมื่อเอนไซม์ให้โปรตอนกับ เอไซด์ แอนไอออนแล้ว มันจึงไม่สามารถให้โปรตอนกับสับสเตรต และเกิดการย่อยได้

        เอนไซม์กลุคแนคเอสจากเชื้อ *Vibrio harveyi* (*Vh*GlcNAcase) ซึ่งจัดอยู่ในกลุ่มไกลโคไซไฮโดรเลสแฟมิลี 20 (GH-20) ทำหน้าที่ย่อยสลายน้ำตาลโอลิโกแซคคาไรด์สายสั้นจากทางด้าน non-reducing end ผ่านกลไกที่เรียกว่า substrate-assisted retaining โดยผลการทดลองของผลกระทบของเกลือโซเดียมต่อปฏิกิริยาการย่อยสลายของเอนไซม์กลุคแนคเอส พบว่า โซเดียม เอไซด์ และ โซเดียม ไนเตรต แสดงการยับยั้งการทำงานของเอนไซม์กลุคแนคเอสได้ดีที่สุด โดยผลการทดลองนี้ถูกยืนยันด้วยการหาค่า IC_{50} และ TLC และจากค่าคงที่ทางจลนพลศาสน์ของกราฟ Michaelis-Menten พบว่าค่า K_m เพิ่มขึ้นและ k_{cat} คงที่ เมื่อความเข้มข้นโซเดียม เอไซด์ และโซเดียม ไนเตรต เพิ่มขึ้น แสดงให้เห็นว่าโซเดียม เอไซด์ และ โซเดียม ไนเตรต แสดงการยับยั้งแบบแข่งขันต่อ pNP-GlcNAc โดยการยับยั้งนี้ได้ถูกยืนยันด้วยกราฟจาก Lineweaver-Burk plots ซึ่งเป็นกราฟส่วนกลับระหว่าง $1/v_0$ ต่อ $1/[S]$ ที่ความเข้มข้นต่างๆ ของโซเดียม เอไซด์ และ โซเดียม ไนเตรต โดยค่า K_i ของ โซเดียม เอไซด์ มีค่าเท่ากับ 0.20 ± 0.03 M และ ของ โซเดียม ไนเตรต มีค่าเท่ากับ 0.20 ± 0.05 M

สาขาวิชาชีวเคมี   ลายมือชื่อนักศึกษา _____

ปีการศึกษา 2557   ลายมือชื่ออาจารย์ที่ปรึกษา _____

PAKNISA SIRIMONTREE : STUDIES ON CHITINOLYTIC ENZYMES

FROM *VIBRIO HARVEYI*: TRANSGLYCOSYLATION REACTION AND

INHIBITION KINETICS OF SODIUM SALTS. THESIS ADVISOR :

ASSOC. PROF. WIPA SUGINTA, Ph.D. 137 PP.

CHITINOLYTIC ENZYMES, *VIBRIO HARVEYI*, TRANSGLYCOSYLATION

REACTION, INHIBITION KINETICS, SODIUM SALTS

Enhancing the transglycosylation activity of glycoside hydrolases does not always result in the production of oligosaccharides with longer chains, because the TG products are often decomposed into shorter oligosaccharides. Here, we investigated mutation strategies for obtaining chitooligosaccharides with longer chains by means of TG reaction catalyzed by family GH18 chitinase A from *Vibrio harveyi* (*Vh*ChiA). HPLC analysis of the TG products from incubation of chitooligosaccharide substrates (GlcNAc$_n$) with several mutant *Vh*ChiAs suggested that the mutation W570G (mutation of Trp570 to Gly) and the mutation D392N (mutation of Asp392 to Asn) significantly enhanced TG activity, but the TG products were immediately hydrolyzed into shorter GlcNAc$_n$. On the other hand, the TG products obtained from the mutants D313A and D313N (mutations of Asp313 to Ala and Asn, respectively) were not further hydrolyzed, leading to the accumulation of oligosaccharides with longer chains. The data obtained from the mutant *Vh*ChiAs suggested that mutations of Asp313, the middle aspartic acid residue of the DxDxE catalytic motif, to Ala and Asn are most effective for obtaining chitooligosaccharides with longer chains.

*Vibrio harvey*i chitinase A (*Vh*ChiA) catalyzes chitin degradation through the substrate-assisted retaining mechanism. This research aims to investigate the effects of

sodium salts on the hydrolytic activities of the chitinase variants. Determination of IC_{50} and TLC suggests that the compound was most active against the wild-type enzyme. Michaelis-Menten plots yield decreasing K_m and k_{cat} upon increasing concentrations of sodium azide, providing an idea that sodium azide acts mixed-type inhibition towards pNP-GlcNAc$_2$. Lineweaver-Burk plots between $1/v_0$ versus $1/[S]$ with different sodium azide concentrations also confirm mixed-type inhibition. The value of the K_i of the EI complex was found to be 1.5 $\pm$ 0.1 M and that of αK of the ESI complex to be 0.4 ± 0.02 M. The results suggested that sodium azide reacted much more efficiently to the ES complex than the free enzyme. Based on the data obtained from this study, it has been proposed that the azide anion abstracts the proton from the γ-COOH side chain of the catalytic residue Glu315, thereby preventing bond cleaving.

Family GH20 GlcNAcase from *Vibrio harveyi* (*Vh*GlcNAcase) sequentially degrades chitooligosaccharides from the non-reducing end through the substrate-assisted retaining mechanism. The results of the effects of sodium salts on the GlcNAcase activity showed that sodium azide and sodium nitrate considerably inhibited the activity of *Vh*GlcNAcase. The inhibitory effects of both compounds were also comfirm by IC_{50} and TLC. Michaelis-Menten plots yield increasing K_m with fairly steady k_{cat} upon increasing concentrations of sodium azide and sodium nitrate, providing an idea that sodium azide and sodium nitrate act competitively. Lineweaver-Burk plots between $1/v_0$ versus $1/[S]$ with different sodium azide and sodium nitrate concentrations also confirm competitive inhibition with the apparent K_i of 0.2 ± 0.03 M and 0.2 ± 0.05 M, respectively.

School of Biochemistry   Student's signature_____

Academic Year 2014   Advisor's signature_____

ACKNOWLEDGEMENTS

I would also like to thank my family for their unconditional love, care, support, understanding, and encouragement. Without them, I would not be what am I today.

Paknisa Sirimontree

CONTENTS

CONTENTS (Continued)

CONTENTS (Continued)

CONTENTS (Continued)

CONTENTS (Continued)

CONTENTS (Continued)

LIST OF TABLES

LIST OF FIGURES

LIST OF FIGURES (Continued)

LIST OF FIGURES (Continued)

LIST OF ABBREVIATIONS

Abs	Absorbance
BSA	Bovine serum albumin
GH	Glycoside hydrolase
GH18	Glycoside hydrolase family 18
GH20	Glycoside hydrolase family 20
GlcNAc	*N*-acetyl-glucosamine
$GlcNAc_2$	di-*N*-acetyl-chitobiose
$GlcNAc_3$	tri-*N*-acetylchitotriose
$GlcNAc_4$	tetra-*N*-acetyl-chitotetraose
$GlcNAc_5$	penta-*N*-acetyl-chitopentaose
$GlcNAc_6$	hexa-*N*-acetylchitohexaose
HPLC	High performance liquid chromatography
IPTG	Isopropyl thio-β-D-galactoside
LB	Luria-Bertani lysogeny broth
nm	nanometer(s)
Ni-NTA	Ni-nitrilotriacetic acid
PMSF	Phenylmethylsulfonylfluoride
*p*NP	*para*-nitrophenyl
*p*NP-GlcNAc	*para*-nitrophenyl-*N*-acetyl-glucosaminide
pNP-$GlcNAc_2$	*para*-nitrophenyl- di-*N*-acetyl-chitobioside
rpm	Round(s) per minute

LIST OF ABBREVIATIONS (Continued)

SDS   Sodium dodecyl sulfate

TEMED   Tetramethylenediamine

Tris   Tris-(hydroxymethyl)-aminoethane
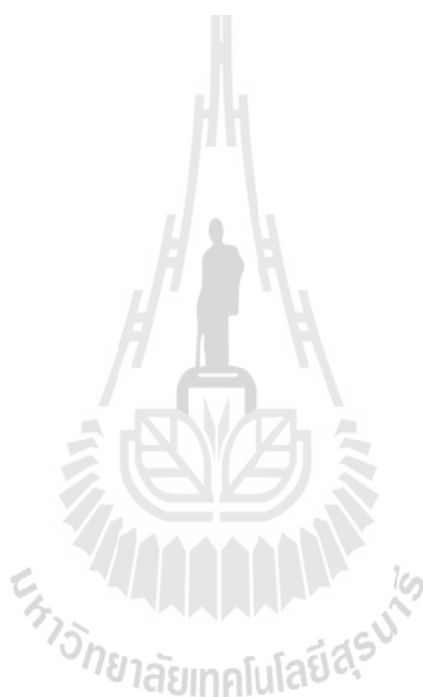
CHAPTER I

INTRODUCTION

1.1 Chitin and applications

Chitin, the second most abundant biopolymer in nature after cellulose, is an insoluble polysaccharide consisting of β-(1,4)-linked *N*-acetylglucosamine (GlcNAc) units (Figure 1.1). Chitin is generally found in the shells of crustaceans, such as crabs and shrimps, the exoskeletons of insects, and the cell walls of fungi (Kadokura, Rokutani, Yamamoto, Ikegami, Sugita, Itoi, Hakamata, Oku, and Nishio, 2007; Kubota, Miyamoto, Yasuda, Inamori, and Tsujibo, 2004; Rinaudo, 2006).
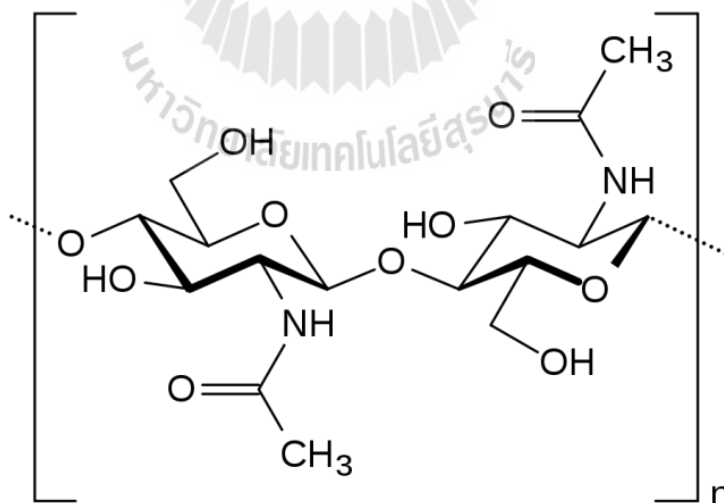
Figure 1.1 Chemical structure of chitin, poly (β-(1-4)-*N*-acetyl-D-glucosamine) repeat units (http://en.wikipedia.org/wiki/Chitin).

Chitin is hydrolyzed into chitooligosaccharide fragments and GlcNAc residues by chemical or enzymatic methods (Ilankovan, Hein, Ng, Trung, and Stevens, 2006). The chemical method can be performed through hydrolysis using a strong acid, such as HCl. However, there appears to be several problems in producing $GlcNAc_n$ by the limited acid hydrolysis of chitin, including high cost, low yield, and acidic waste created by the use of HCl. On the other hand, the enzymatic method occurs under mild conditions, in which the selectivity of the end products depending on the substrate specificity of chitinolytic enzymes. In addition, the enzymatic reaction occurs quickly and completely with less time consuming, lower cost, and no pollutants released to nearby environment (Chen, Shen, and Liu, 2010; Sashiwa, Fujishima, Yamano, Kawasakia, Nakayama, Murakia, Sukwattanasinitt, Pichyangkura, and Aiba, 2003).

A complete enzymatic degradation of chitin involves endochitinases (EC 3.2.1.14), exochitinases (EC 3.2.1.14) and β-N-acetylglucosaminidases or GlcNAcases (EC 3.2.1.52) (Dı́ez, Rodrı́guez-Saı́z, de la Fuente, Moreno, and Barredo, 2005). The reactions usually take place in two successive steps. In the first step, chitinases catalyze the insoluble chitin by cleaving the glycosidic bonds between GlcNAc residues, yielding chitooligosaccharide fragments with $GlcNAc_2$ as the major product (Cohen-Kupiec and Chet, 1998). Endochitinases cleave chitin randomly at internal sites, whereas exochitinases release $GlcNAc_2$ or $GlcNAc_3$ units from the non-reducing end of chitin chain. In the second step, the resultant chitooligosaccharides are further hydrolyzed from the terminal, non-reducing end to produce GlcNAc residues by GlcNAcases (Cohen-Kupiec and Chet, 1998; Matsuo, Kurita, Park, Tanaka, Nakagawa, Kawamukai, and Matsuda, 1999; Nogawa, Takahashi,

Kashiwagi, Ohshima, Okada, and Morikawa, 1998; Ueda, Fujita, Kawaguchi, and Araai, 2000).

Chitinases and GlcNAcases are widely distributed in various organisms, including bacteria, fungi, insects, plants, animals and humans (Kim, Matsuo, Ajisaka, Nakajima, and Kitamoto, 2002; Li, Morimoto, Katagiri, Kimura, Sakka, Lun, and Ohmiya, 2002). Bacteria produce chitinases and GlcNAcases that hydrolyze chitin into GlcNAc, which is finally metabolized intracellularly to produce nutrition and energy required for bacterial growth (Tews, Perrakis, Oppenheim, Dauter, Wilson, and Vorgias, 1996). Fungal chitinases and GlcNAcases seem to play important roles in many biological processes, including cell wall digestion, germination, hyphal growth, hyphal branching and hyphal autolysis (Kim *et al*., 2002). The cuticles of insects are hydrolyzed during the molting process by chitinases and GlcNAcases (Ikegami, Okada, Hashimoto, Seino, Watanabe, and Shirakawa, 2000). Plants use chitinases and GlcNAcases to act against pathogenic fungi (Ikegami *et al*., 2000). In animals, chitinases and GlcNAcases are involved in the digestive system (Rinaudo, 2006). In human, chitinases and GlcNAcases are found to be highly expressed in macrophages that are involved in inflammatory and lysosomal disease (Kanneganti, Kamba, and Mizoguchi, 2013; Kim *et al*., 2002; Kzhyshkowska, Gratchev, and Goerdt, 2007; Rosa, Malaguarnera, Gregorio, Drago, and Malaguarnera, 2012). Both human chitinases and GlcNAcases have been detected at high levels in patients infected with *Plasmodium falciparum*. This suggests that the enzyme's induction may reflect an immunological response to malarial infection (Patil, Ghormade, and Deshpande, 2000). Recently, human chitinases have been reported to be particularly associated with anti-inflammatory effect against the T helper-2 driven diseases, such

as allergic asthma (Donnelly and Barnes, 2004; Wills-Karp and Karp, 2004; Zhu, Zheng, Homer, Kim, Chen, Cohn, Hamid, and Elias, 2004).

Chitin and its degradation derivatives are important for biomedical, pharmacological, agricultural, and biotechnological applications (Rinaudo, 2006). For examples, chitooligosaccharides are potentially used for fatty acid absorption, decreasing LDL and increasing HDL cholesterols, decreasing blood sugar level, and enhancing calcium absorption (Koide, 1998). Chitin degradation products can stimulate the immune system to respond to microbial infections (Kumar, Varadaraj, Gowda, and Tharanathan, 2005; Patil *et al*., 2000). Chitooligosaccharides and GlcNAc residues have been reported for their anti-inflammatory activity and are used for treatment of ulcerative colitis and gastrointestinal inflammation disorders. GlcNAc residues have also been used as a nutritional substrate for pediatric chronic inflammatory bowel disease and pharmaceutical therapy of osteoarthritis (Park, Kim, and Park, 2010). Chitin derivatives are used for food and drink supplements to improve the function of connective tissues and joints (Qin, Li, Xiao, Liu, Zhu, Du, 2006). The abundance of chitin in nature has stimulated research on isolation and characterization of chitinolytic enzymes from different sources.

1.2 Classification of chitinases and GlcNAcases

Chitinases (EC 3.2.1.14) are classified into glycoside hydrolases family 18 (GH-18) and family 19 (GH-19), depending on the amino acid sequence identity of their catalytic domains and the mode of enzyme action (http://www.cazy.org/; Brameld and Goddard, 1998; Fukamizo, Miyake, Tamura, Ohnuma, Skriver, Pursiainen, and Juffer, 2009; Funkhouser and Aronson, 2006; Hoell, Dalhus, Heggset,

Aspmo, and Eijsink, 2006; Kawase, Saito, Sato, Kanai, Fujii, Nikaidou, Miyashita, and Watanabe, 2004; Suginta, Songsiriritthigul, Kobdaj, Opassiri, and Svasti, 2007; van Aalten, Komander, Synstad, Gåseidnes, Peter, and Eijsink, 2001; van Scheltinga, Hennig, and Dijkstra, 1996). Family 18 chitinases are found in a variety of prokaryotic and eukaryotic organisms, such as viruses, bacteria, fungi, plants, insects and mammals, whereas family 19 chitinases are mainly found in higher plants and in the gram-positive bacterium *Streptomyces* (Brameld *et al*., 1998; Iseli, Armand, Boller, Neuhaus, and Henrissat, 1996; Sasaki, Yokoyama, Itoh, Hashimoto, Watanabe, and Fukamizo, 2002). The catalytic domain of family 18 chitinases has a long deep substrate-binding groove located at the top of the $(\beta/\alpha)_8$ TIM (triosephosphate isomerase) barrel fold with a conserved DxDxE motif on the $\beta 4$-strand (Figure 1.2) (Aronson, Halloran, Alexyev, Amable, Madura, Pasupulati, Worth, and Roey, 2003; Papanikolau, Prag, Tavlas, Vorgias, Oppenheim, and Petratos, 2001; Papanikolau, Prag, Tavlas, Vorgias, and Petratos, 2003; Perrakis, Tews, Dauter, Oppenheim, Chet, Wilson, and Vorgias, 1994; van Aalten *et al*., 2001). On the other hand, the catalytic domain of family 19 chitinases comprises of two lobes, each of which is rich in α-helical structure. The substrate binding cleft of the enzymes is positioned between the two lobes (Figure 1.2) (Davies and Henrissat, 1995; Hart, Pfluger, Monzingo, Hollis, and Robertus, 1995; Henrissat and Davies, 2000).
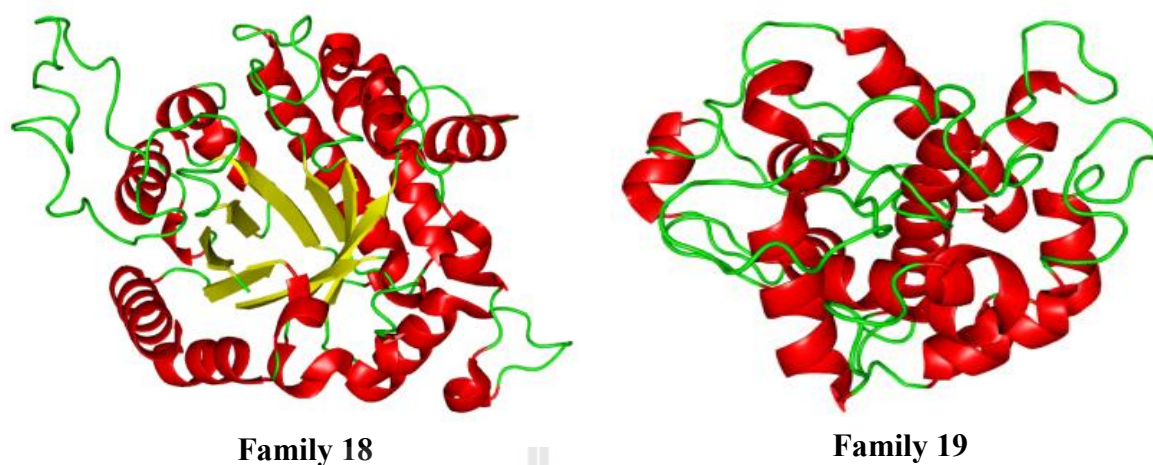
Family 18 **Family 19**

Figure 1.2 A ribbon representation of the main characteristics of the catalytic domains of GH- 18 (PDB code: 1NH6) and GH- 19 (PDB code: 3CQL) chitinases.

The mode of enzyme action of family 18 chitinases has been proposed to be the substrate-assisted retaining mechanism, which contains a catalytic acid/base residue and the *N*-acetyl group of the sugar in the -1 subsite acts as a nucleophile. The hydrolytic products of this mechanism are in the *β*-anomeric form (Armand, Tomita, Heyraud, Gey, Watanabe, and Henrissat, 1994; Aronson *et al*., 2003; Brameld *et al*., 1998; Fukamizo, Sasaki, Schelp, Bortone, and Robertus, 2001; Hollis, Honda, Fukamizo, Marcotte, Day, and Robertus, 1997; Vuong and Wilson, 2010). In contrast, the mode of enzyme action of family 19 chitinases employs the single displacement inverting mechanism. The hydrolytic reaction requires a catalytic acid residue and a catalytic base residue, which yields an inversion of anomeric configuration with a predominant α-anomeric product (Fukamizo, Koga, and Goto, 1995; Hollis *et al*., 1997).

GlcNAcases are classified into glycoside hydrolase family 3 (GH-3) and family 20 (GH-20) based on the amino acid sequence similarity of their catalytic domains and the mode of enzyme action (http://www.cazy.org/; Henrissat and Bairoch, 1993; Henrissat and Daviest 1997; Li *et al*., 2002). Family 3 glycoside hydrolases include *β*-D-glucosidases (EC 3.2.1.21), *β*-D-xylopyranosidases (EC 3.2.1.37), *β*-*N*-acetylglucosaminidases (GlcNAcases) (EC 3.2.1.52), and *α*-L-arabinofuranosidases (EC 3.2.1.55) (Harvey, Hrmova, De Gori, Varghese, and Fincher, 2000). Family 20 glycoside hydrolases include *β*-*N*-acetylglucosaminidases (GlcNAcases) (EC 3.2.1.52) and *β*-hexosaminidases (*β*-*N*-acetylhexosaminidases) (EC 3.2.1.52). While, GlcNAcases hydrolyze *β*-1,4 linkages *N*-acetylglucosamine oligomers, *β*-hexosaminidases also hydrolyze *β*-1,4 linkages between *N*-acetylgalactosamine and galactosamine moieties (Tews *et al*., 1996). Most of bacterial GlcNAcases are grouped into family 20 GlcNAcases, such as chitobiase from *Serratia marcescense* (Tews *et al*., 1996), *β*-hexosaminidase from *Streptomyces plicatus* (Mark, Vocadlo, Knapp, Triggs-Raine, Withers, and James, 2001), disperin B (*β*-1,6-*N*-acetylglucosaminidase) from *Actinobacillus actinomycetemcomitans* (Ramasubbu, Thomas, Ragunath, and Kaplan, 2005), *N*-acetyl-*β*-D-glucosaminidase from *Streptococcus gordonii* (Langley, Harty, Jacques, Hunter, Guss, and Collyer, 2008), *β*-*N*-acetylhexosaminidase from *Paenibacillus* sp. (Sumida, Ishii, Yanagisawa, Yokoyama, and Ito, 2009), and *β*-*N*-acetylglucosaminidases from *Vibrio harveyi* 650 (Suginta, Chuenark, Mizuhara, and Fukamizo, 2010). While, only five bacterial GH-3 GlcNAcases have been characterized, including ExoII or NagZ from *Vibrio furnissii* (Chitlaru and Roseman, 1996), Nag3A from *Clostridium paraputrificum* M-21 (Li *et al*., 2002), NagA from *Streptomyces thermoviolaceus* OPV-520 (Kubota *et al*., 2004),

NagA from *Thermotoga maritime*, and CbsA from *T. neapolitana* (Choi, Seo, Park, Park, and Cha, 2009). The mode of enzyme action of family 3 GlcNAcases has been proposed to be the double displacement retaining mechanism, while the mode of enzyme action of family 20 GlcNAcases employs the substrate-assisted retaining mechanism which is similar to family 18 chitinases (Vocadlo and Withers, 2005).

1.3 Catalytic mechanisms of family 18 chitinases and family 20 GlcNAcases

Family 18 chitinases catalyze the hydrolytic reaction through the substrate-assisted retaining mechanism that the nucleophilic attack is carried out by the *N*-acetamido group of the sugar bound to the -1 subsite to form an oxazolinium ion. The position and nucleophilicity of the acetamido group are affected by certain acidic residues located within the conserved DxDxE motif. These residues include the catalytic acid/base (Glu144 and Asp140 and Asp142 in *Sm*ChiB) that are buried in the core of the $(\beta/\alpha)_8$ fold. According to this mechanism, the catalytic residue Glu acts as a proton donor, and its position, is in the vicinity to donate a proton to the oxygen O4 of +1 sugar unit. Subsequent cleavage of the glycosidic C1(-1)-O4(+1) bond leads to the formation of an oxazolinium ion intermediate that is stabilized by hydrogen bonding interaction with the protonated Asp142 in *Sm*ChiB (Figure 1.3A-B). Then, a proton from a water molecule was taken up by the γ-carboxylate of Glu144 in *Sm*ChiB, and the remaining hydroxide anion was taken up by the C1 carbon of -1 sugar, yields the hydrolytic product, which retains the initial anomeric configuration (Figure 1.3C). The rotation of Asp142 is not only for stabilizing the oxazolinium ion intermediate, but also for donating a proton. The rotation of Asp142 also causes

lowering *p*Ka of Glu144, which triggers the hydrolysis of the *O*-glycosidic linkage at the cleavage site (Papanikolau *et al*., 2001; Perrakis *et al*., 1994; van Aalten *et al*., 2001). In addition, the study recently found that the enzyme-substrate interactions of *Vh*ChiA revealed two conformations of Asp313 and (-1) sugar unit. The first conformation, likely to be the initial conformation, showed that the *β*-COOH of Asp313 detaches from Asp311 and rotates to form hydrogen-bond only with the − C=O of the *N*-acetamido group of the (-1) sugar unit (Figure 1.4A-B). The second conformation, formed from the first by concerted bond rotations, demonstrated hydrogen bonds between the Asp313 side chain and the −NH of the *N*-acetyl group and the *γ*-COOH of Glu315. Then, the glycosidic bond of the substrate is cleaved by nucleophilic attack on C-1 by the –C=O of the *N*-acetamido group, with protonation of the glycosidic oxygen by Glu315, generating an oxazolinium ion intermediate, which is stabilized by Asp313 (Figure 1.4C). The cycle is completed after the second nucleophilic attack on the intermediate by –OH group of a water molecule (Figure 1.4D) (Suginta and Sritho, 2012).
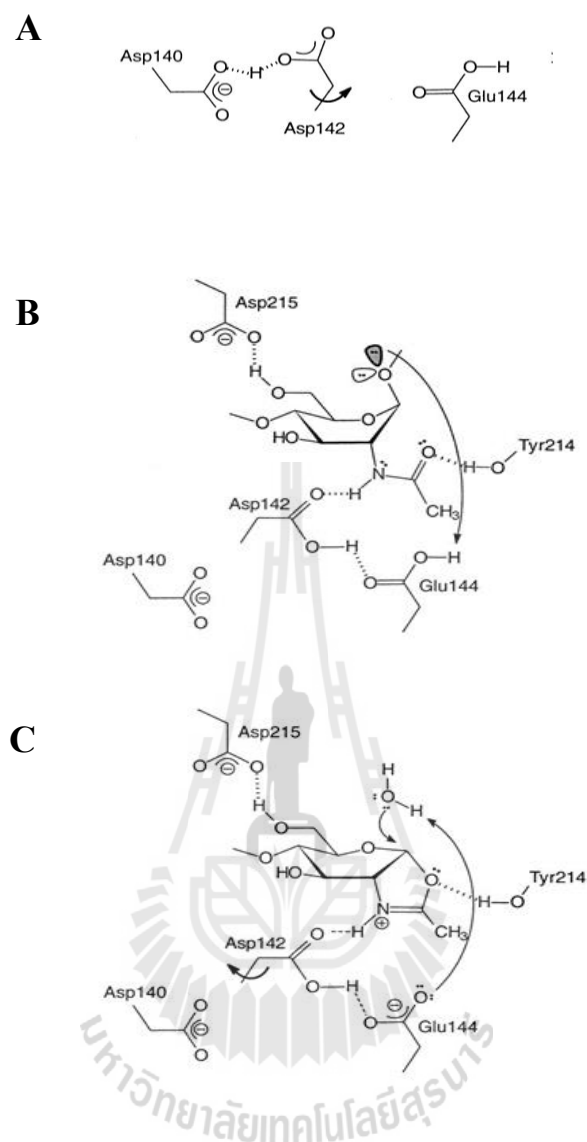
Figure 1.3 The catalytic mechanism of family 18 chitinases B from *Serratia marcescens* (*Sm*ChiB). (A) Resting enzyme. (B) Substrate binding and rotation of Asp 142 toward Glu 144, enabling hydrogen bond interactions between the hydrogen of the acetamido group, Asp 142 and Glu 144. (C) Hydrolysis of the oxazolinium ion intermediate leads to protonation of Glu 144 and rotation of Asp 142 to its original position where it shares a proton with Asp 140 (van Aalten *et al*., 2001).
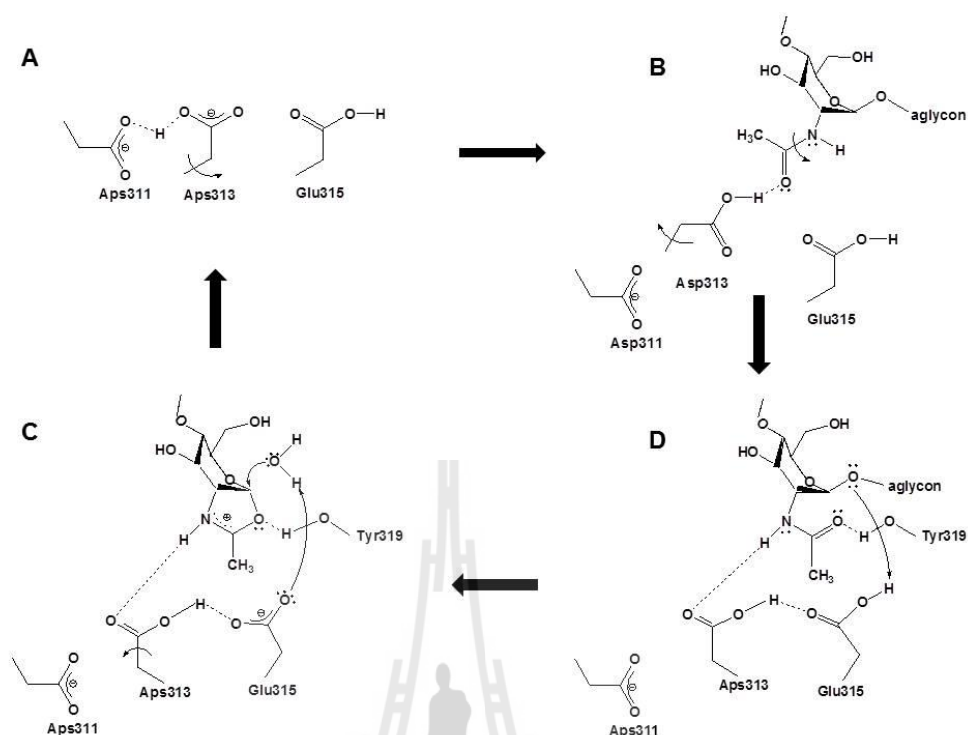
Figure 1.4 The refined catalytic cycle of chitin degradation of family 18 *Vibrio harveyi* chitinase A (*Vh*ChiA). (A) Pre-priming, (B) Substrate binding, (C) Bond cleavage, and (D) Formation of reaction intermediate (Suginta and Sritho, 2012).

The catalytic mechanism of family 3 GlcNAcases catalyzes the hydrolytic reaction through the double displacement mechanism, involving the formation and breakdown of a covalent α-glycosyl enzyme intermediate formed on an aspartate residue (Figure 1.4A) (Vocadlo *et al*., 2005). In the first step of the reaction, the formation of the intermediate, departure of the aglycon leaving group is typically facilitated by a general acid/base catalytic residue, which donates a hydrogen atom to the glycosyl oxygen atom while the nucleophile forms the glycosyl-enzyme intermediate. In the second step of the reaction, the breakdown of the intermediate,

the same catalytic residue acts as a general base, enhancing the nucleophilicity of a water molecule poised near the anomeric center. The water molecule attacks the anomeric center with the net result being the formation of the hemiacetal product with retained stereochemistry (Vocadlo *et al*., 2005). In contrast, the catalytic mechanism of family 20 GlcNAcases employs the substrate-assisted retaining mechanism, involving the carbonyl of the 2-acetamido group that acts as a nucleophile to displace the aglycon leaving group with the net result being the formation of an oxazolinium ion intermediate. Afterwards, a water molecule attacks the anomeric center, breaking down the oxazolinium ring to generate the hemiacetal product with retained stereochemistry (Figure 1.4B) (Vocadlo *et al*., 2005). The two key catalytic residues of family 20 glycoside hydrolases were identified previously by both structural and kinetic studies. The catalytic cycle employs an Asp-Glu catalytic pair, where the aspartate and glutamate residues are immediately adjacent to each other in the sequence (Centinbas, Macauley, Stubbs, Drapala, and Vocadlo, 2006). For family 20 GlcNAcases, an alternative mechanism has been proposed, involving the formation of an oxocarbenium ion intermediate stabilized by the acetamido group that protects the bottom face of the saccharide ring (Figure 1.4C) (Vocadlo *et al*., 2005).
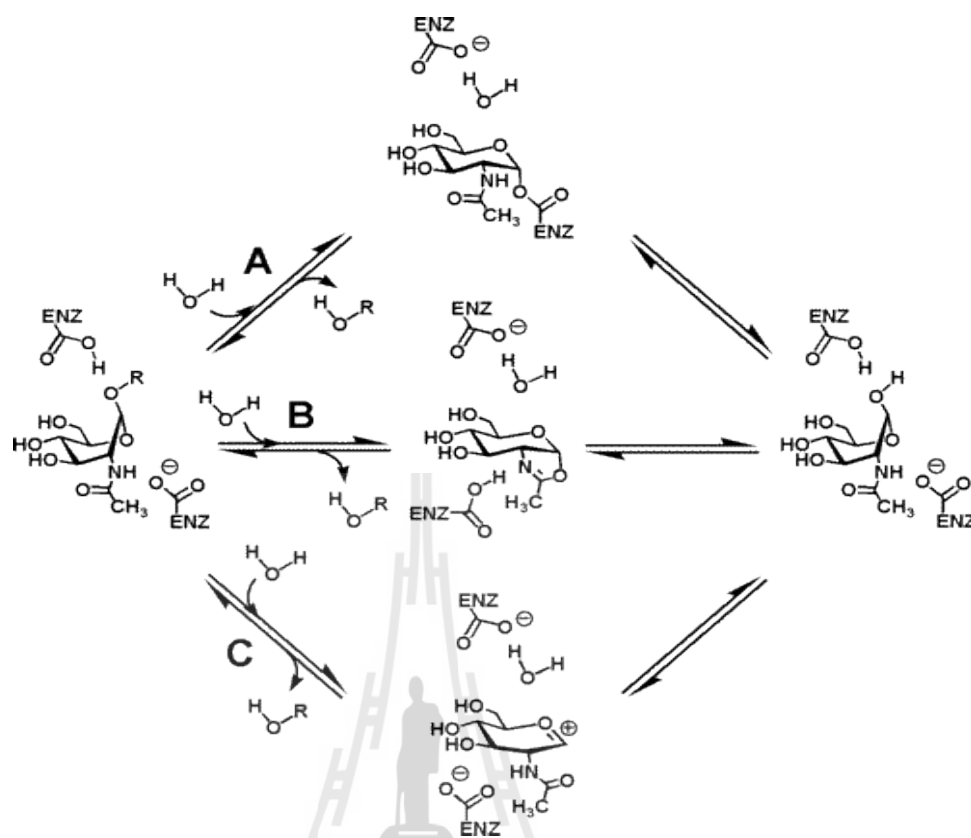
Figure 1.5 The catalytic mechanisms of the two classes of GlcNAcases. (A) Family 3 GlcNAcases use an anionic enzymic carboxylate group as the nucleophile to form a covalent glycosyl enzyme intermediate. (B) Family 20 GlcNAcases use the 2-acetamido group of the substrate acts as nucleophile to form an oxazolinium ion intermediate. (C) An alternative mechanism has been proposed for Family 20 GlcNAcases involving the formation of an oxocarbenium ion intermediate stabilized by the acetamido group (Vocadlo *et al*., 2005).

1.4 Studies of the effect of sodium azide on the catalytic activity of the retaining enzymes

Several reports employed sodium azide as a chemical rescue to probe the catalytic acid/base and the catalytic nucleophile residues of the retaining glycoside hydrolases, such as *Cellulomas fimi* GH-85 exoglucanase/xylanase (MacLeod, Lindhorst, Withers, and Warrent, 1994), *Bacillus licheniformis* 1,3-1,4-*β*-glucanase (Viladot, Ramon, Durany, and Planas, 1998), *Streptomyces* sp. GH-1 *β*-glucosidase (Vallmitjana, Ferrer-Navarro, Planell, Abel, Ausı´n, Querol, Planas, and Pe´rez-Pons, 2001), *Geobacillus stearothermophilus* T-6 GH-51 α-L-arabinofuranosidase (Shallom, Belakhov, Solomon, Shoham, Baasov, and Shoham, 2002), *Streptomyces plicatus* GH-20 hexoxaminidase (*Sp*Hex) (Williams, Mark, Vocadlo, James, and Withers, 2002), *Sulfolobus solfataricus* GH-29 α-L-fucosidase (Cobucci-Ponzano, Trincone, Giordano, Rossi, and Moracci, 2003), *Paenibacillus* sp. TS12 glucosylceraminidase (Paal, Ito, and Withers, 2004), and *Arthrobacter protophormiae* GH-85 endo-*β*-N-acetylglucosaminidase (Endo A) (Fujita, Sato, Toma, Kitahara, Suganuma, Yamamoto, and Takegawa, 2007). All of those studies demonstrated that sodium azide significantly recovered the glycoside hydrolase activity of the inactive mutant, in which one residue in the catalytic D-E pair was mutated. The results proposed that the azide anion acts as an alternative nucleophile to form *α*-glycosyl azide in the glycosylation step or *β*-glycosyl azide in the deglycosylation step of the retaining glycosidase mechanism (MacLeod *et al*., 1994; Viladot *et al*., 1998). For example, the activity of *Arthrobacter protophormiae* endo-*β-N*-acetylglucosaminidase (Endo A) inactive mutant E173A was increased by 127-fold when 2 M sodium azide was added in the assayed reaction (Fujita *et al*., 2007). The

role of the key catalytic residues Glu134 and Glu138 of *Bacillus licheniformis* 1,3-1,4-β-glucanase is probed by a chemical rescue methodology, based on enzyme activation of inactive mutants by the action of added sodium azide that acts as an exogenous nucleophile. The inactive mutants E138A and E134A were produced by site-directed mutagenesis. Addition of sodium azide re-activates the mutants. The chemical rescue operates by a different mechanism, depending on the mutant as deduced from ^{1}H NMR monitoring and kinetic analysis of enzyme reactivation. E138A yields the β-glycosyl azide product arising from nucleophilic attack of azide anion on the glycosyl-enzyme intermediate in the deglycosylation step suggested that Glu138 is the general acid-base residue. In contrast, azide anion reactivates E134A mutant through a single inverting displacement to give the α-glycosyl azide product in the glycosylation step suggested that Glu134 is the catalytic nucleophile (Viladot *et al*., 1998). In contrast, sodium azide was found to inhibit the wild-type *Bacillus licheniformis* 1,3-1,4-β-glucanase activity using mixed type and competitive mode when G4G3G-MU and G4G3G-2,4DNP as the substrates, respectively (Viladot *et al*., 1998).

The most relevant case to family 18 chitinases and family 20 GlcNAcases are a report on *Sp*Hex, a retaining family 20 glycosidase from *Streptomyces plicatus* (Williams *et al*., 2002). *Sp*Hex catalyzes the hydrolysis of *N*-acetyl-β-hexosaminides. An acidic pair (Asp313-Glu314) is identified to be the most essential resides in the catalysis. Functional roles of Asp313 are predicted to aid the 2-acetamido group of -1 GlcNAc to act as a powerful nucleophile and to stabilize the oxazolinium ion intermediate. On the other hand, Glu314 acts as the catalytic residue that directly attacks the β-1,4-glycosidic bond at the cleavage site. Single mutation of Asp313 of

*Sp*Hex to Ala or Asn (mutant D313A or D313N) almost abolished the hydrolytic activity of *Sp*Hex. However, k_{cat} of mutant D313A was increased up to 16 fold of the original rate when sodium azide was added in the assayed reaction. It has been concluded that the azide ion acts as an alternative nucleophile to water and open the oxazolinium ion intermediate formed after acid catalysis by Glu314 (Williams *et al*., 2002). The activation of sodium azide on the inactive mutant may occur in 2 ways: i) Azide anion could provide charge stabilization of the transition state that flanks the oxazolinium ion intermediate, instead of the mutant D313A that the acidic side chain has been removed. Alternatively, azide anion may reactivate the mutant by acting as a nucleophile that competes with the hydroxyl group from the water to interact the oxazolinium ion intermediate to give the *β*-glycosyl azide product in the deglycosylation step (Figure 1.5) (Williams *et al*., 2002).
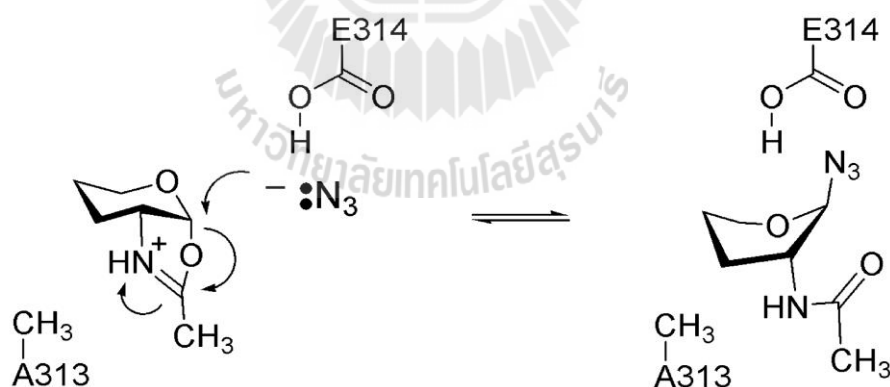
Figure 1.6 Proposed mechanism of azide anion rescues the *Sp*Hex D313A variant activity. Azide as an alternative nucleophile to water acts to open the oxazolinium ion intermediate (Williams *et al*., 2002).

1.5 Studies of transglycosylation reaction of family 18 chitinases

In nature, degradation of insoluble chitin polymer by chitinases generates water-soluble chitooligosaccharide fragments (Rinaudo, 2006). Chitooligosaccharides have various biological functions. For example, they can stimulate plant immune system to respond to microbial infections, so as they can be used as antimicrobial agents (Kaku, Nishizawa, Ishii-Minami, Akimoto-Tomiyama, Dohmae, Takio, Minami, and Shibuya, 2006; Miya, Albert, Shinya, Desaki, Ichimura, Shirasu, Narusaka, Kawakami, Kaku, and Shibuya, 2007; Kumar *et al.*, 2005; Yamaguchi, Yamada, Ishikawa, Yoshimura, Hayashi, Uchihashi, Ishihama, Kishi-Kaboshi, Takahashi, Tsuge, Ochiai, Tada, Shimamoto, Yoshioka, and Kawasaki, 2013). However, the biological activities of chitooligosaccharides are most efficient, when the chain lengths are more than five or six (Kumar *et al.*, 2005; Petutschnig, Jones, Serazetdinova, Lipka, and Lipka, 2010). Usually, chemical synthesis of chitooligosaccharides with such longer chains is cumbersome and costly due to the selective protection and subsequent manipulation of various monosaccharide donors and acceptors (Aly, Ibrahim, Ashry, and Schmidt, 2001; Kanie, Ito, and Ogawa, 1994). Therefore, enzymatic synthesis employing the transglycosylation activity of chitinases may serve as a better biological tool for a large-scale production of such biologically-active compounds.

Transglycosylation (TG) catalyzed by family 18 chitinases usually takes place through two steps (Aronson, Halloran, Alexeyev, Zhou, Wang, Meehan, and Chen, 2006; Fukamizo, Sasaki, Schelp, Bortone, and Robertus, 2001; Zakariassen, Hansen, Jøranli, Eijsink, and Sørlie, 2011). In the first step, the glycosidic oxygen is protonated by a catalytic acid to cleave the β-1,4-glycosidic linkage and to form the

oxazolinium ion intermediate, in which the C1 carbon of the -1 sugar is stabilized by anchimeric assistance of the sugar N acetamido group. In the second step, the oxazolinium ion intermediate is attacked by a water molecule from the β-side, leading to hydrolysis with net retention of anomeric form. When a water molecule is outcompeted by another acceptor, such as carbohydrates, TG reaction takes place, resulting in formation of a glycosidic linkage and yielding longer-chain chitooligosaccharides instead.

Chitinases from various sources have been reported to potentially catalyze TG reaction. For examples, a chitinase from *Nocardia orientalis* was reported to convert $GlcNAc_4$ substrate to $GlcNAc_6$ under high ammonium sulfate concentration (Nanjo, Sakai, Ishikawa, Isobe, and Usui, 1989). Recently, *Serratia proteamaculans* chitinase D (*Sp*ChiD) showed high TG activity with $GlcNAc_{3-6}$ substrates, generating $GlcNAc_{7-13}$ products, which were hydrolyzed into smaller $GlcNAc_n$ after 90 min of the reaction (Purushotham and Podile, 2012). Mutations of some amino acids located close to the catalytic cleft were found to enhance TG activity in various family 18 chitinases. For examples, *Serratia marcescens* chitinase A (*Sm*ChiA) showed that mutation of Trp167 at the -3 subsite to Ala (mutant W167A) enhanced TG activity producing $GlcNAc_n$, of which the polymerization degree is higher than that of $GlcNAc_4$ and $GlcNAc_5$ substrates (Aronson *et al*., 2006). Additionally, two mutants from different chitinase homologs (*Sm*ChiA D313N and *Sm*ChiB D142N) were found to improve TG activity, especially the double mutant D313N/F396W at the +2 subsite in *Sm*ChiA showed two-fold increase in the TG rate as compared to the single mutant D313N (Zakariassen *et al*., 2011). Another report on mutants D200A and D202A of *Bacillus circulans* WL-12 chitinase A1 and on mutants D170N and D170A of *Trichoderma*

harzanium chitinase 42 displayed higher TG activity, whereas their hydrolytic activity was dramatically diminished (Martinez, Boer, Koivula, Samain, Driguez, Armand, and Cottaz, 2012). On the other hands, mutants M226A, Y228A, R284A, F64W, F125A, G119S, S116G and W247A of *Sp*ChiD displayed the TG products that were stable for an extended period of up to 6 h (Madhuprakash, Tanneeru, Purushotham, Guruprasad, and Podile, 2012).

1.6 Studies of *Vibrio harveyi* chitinase A

The marine bacterium, *Vibrio harveyi* (formerly *V. carchariae*), chitinase A (*Vh*ChiA) is a member of family 18 glycoside hydrolases (GH-18) that is mainly responsible for the hydrolysis of *β*-1,4 glycosidic linkages of chitin biomaterials in the marine ecosystem (Suginta, Robertson, Austin, Fry, and Fothergill-Gilmore, 2000). *Vh*ChiA is active as a monomer of M_r 63,000 (Suginta *et al*., 2000). Analysis of chitin hydrolysis using HPLC/ESI-MS suggested that this enzyme acts as an endochitinase (Suginta, Vongsuwan, Songsiriritthigul, Prinz, Estibeiro, Duncan, Svasti, and Fothergill-Gilmore, 2004). The enzyme primarily generated *β*-anomeric products indicating that it catalyzed the hydrolysis through the substrate assisted retaining mechanism (Suginta, Vongsuwan, Songsiriritthigul, Svasti, and Prinz, 2005). The hydrolytic activity of mutants *Vh*ChiA E315M, E315Q and D392N towards glycol chitin showed that the mutant D392N retained significant chitinase activity in the gel activity assay, while the mutants E315M and E314Q showed the complete loss of substrate utilization suggested that Glu315 is an essential residue in the enzyme catalysis (Suginta *et al*., 2005). In addition, all chitinases also exhibited transglycosylation activity towards chitooligosaccharides and *p*NP-glycosides,

especially the mutant D392N that showed strikingly greater efficiency in oligosaccharide synthesis than the wild-type enzyme (Suginta *et al*., 2005).

The effects of point mutation of the residues Trp168, Tyr171, Trp275, Trp397 and Trp570 were studied. All the mutant residues located in the substrate binding cleft of the modeled 3D structure of *Vh*ChiA. Mutations of Trp168, Tyr171 and Trp570 completely abolished the hydrolyzing activity against colloidal chitin, and greatly reduced the hydrolyzing activity against the *p*NP substrate (Suginta *et al*., 2007). Mutant W570G showed the most severe effects on the hydrolyzing activity, having no activity against colloidal chitin and least activity against *p*NP-GlcNAc$_2$ (Suginta *et al*., 2007). In the modeled 3D structure, Trp570 was closest to the sugar ring at subsite -1 that is likely to be responsible for holding the GlcNAc ring at this position in place so that cleavage of the glycosidic bond between subsites -1 and +1 can occur (Suginta *et al*., 2007). The time course study of G4-G6 hydrolysis by thin layer chromatography (TLC) showed higher efficiency of the mutants W275G and W397F over the wild-type enzyme. Although the time course of colloidal chitin hydrolysis displayed no difference in the cleavage behavior of the chitinase variants, the time course of G6 hydrolysis exhibited distinct hydrolytic patterns between the wild-type and the mutants W275G and W397F. The results suggested that residues Trp275 and Trp397 are involved in defining the binding selectivity of the enzyme to soluble substrates (Suginta *et al*., 2007).

The X-ray structure of wild-type *Vh*ChiA showed that the overall structure of *Vh*ChiA consists of three distinct domains, which are the *N*-terminal chitin-binding domain, the main catalytic $(\alpha/\beta)_8$ TIM-barrel domain and the small $(\alpha+\beta)$ insertion domain. The structure of the catalytic cleft of the inactive mutant *Vh*ChiA (E315M)

complexes with GlcNAc$_6$ has a long, deep groove, which contains six substrate binding sites (-4)(-3)(-2)(-1)(+1)(+2) where subsites -4 to -1 are the glycone sites and subsites +1 and +2 are the aglycone sites. The cleavage site is located between subsites -1 and +1 (Figure 1.6) (Songsiriritthigul, Pantoom, Aguda, Robinson, and Suginta, 2008). Recently, the roles of Asp313, which lies at the bottom of the binding cleft catalytic residue 315, in the catalytic cycle of chitin degradation by *Vh*ChiA were investigated. The kinetic and structural evidence suggest that Asp313 in the highly conserved DXDXE sequence motif plays several important roles in the catalytic cycle of *Vh*ChiA. Asp313 contributes to the ability of *Vh*ChiA to bind the chitin substrates. Asp313 participates in the catalytic process by lowering the pK$_a$ of catalytic residue 315, promoting bond cleavage, and stabilizes the oxazolinium ion intermediate (Suginta and Sritho, 2012)
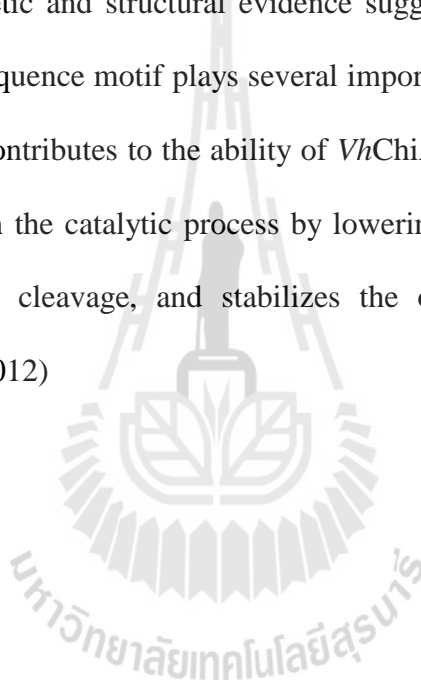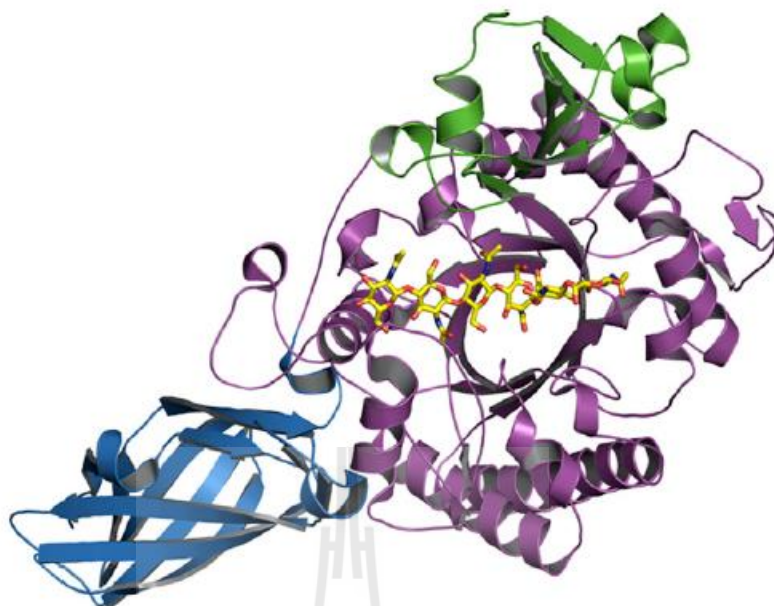
Figure 1.7 The crystal structure of the *Vh*ChiA E315M inactive mutant complexed with GlcNAc$_6$ is that of a typical family 18 glycoside hydrolases comprising three distinct domains. The *N*-terminal chitin-binding domain (ChBD) is in blue, the catalytic $(\alpha/\beta)_8$ TIM-barrel domain is in magenta and the small $(\alpha+\beta)$ insertion domain is in green. The catalytic cleft of chitinase A contains six chitooligosaccharide ring-binding subsites (-4)(-3)(-2)(-1)(+1)(+2) (Songsiriritthigul *et al*., 2008).

1.7 Studies of *Vibrio harveyi* GlcNAcases

The genes encoding two GlcNAcases (*Vh*Nag1 and *Vh*Nag2) from *V. harveyi* are classified as new members of family 20 glycoside hydrolases (Suginta *et al*., 2010). These enzymes were successfully cloned and expressed in *E. coli* M15 host cells. *Vh*Nag1 has a molecular mass of 89 kDa and an optimum pH of 7.5, while *Vh*Nag2 has a molecular mass of 73 kDa and an optimum pH of 7.0. The recombinant GlcNAcases were found to hydrolyze all the natural substrates, *Vh*Nag2 being more

active than *Vh*Nag1. Product analysis by TLC and quantitative HPLC suggested that *Vh*Nag2 degrades chitooligosaccharides in an exo manner releasing GlcNAc as the end product and it has the highest activity toward chitotetraose. Kinetic modeling of the enzymatic reaction revealed that the binding pocket of *Vh*Nag2 contains four substrate binding subsites, designated (-1), (+1), (+2), and (+3).

In living cells, these intracellular enzymes may work after endolytic chitinases to complete chitin degradation (Suginta *et al*., 2010).

1.8 Research objectives

Vibrio harveyi is a marine bacterium responsible for a rapid turnover of chitin biomaterials in the marine enviroment. The bacterium initially secretes chitinase A (*Vh*ChiA), which is a member of family 18 glycoside hydrolases, to degrade chitin polymer, yielding chitooligosaccharide fragments, which can be taken up by the cell through chitoporin. In the periplasm, GlcNAcase (*Vh*GlcNAcase), which is a member of family 20 glycoside hydrolases, is sequentially degrades the transported chitooligosaccharides into GlcNAc monomers that are further metabolized inside the cells. Although *Vh*ChiA and *Vh*GlcNAcase are different classes of glycoside hydrolases, both catalyze the hydrolytic reaction through the substrate-assisted retaining mechanism.

From the studies of transglycosylation (TG) reaction catalyzed by family 18 chitinases, it is obvious that enhancing the TG activity of chitinases does not always result in the production of chitooligosaccharides with longer chains, because the TG products are often decomposed into shorter oligosaccharides. In the first part of this research, we investigated the mutation strategies for obtaining chitooligosaccharides

with longer chains by means of enzymatic TG reaction using family 18 chitinase A from *Vibrio harveyi* (*Vh*ChiA).

Several reports have employed sodium azide as a chemical rescue to probe the catalytic acid-base residues of the catalytically inactive mutant glycoside hydrolases. However, the effects of sodium azide and sodium salts of small nucleophiles on the wild-type and mutants *Vh*ChiA and *Vh*GlcNAcase activities have not been thoroughly investigated. Therefore, the second part of this research aims to investigate the effects of sodium azide and sodium salts on the hydrolytic activity of the two enzymes against *p*NP-glycosides and natural substrates.

The objectives of this research include:

1. To express and purify the wild-type and mutants of *Vh*ChiA and *Vh*GlcNAcase

2. To evaluate the transglycosylation activity of the *Vh*ChiA wild-type and the mutants, including W570G, D392N, D313A and D313N by a quantitative HPLC technique.

3. To investigate the effects of sodium azide and other sodium salts on the hydrolytic activities of the *Vh*ChiA and *Vh*GlcNAcase.

CHAPTER II

MATERIALS AND METHODS

2.1 Bacterial strains and expression plasmids

The genes encoding chitinase A (*Vh*ChiA) and *N*-acetylglucosaminidase from the marine bacterium *Vibrio harveyi* were previously isolated, cloned into the pQE60 expression vector, and expressed in *E. coli* M15 (pREP) type strain, as described elsewhere (Suginta *et al*., 2004; Suginta *et al*., 2010). Both genes were designated *Vh*ChiA and *Vh*GlcNAcase, respectively. In this study, the chitinase constructs used were: pQE-60 vector, harboring wild-type and mutants D392N, W570G, D313A and D313N *chitinase A* gene fragments (Suginta *et al*., 2004; Suginta *et al*., 2005; Suginta *et al*., 2007; Suginta *et al*., 2012). pQE-60 expression vector harboring *β-N-acetyl-glucosaminidase* gene fragment (Suginta *et al*., 2010) was used to express *Vh*GlcNAcase. *Escherichia coli* strain DH5α was used as a routine host for amplification of recombinant plasmids. *E. coli* strain M15 (Qiagen, Valencia, CA, USA) was used for high-level expression of the recombinant chitinase A (*Vh*ChiA) and *β-N*-acetyl-glucosaminidase (*Vh*GlcNAcase).

2.2 Chemicals and reagents

Chemicals and reagents used for protein expression, purification and characterization of *Vh*ChiA and *Vh*GlcNAcase were analytical grade unless otherwise

stated. Acetone, aniline, ammonia solution 30%, buthanol, calcium chloride, ethanol, glacial acetic acid, hydrochloric acid, magnesium chloride, methanol, nickel (II) sulphate, orthophosphoric acid 85%, potassium acetate, potassium dihydrogen phosphate, dipotassium hydrogen phosphate, potassium sodium tartrate, sodium acetate, sodium carbonate, sodium chloride, sodium dihydrogen phosphate, disodium hydrogen phosphate, sodium formate, sodium hydroxide, sodium nitrate, sodium sulphate, Tris-(hydroxymethyl)-aminomethane, sodium dodecyl sulfate (SDS) and water (HPLC grade) were purchased from Carlo Erba (Rodano, Milano, Italy).

Acrylamide, ammonium persulfate, bis-*N, N''*-methylenebisacrylamide, 2-β-mercaptoethanol, bromophenol blue, coomassie brilliant blue R250, ethylenediamine tetra-acetic acid (EDTA), glycerol and *N, N', N'', N'''*-tetramethylethylenediamine (TEMED) were purchased from Sigma-Aldrich (St. Louis, MO, USA). Ampicillin, kanamycin, phenylmethyl sulfonyl fluoride (PMSF), imidazole, hen egg white lysozyme and triton X-100 were purchased from USB Corporation (Cleveland, OH, USA). Tryptone, yeast extract powder and agar powder were purchased from Himedia Laboratories (Marg, Mumbai, India). Diphenylamine was from Acros Organics (Morris Plains, NJ, USA). DNase I was from Bio basic (Markham, Ontario, Canada). Glycine was from Vivantis (Oceanside, CA, USA). Isopropyl thio-*β-D*-galactoside (IPTG) was from Merck Millipore (Billerica, MA, USA). BCA protein assay kit was a product of EMD Chemicals (San Diego, CA, USA).

N-acetyl-chitooligosaccharides (*N*-acetyl-glucosamine, di-*N*-acetyl-chitobiose, tri-*N*-acetylchitotriose, tetra-*N*-acetyl-chitotetraose, penta-*N*-acetyl-chitopentaose and hexa-*N*-acetylchitohexaose) were produced by acid hydrolysis of chitin (Rupley *et al.*, 1964) and purified by gel-filtration column of Gcl-25m (JNC Co., Tokyo, Japan) and

also were purchased from Seikagaku Corporation (Chiyoda-ku, Tokyo, Japan). Chitin from crab shells was purchased from Seikagaku Corporation (Tokyo, Japan) and colloidal chitin was prepared from crab chitin by the method of Hsu and Lockwood (1975). *p*-nitrophenol (*p*NP) and *p*-nitrophenyl-*N*-acetyl-glucosaminide (*p*NP-GlcNAc) were purchased from Sigma-Aldrich (St. Louis, MO, USA). *p*-nitrophenyl-di-*N*-acetyl-chitobioside (*p*NP-GlcNAc$_2$) was purchased from Toronto research chemicals (Ontario, Canada).

Ni-nitrilotriacetic acid (Ni-NTA) agarose resins were purchased from Qiagen (Valencia, CA, USA) and Bio-Rad Laboratories (Hercules, CA, USA). Ni-NTA agarose columns (1x5 ml) were purchased from Qiagen GmbH (Qiagen, Hilden, Germany). HiPrep 16/60 Sephacryl S-100 HR and S-200 HR columns were products of GE Healthcare (Munich, Germany). Vivaspin-20 ultrafiltration membrane concentrators (M_r 10,000 cut-off) were products of Vivascience (AG, Hannover, Germany). A 96-well microtiter plate was from Nunc (Roskilde, Denmark). A TCL Silica gel 60 F$_{254}$ Aluminum sheet (10 cm x 10 cm) and a TLC developing tank were from Merck (Berlin, Germany).

2.3 Instrumentation

The instruments required for protein expression, purification and characterization are located at the Biochemistry-Electrochemistry Research Unit at the Center for Scientific and Technology Equipment (F9 building), Suranaree University of Technology, Nakhon Ratchasima, Thailand. These instruments included a Mini-PROTEAN® 3 Cell (Bio-Rad, Hercules, CA, USA), a Biochrom Anthos Multiread 400 Microplate Reader (Biochrom, Cambridge, UK), a Multi Read 400

Microplate Reader (Becthai Bangkok Equipment & Chemical Co., Ltd., Bangkok, Thailand), a Shaking incubator (MRC, Holon, Israel), a Thermomixer comfort (Eppendorf AG, Hamburg, Germany), a microcentrifuge Denville 26OD (Denville Scientific, Metuchen, NJ, USA), a High-speed microentrifuge CF16RX II (Hitachi, Tokyo, Japan), a LS-55 fluorescence spectrometer (Perkin-Elmer, Bangkok, Thailand) and an ÄKTA purifier system (Amersham Bioscience, Piscataway, NJ, USA).

The instruments used for transglycosylation reaction that located at Kinki University, Nara, Japan were an FPLC purifier system (GE Healthcare, Munich, Germany) and a gel filtration column of TSK-1 GEL G2000PW (7.5 mm × 600 mm) connected with a Hitachi L-7000 HPLC system (Hitachi Koki Co., Ltd, Tokyo, Japan).

2.4 Recombinant expression of *Vh*ChiA and *Vh*GlcNAcase variants

For recombinant protein expression, the recombinant plasmids were transformed into *E. coli* M15 competent cells. Then, the ampicillin/kanamycin resistant colonies were picked from single colonies, and grown overnight at 37 $^{\circ}$C in Luria-Bertani (LB) broth containing 100 μg/mL ampicillin and 25 μg/mL kanamycin with shaking at 200 rpm. The freshly inoculated culture was diluted to a ratio of 1:100 with LB broth, containing the same concentrations of ampicillin and kanamycin, and further grown at 37 $^{\circ}$C until the OD_{600} reaches 0.4-0.6. To induce protein expression, isopropyl thio-*β-D*-galactoside (IPTG) was added to a final concentration of 0.5 mM, and the culture was further incubated overnight at 25 $^{\circ}$C for *Vh*ChiA or 20 $^{\circ}$C for *Vh*GlcNAcase for an additional 18 hr with shaking at 200 rpm. The IPTG-induced cells were harvested by centrifugation at 4,500 rpm at 4 $^{\circ}$C for 30 min, and the cell

pellet was kept at -80 ^{o}C for 60 min or longer until used. The cell pellet was re-suspended in lysis buffer (1 mg/mL lysozyme, 1 mM phenylmethyl sulfonyl fluoride (PMSF), 1% (v/v) Triton X-100, 2 mM MgCl$_2$, DNase I, 5 mM Imidazole and 20 mM Tris-HCl buffer, pH 8.0 containing 150 mM NaCl), and further incubated at room temperature for 30 min. Cell debris was removed by centrifugation at 12,000 rpm at 4 ^{o}C for 1 hr, while supernatant containing recombinant proteins was collected for purification.

2.5 Purification of *Vh*ChiA and *Vh*GlcNAcase variants

Both *Vh*ChiA and *Vh*GlcNAcase were expressed in *E. coli* M15 cells with hexahistidine tag attached at their C-terminal ends to aid purification by affinity chromatography. Purification of the recombinant proteins was carried out initially using Ni-NTA agarose resin (Qiagen, CA, USA) at 4 ^{o}C. The supernatant containing soluble proteins prepared as described in Section 2.4 was gravitationally applied onto a Ni-NTA agarose affinity column (1x5 ml, Qiagen GmbH, Hilden, Germany). The Ni-NTA agarose column was equilibrated with the equilibration buffer (20 mM Tris-HCl, pH 8.0 containing 150 mM NaCl). After sample loading, the column was washed thoroughly with the equilibration buffer, followed by the equilibration buffer containing 5 mM and 20 mM imidazole, and then eluted with 250 mM imidazole. The eluted fractions were concentrated to 5 ml using a Vivaspin-20 membrane concentrator (M$_r$ 10,000 cut-off, Vivascience AG, Hannover, Germany). The concentrated protein was further purified by gel filtration chromatography on a HiPrep 16/60 Sephacryl S-200 HR column connected to an ÄKTA purifier system (Amersham Bioscience, NJ, USA). Fractions of 2 mL were collected and analyzed by

SDS-PAGE on a 12% acrylamide gel for purity verification. The protein-containing fractions were pooled and concentrated to a small volume with the same type of the Vivaspin membrane concentrator. The final protein concentration was determined by BCA protein assay kit (EMD Chemicals, CA, USA).

The protocol for purification of *Vh*ChiA variants for transglycosylation study was modified slightly, since this part of research was carried out abroad. After the recombinant proteins were highly expressed in *E. coli* M15 cells as described in Section 2.4, the IPTG-induced cells were collected by centrifugation, re-suspended in 30 ml of 20 mM Tris-HCl, pH 8.0 containing 150 mM NaCl, and then lysed on ice using an Ultrasonic disruptor with a 1.5-cm-diameter probe. The supernatant obtained after centrifugation at 12,000 rpm for 60 min was applied to a Ni-NTA agarose affinity column (Bio-Rad Laboratories, CA, USA), washed thoroughly with 5 mM and 20 mM imidazole, and then eluted with 250 mM imidazole prepared in 20 mM Tris-HCl, pH 8.0 containing 150 mM NaCl. Then, the eluted fractions were concentrated to 5 ml using a Vivaspin-20 membrane concentrator (M_r 10,000 cut-off, Vivascience AG, Hannover, Germany). The concentrated proteins were further purified by gel filtration chromatography on a HiPrep 16/60 Sephacryl S-100 HR column connected to an FPLC purifier system (GE Healthcare, Munich, Germany). Fractions of 2 ml were collected and analyzed on SDS-PAGE for purity verification. The chitinase-containing fractions were pooled, then dialyzed with 20 mM phosphate buffer, pH 7.0, and concentrated to a small volume with the same type of the Vivaspin-20 membrane concentrator. A final protein concentration was determined by UV absorbance at 280 nm.

2.6 Time-course study of transglycosylation reaction by quantitative HPLC

A reaction mixture (100 μl) contained chitooligosaccharide substrate (6.8 mM GlcNAc$_4$, 5.5 mM GlcNAc$_5$, or 4.6 mM GlcNAc$_6$) and *Vh*ChiA (5 μM of wild-type, W570G, or D392N, 16 μM of D313A, or 8 μM of D313N) in 20 mM sodium phosphate buffer, pH 7.0. The reaction mixture was incubated at 40 $^{\circ}$C, and then an aliquot of 10 μL was transferred to a new microcentrifuge tube containing 10 μl of 0.1 M NaOH to terminate the enzymatic reaction at various times of incubation. To determine the enzymatic products, the resultant solution was immediately applied onto a gel filtration column of TSK-1 GEL G2000PW (7.5 mm × 600 mm) connected with a Hitachi L-7000 HPLC system (Hitachi Koki Co., Ltd, Tokyo, Japan). Elution was conducted with Milli-Q water at a constant flow rate of 0.3 ml/min. The oligosaccharide products in the effluent were monitored by UV absorption at 220 nm. Peak area of each GlcNAc$_n$ obtained from the elution profile was then converted into molar concentration using the standard calibration curve of the GlcNAc$_n$ (n=1-6) mixture with known concentrations.

2.7 Study of effects of azide salts on *Vh*ChiA and *Vh*GlcNAcase activity

2.7.1 Effects of sodium salts on specific hydrolyzing activity of *Vh*ChiA and *Vh*GlcNAcase

Sodium derivatives including sodium azide, sodium formate, sodium chloride, sodium acetate, and sodium nitrate were used to investigate the effects of

several salts on *Vh*ChiA and *Vh*GlcNAcase in hydrolyzing *p*NP-GlcNAc$_2$ and *p*NP-GlcNAc glycosides, respectively. The activity towards *p*NP-glycosides was determined in a 96-well microtiter plate. A 100-µl assay mixture contained 500 µM *p*NP-GlcNAc$_2$ or *p*NP-GlcNAc, 1 µg *Vh*ChiA or 3 µg *Vh*GlcNAcase and 2 M sodium derivatives in 100 mM potassium acetate, pH 5.5 or 100 mM potassium phosphate, pH 7.5. The reaction mixture was incubated at 37 $^{\circ}$C for 10 min with constant agitating, and then the enzymatic reaction was terminated by the addition of 100 µl of 3 M Na$_2$CO$_3$. The amount of *p*-nitrophenol (*p*NP) released was determined spectrophotometrically at 405 nm in a Biochrom Anthos Multiread 400 Microplate Reader (Biochrom, Cambridge, UK). The molar concentrations of *p*NP were calculated from a calibration curve constructed with *p*NP standard varying from 0-20 nmol. One unit of enzyme is defined as 1 nmol of *p*NP released in 1 min at 37 $^{\circ}$C.

The effect of sodium azide on the hydrolytic activity of *Vh*ChiA mutants D313A and D313N was measured using synthetic glycoside. The activity towards *p*NP-GlcNAc$_2$ was determined in a 96-well microtiter plate. A 100-µl assay mixture contained 500 µM *p*NP-GlcNac$_2$, 1 µg wild-type, 20 µg D313A or 10 µg D313N and 0, 0.1, 0.2, 0.5, 1.0, 1.5 or 2.0 M sodium azide in 100 mM sodium phosphate buffer, pH 7.5. The reaction mixture was incubated at 37 $^{\circ}$C for 10 min with constant agitating, and then the enzymatic reaction was terminated by the addition of 100 µl 3 M Na$_2$CO$_3$. The amount of *p*NP released was calculated as described in the previous section.

2.7.2 Time-courses analysis of sodium azide and potassium azide on *Vh*ChiA and *Vh*GlcNAcase activities

The effects of cations on the hydrolytic activities of *Vh*ChiA and *Vh*GlcNAcase were investigated using *p*NP-GlcNAc$_2$ and *p*NP-GlcNAc as substrates, respectively. The activity towards *p*NP-glycosides was determined in a 96-well microtiter plate. A 100-µl assay mixture contained 500 µM *p*NP-GlcNAc$_2$ or *p*NP-GlcNAc, 1 µg *Vh*ChiA or 3 µg *Vh*GlcNAcase and 0.1, 0.5, 1.0 or 2.0 M sodium azide or potassium azide in 100 mM potassium phosphate, pH 7.5. The reaction mixture was incubated at 37 ^{o}C for various times of 0, 2.5, 5, 10, 30, and 60 min with constant agitating, and then the enzymatic reaction was terminated by the addition of 100 µL of 3 M Na$_2$CO$_3$. The amount of *p*NP released was calculated as described in Section 2.7.1.

2.7.3 Study of buffer concentrations on *Vh*ChiA and *Vh*GlcNAcase activities

The concentrations of sodium and potassium phosphate buffers, pH 7.5 were varied to investigate the effects of different buffer concentrations on *Vh*ChiA and *Vh*GlcNAcase in hydrolyzing *p*NP-GlcNAc$_2$ and *p*NP-GlcNAc glycosides, respectively. The activity towards *p*NP-glycosides was determined in a 96-well microtiter plate. A 100-µL assay mixture contained 500 µM *p*NP-GlcNAc$_2$ or *p*NP-GlcNAc, 1 µg *Vh*ChiA or 3 µg *Vh*GlcNAcase in various concentrations (0.1, 0.5, 1.0, and 2.0 M) of sodium or potassium phosphate buffer, pH 7.5. The reaction mixture was incubated at 37 ^{o}C for 10 min with constant agitating, and then the enzymatic

reaction was terminated by the addition of 100 µl of 3M Na_2CO_3. The amount of pNP released was calculated as described in Section 2.7.1.

2.8 Time-course analysis of reversible inhibition of sodium azide on *Vh*ChiA activity

A reaction mixture (500 µl) contained 250 µg *Vh*ChiA and 2 M sodium azide in 20 mM Tris-HCl, pH 8.0, was incubated at 37 ^{o}C with shaking. After 10 min, the enzyme containing sodium azide was dialyzed with 20 mM Tris-HCl, pH 8.0 to remove sodium azide, and then the enzymatic activity was determined in a 96-well microtiter plate. The reaction mixture contained 500 µM pNP-GlcNAc$_2$ and 1 µg *Vh*ChiA (after dialysis) in 100 mM sodium phosphate buffer, pH 7.5, was incubated at 37 ^{o}C for various times of 0, 2.5, 5, 10, 30 and 60 min with constant agitating, and then terminated by the addition of 100 µl 3M Na_2CO_3. The amount of pNP released was estimated as described in Section 2.7.1. To determine whether the inhibition by azide ions was reversible or non-reversible, the enzyme containing sodium azide in 1.5 ml tube was covered with dialysis membrane, and then dialyzed in 500 ml of 20 mM Tris-HCl, pH 8.0 for 1 hr with 3 times. The enzyme activity after dialysis was compared with the enzyme activity before dialysis.

2.9 Study of sodium azide on structural integrity of *Vh*ChiA and *Vh*GlcNAcase by fluorescence spectrophotometry

The purified wild-type enzymes: *Vh*ChiA and *Vh*GlcNAcase, were investigated with different concentrations of sodium azide and sodium nitrate to see

the effects of sodium salts on the structural integrity of both enzymes. A reaction mixture (500 µl) contained 2 µg of *Vh*ChiA or 4 µg of *Vh*GlcNAcase and 0, 0.2, 0.5, 1.0, 1.5, or 3.0 M sodium azide or sodium nitrate in 20 mM Tris-HCl, pH 8.0, was pre-incubated at 25 $^{\circ}$C for 1 min with constant agitating, and then the reaction was further measured by fluorescence spectrophotometry. For the control reactions, the enzymes were heated at 100 $^{\circ}$C for 10 min or dissolved in 8 M urea in 20 mM Tris-HCl, pH 8.0 to denature the protein structures. The reactions were measured as described in previously.

The changes in intrinsic tryptophan fluorescence were directly monitored on a LS-55 fluorescence spectrometer (Perkin-Elmer, Bangkok, Thailand). The measurements were conducted at 25 °C. The excitation wavelength was 295 nm and emission intensities were collected over 300-500 nm with the excitation and emission slit widths being kept at 5 nm. Each protein spectrum was corrected for the buffer spectrum. The fluorescence intensity data were analyzed by a nonlinear regression function available in GraphPad Prism version 5.0 (GraphPad Software, California, USA).

The protein spectrum of each reaction was subtracted with the buffer that contained each sodium azide or sodium nitrate concentration.

2.10 Steady-state kinetics of inhibition

2.10.1 Kinetics of sodium azide inhibition on the hydrolytic activity of *Vh*ChiA

Inhibitory effects on kinetic properties of *Vh*ChiA were investigated using *p*NP-GlcNAc$_2$ as the substrate. A reaction mixture (100 µl) prepared in a 96-

well microtiter plate and contained 0-800 μM pNP-GlcNAc$_2$, 1 μg VhChiA and different concentrations of sodium azide (0, 0.5, 1.0, 1.5 and 2.0 M) in 100 mM sodium phosphate buffer, pH 7.5. The reaction mixture was incubated at 37 °C for 10 min with constant agitating, and then terminated by the addition of 100 μl of 3 M Na$_2$CO$_3$. The amount of pNP released was estimated as described in Section 2.6.1. The kinetic parameters (V_{max}, K_m and k_{cat}) were evaluated from the experiments carried out in triplicate using the nonlinear regression function available in GraphPad Prism version 5.0 (GraphPad Software, California, USA). Type of inhibition was assessed from Lineweaver-Burk plots (also available in GraphPad Prism version 5.0). For K_i and αK_i values were determined from Dixon plot of sodium azide concentrations against slope of Lineweaver-Burk plots and inverse V_{max} apparent of Michaelis-Menten plots, respectively. The K_i suggests the affinity between inhibitor and free enzyme whereas the αK_i suggests the affinity between inhibitor and enzyme-substrate complex.

2.10.2 Kinetics of sodium azide and sodium nitrate inhibitions on the hydrolytic activity of VhGlcNAcase

Inhibitory effects on kinetic properties of VhGlcNAcase were investigated using pNP-GlcNAc as the substrate. A reaction mixture (100 μl) prepared in a 96-well microtiter plate and contained 0-800 μM of pNP-GlcNAc, 3 μg of VhGlcNAcase and different concentrations of sodium azide or sodium nitrate (0, 0.3, 0.4, 0.5 and 0.6 M) in 100 mM sodium phosphate buffer, pH 7.5. The reaction mixture was incubated at 37 °C for 10 min with constant agitating, and then terminated by the addition of 100 μl 3 M Na$_2$CO$_3$. The amount of pNP released was

estimated as described in Section 2.10.1. The kinetic parameters (V_{max}, K_m and k_{cat}) were obtained from the nonlinear regression function and types of inhibition were assessed from Lineweaver-Burk plots available in GraphPad Prism version 5.0 (GraphPad Software, California, USA). The K_i values of sodium azide and sodium nitrate were determined as described in Section 2.7.1.

2.11 Determination of IC$_{50}$ values

Dose-response curves representing sodium azide inhibition on the hydrolytic activity of *Vh*ChiA were determined using *p*NP-GlcNAc$_2$ as substrate. A reaction mixture (100 μL) prepared in a 96-well microtiter plate contained 500 μM *p*NP-GlcNAc$_2$, 1 μg *Vh*ChiA and varied concentrations of sodium azide with a two-fold dilution series to obtain a concentration range of 0-4 M in 100 mM sodium phosphate buffer, pH 7.5. The reaction mixture was incubated at 37 ^{o}C for 10 min with constant agitating, and then terminated by the addition of 100 μl 3 M Na$_2$CO$_3$. The enzyme activity was estimated from the liberated *p*NP, which is quantitated as described in Section 2.6.1. The IC$_{50}$ value of sodium azide was obtained from the plot of logarithmic values of sodium azide concentrations versus the ratio of the initial velocity of the enzyme in the presence of sodium azide at concentration and the initial velocity of the enzyme in the absence of sodium azide in GraphPad Prism version 5.0. (GraphPad Software, California, USA).

Dose-response curves representing sodium azide and sodium nitrate inhibitions on the hydrolytic activity of *Vh*GlcNAcase were carried out using *p*NP-GlcNAc as substrate. The reaction mixture (100 μl) prepared in a 96-well microtiter plate contained 500 μM *p*NP-GlcNAc, 3 μg *Vh*GlcNAcase and varied concentrations

of sodium azide or sodium nitrate with a two-fold dilution series to obtain a concentration range of 0-4 M in 100 mM sodium phosphate buffer, pH 7.5. The reaction mixture was incubated at 37 $^{\circ}$C for 10 min with constant agitating, and then terminated by the addition of 100 μl 3 M Na_2CO_3. The amount of *p*NP released was estimated as described in Section 2.7.1 and the IC_{50} values of sodium azide and sodium nitrate were obtained as described in previously.

2.12 Time-course analysis of the hydrolytic products of *Vh*ChiA and *Vh*GlcNAcase by TLC (thin-layer chromatography)

The inhibition of sodium azide on hydrolysis of $GlcNAc_6$ by *Vh*ChiA was carried out in a 20 μL reaction mixture that contained 2.5 mM $GlcNAc_6$, 1 μg *Vh*ChiA and 2 M sodium azide in 100 mM phosphate buffer, pH 7.5. The reaction mixture was incubated at 37 $^{\circ}$C for various times of 2, 5, 10, 15, 30, 60 and 180 min before termination by boiling at 100 $^{\circ}$C for 5 min. For product analysis, each reaction mixture was applied five times (1 μl each) to a TCL Silica gel 60 F_{254} Aluminum sheet (10 cm x 10 cm) (Merck, Berlin, Germany), and then chromatographed three times (1 h each) in a mobile phase containing *n*-butanol: methanol: 28% ammonia solution: H_2O (10:8:4:2) (v/v), followed by spraying with aniline-diphenylamine reagent and baking at 180 $^{\circ}$C for 3 min. The inhibitions of sodium azide and sodium nitrate on hydrolysis of $GlcNAc_2$ and $GlcNAc_4$ by *Vh*GlcNAcase were further studied under the same condition with varied time points of 2, 5, 10, 15, 30, 60, 180 min and 18 h.

For time-course of colloidal chitin hydrolysis, the reaction mixture (400 μL) contained 5% (w/v) colloidal chitin, 10 μg *Vh*ChiA and 2 M sodium azide in 100 mM

phosphate buffer, pH 7.5. After incubation at 37 $^{\circ}$C with shaking at 350 rpm for variable times of 2, 5, 10, 15, 30, 60, 180 min and 18 h, the reaction mixture was centrifuged to precipitate the remaining chitin. Then, the degradation products were analyzed by TLC as described for GlcNAc$_{2-6}$ hydrolysis.

CHAPTER III

RESULTS

3.1 Mutation strategies for obtaining chitooligosaccharides with longer chains by transglycosylation reaction of a family GH18 chitinase A from *Vibrio harveyi*

3.1.1 Mutation targets

To enhance the transglycosylation (TG) activity, two strategies were proposed: (1) enhancing the acceptor binding ability (Umemoto, Ohnuma, Mizuhara, Sato, Skriver, and Fukamizo, 2013) and (2) suppressing the attack of a nucleophilic water molecule to the transition state (Hurtado-Guerrero, Schuttelkopf, Mouyna, Ibrahim, Shepherd, Fontaine, Latge, and van Aalten, 2009; Zakariassen *et al*., 2011). Since the acceptor binding site (+1 and +2) of wild type enzymes are evolutionarily optimized for efficiently accepting their natural substrates, the mutations introduced into the acceptor binding site usually reduce the acceptor binding ability. Thus, mutations for enhancing the binding ability are quite difficult. In the former studies, mutations were introduced into the glycon-binding site (-2 and -1) to suppress the sugar binding ability of the negatively-numbered subsites. The suppression of the sugar-binding to the negatively numbered subsites may relatively enhance the binding ability toward the positively-numbered subsites (acceptor-binding site) (Aronson *et*

al., 2006; Fukamizo, Goto, Torikata, and Araki, 1989). In fact, mutation of Trp168 (subsite -3) of *Serratia marcescens* chitinase A enhanced the TG activity (Aronson *et al*., 2006). Here, we tried to mutate Trp570, which is responsible for the sugar-residue binding at subsites -1 and -2 (Figure 3.1.1) to glycine (Songsiriritthigul *et al*., 2008; Suginta *et al*., 2007). Asp392, which is supposed to be responsible for the acceptor-binding at subsites +1 and +2 (Figure 3.1.1), was also mutated to asparagine, which may facilitate hydrogen binding interaction with the sugar residue (Songsiriritthigul *et al*., 2008). In addition to these mutations, we also mutated the middle aspartic acid residue (Asp313) in the DxDxE catalytic motif (Figure 3.1.1), because this mutation was reported to significantly enhance the TG activity of *S. marcescens* chitinases (Martinez *et al*., 2012; Zakariassen *et al*., 2011).
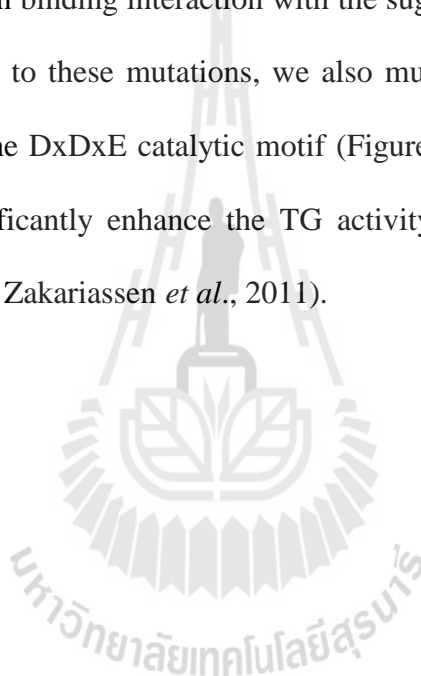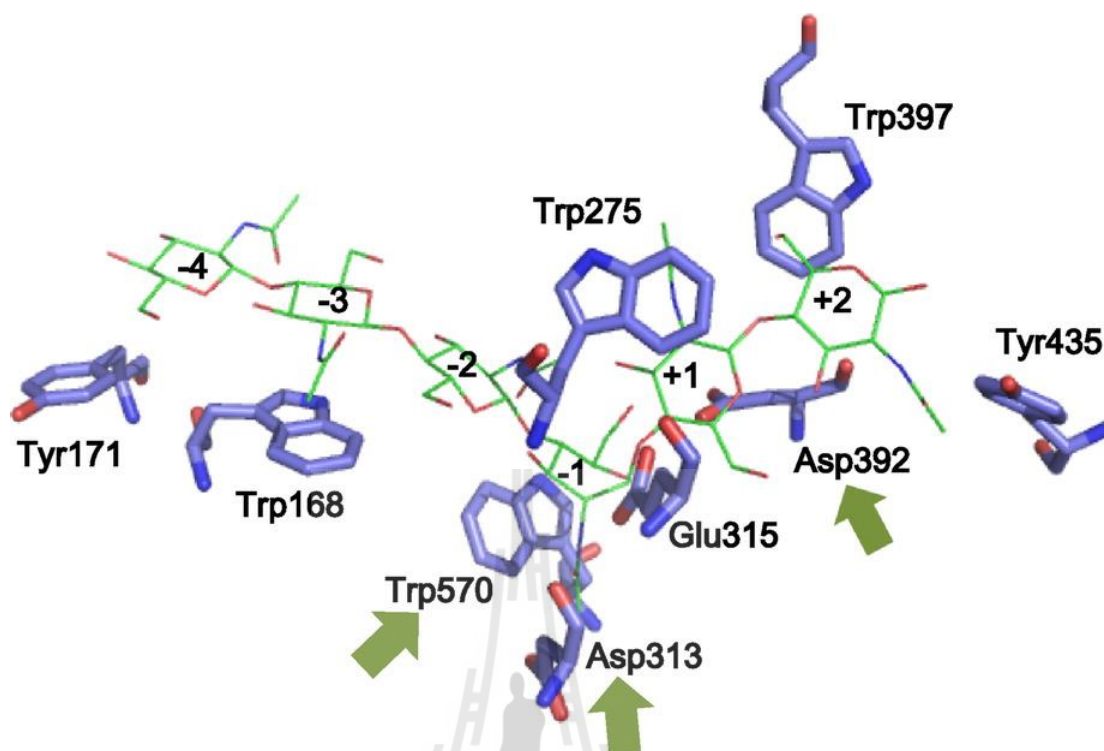
Figure 3.1.1 Superimposition of the active site structure of ligand-free wild-type *Vh*ChiA and *Vh*ChiA E315M mutant complexed with GlcNAc$_6$ (only GlcNAc$_6$ shown as green; PDB code, 3B9A). GlcNAc-binding subsites are indicated by integers based on the nomenclature suggested by Davies *et al.*, 1997 (Davies, Wilson, and Henrissat, 1997). The amino acid residues presented as the stick model are important for chitooligosaccharide binding. The structure of ligand-free wild-type *Vh*ChiA was obtained from the PDB database (PDB code, 3B8S) (Songsiriritthigul *et al.*, 2008) and displayed by the program PyMol (http://www.pymol.org/). The arrows indicate the mutation targets.

3.1.2 Time-courses of chitooligosaccharide degradation catalyzed by wild-type *Vh*ChiA

We first evaluated TG activity of the wild-type *Vh*ChiA (WT). Incubation of WT with the $GlcNAc_4$ substrate produced $GlcNAc_2$ as the major hydrolytic product after 3 h of reaction (Figure 3.1.2A). A small but significant amount of $GlcNAc_3$ was also produced after 3 h, but no GlcNAc was detected at all. From the $GlcNAc_5$ substrate, $GlcNAc_2$ and $GlcNAc_3$ were formed as the major hydrolytic products, and a trivial amount of $GlcNAc_4$ was also formed at 2 h (Figure 3.1.2B). The $GlcNAc_4$ formation from $GlcNAc_5$ was not accompanied by GlcNAc formation. The $GlcNAc_3$ product from $GlcNAc_4$ and the $GlcNAc_4$ product from $GlcNAc_5$ were not derived from a simple hydrolysis of the initial substrates. Aronson *et al*., 2006 reported a similar hydrolytic profile obtained by *Serratia marcescens* chitinase A. Plant class V chitinase from cycad also exhibited a similar reaction profile (Taira, Fujiwara, Dennhart, Hayashi, Onaga, Ohnuma, Letzel, Sakuda, and Fukamizo, 2010). Both reports explained that $GlcNAc_3$ is produced from initial substrate $GlcNAc_4$ through the TG product $GlcNAc_6$, as shown in Figure 3.1.3 $GlcNAc_4$ was first hydrolyzed into $GlcNAc_2$ + $GlcNAc_2$ (Step I). After the latter $GlcNAc_2$ is released from the enzyme, the acceptor $GlcNAc_4$ binds to the acceptor-binding site (the positively-numbered subsites) (Step IIb), and then attacks the oxazolinium ion intermediate at subsite -1, producing $GlcNAc_6$ as the TG product (Step III). The $GlcNAc_6$ produced is relocated to the more stable binding mode (-3, -2, -1, +1, +2) (Step IV), and hydrolyzed into $GlcNAc_3$ + $GlcNAc_3$ (Step V). In the case of the initial substrate $GlcNAc_5$, WT produced $GlcNAc_2$ and $GlcNAc_3$ and a small amount of $GlcNAc_4$ at 2 hr. Since $GlcNAc_5$ is assumed to act as an acceptor

molecule as well as a substrate in the mechanism shown in Figure 3.1.3, GlcNAc$_4$ is most likely produced through the TG product GlcNAc$_7$. Thus, we concluded that the WT enzyme has a very low TG activity. From the initial substrate GlcNAc$_6$, WT produced GlcNAc$_2$, GlcNAc$_3$, and GlcNAc$_4$ (Figure 3.1.2C). No evidence for TG reaction was obtained from the reaction toward GlcNAc$_6$. The result suggested that WT not only catalyzes the hydrolysis of the chitooligosaccharide substrates, but also catalyzes TG reaction much less efficiently with the substrates GlcNAc$_4$ and GlcNAc$_5$.
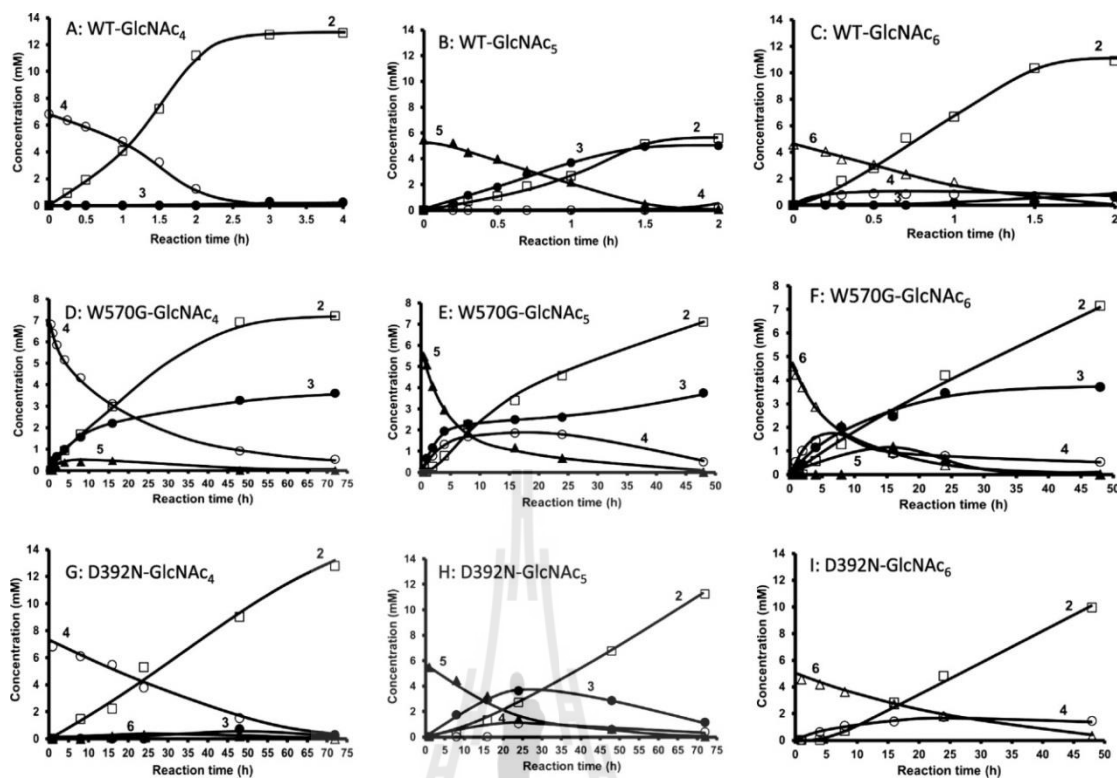
Figure 3.1.2 Reaction time courses of the wild-type and mutated *Vh*ChiA toward chitooligosaccharide substrates GlcNAc$_{4-6}$. The wild-type *Vh*ChiA (5 μM) was incubated with 6.8 mM GlcNAc$_4$ (A), 5.5 mM GlcNAc$_5$ (B), or 4.6 mM GlcNAc$_6$ (C), W570G *Vh*ChiA (5 μM) was incubated with 6.8 mM GlcNAc$_4$ (D), 5.5 mM GlcNAc$_5$ (E), or 4.6 mM GlcNAc$_6$ (F). D392N *Vh*ChiA (5 μM) was incubated with 6.8 mM GlcNAc$_4$ (G), 5.5 mM GlcNAc$_5$ (H), or 4.6 mM GlcNAc$_6$ (I). Individual reactions were conducted in 20 mM phosphate buffer, pH 7.0 at 40 ^{o}C. The products were analyzed by gel-filtration HPLC at various times of incubation. Numbers represent the degree of polymerization. Symbols are open squares, GlcNAc$_2$; black squares, GlcNAc$_3$; open circles, GlcNAc$_4$; black triangles, GlcNAc$_5$; o, GlcNAc$_6$.
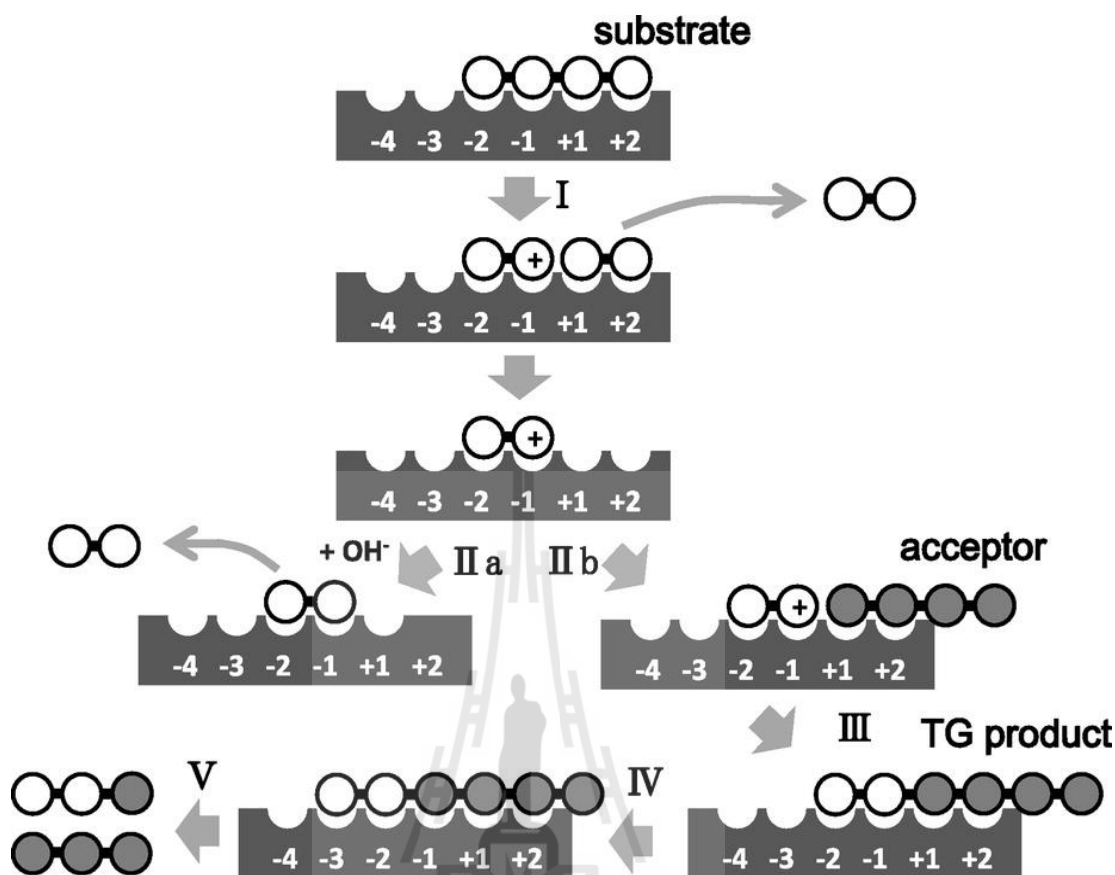
Figure 3.1.3 The reaction scheme for hydrolysis/TG catalyzed by *Vh*ChiA with GlcNAc$_4$ substrate. Step I: Bond cleavage; GlcNAc$_4$ binds to the -2 to $+2$ subsites and the glycosidic linkage located between the -1 and $+1$ subsites is cleaved by the action of Glu315 to form GlcNAc$_2$ with an oxazolinium ion intermediate at subsites -2 and -1 and the intact GlcNAc$_2$ product at subsites $+1$ and $+2$, which will diffuse away. Step IIa: Hydration; a water molecule attacks the C1 carbon of the oxazolinium ion intermediate to release the product of GlcNAc$_2$. Steps IIb and III: Acceptor binding and formation of glycosidic linkage; an incoming GlcNAc4 attacks the intermediate instead of a water molecule to form a new glycosidic linkage, producing the TG product of GlcNAc$_6$. Step IV: Shifting the binding mode of GlcNAc$_6$ to subsites -3 to +2. Step V: the newly formed GlcNAc$_6$ is then hydrolyzed to form two

molecules of GlcNAc$_3$. GlcNAc residues are represented by open circles, an incoming of GlcNAc$_4$ molecule is represented by grey circles, the oxazolinium ion intermediate is represented by positive signs in open circles and the binding subsites of the enzyme given as integers based on the nomenclature suggested by Davies *et al.*, 1997. Formation of the TG products by the mutants *Vh*ChiA D313A and D313N is represented from Step I to Step III, while the additional steps (Step IV and Step V) should be introduced for the reactions catalyzed by the mutants W570G and D392N.

3.1.3 Time courses of chitooligosaccharide degradation catalyzed by the W570G mutant

The hydrolytic activities of mutant W570G toward the substrates GlcNAc$_{4-6}$ were much less than those of WT (Figures 3.1.2D, 3.1.2E, and 3.1.2F), and the results were consistent with the specific activity data reported previously (Suginta *et al.*, 2007). However, a considerable amount of GlcNAc$_3$ was produced in addition to GlcNAc$_2$ from the initial substrate GlcNAc$_4$ (Figure 3.1.2D). The GlcNAc$_3$ produced was clearly derived from the mechanism shown in Figure 3.1.3, because no GlcNAc was found in the products. GlcNAc$_5$, which may be derived from the TG reaction between the donor GlcNAc$_2$ and the acceptor GlcNAc$_3$, was also detected in the early stage of the reaction. The productions of GlcNAc$_3$ and GlcNAc$_5$ indicate that TG activity was significantly enhanced in W570G. The time-course profiles of mutant W570G with GlcNAc$_5$ substrate (Figure 3.1.2E) showed that GlcNAc$_2$ and GlcNAc$_3$ were the major hydrolytic products. GlcNAc$_4$ was also produced without formation of GlcNAc, and the maximum level of GlcNAc$_4$ was approximately 2 mM at 16 h of incubation. GlcNAc$_4$ was then gradually degraded to GlcNAc$_2$, and only 0.5 mM

remained at 48 h. The $GlcNAc_4$ product may be derived from the mechanism shown in Figure 3.1.3, where the substrate and the acceptor molecules should be replaced with $GlcNAc_5$. Mutant W570G hydrolyzed $GlcNAc_6$ substrate to $GlcNAc_2$, along with $GlcNAc_3$ and $GlcNAc_4$ (Figure 3.1.2F). $GlcNAc_5$ was also detected, but GlcNAc was not. Thus, the $GlcNAc_5$ product may be produced through the TG product $GlcNAc_8$ as shown in Figure 3.1.3, where the substrate and the acceptor molecules should be replaced with $GlcNAc_6$. The results obtained from this set of experiments suggested that mutation of Trp570 located in between subsites -2 and -1 strongly enhanced TG activity, but the TG products obtained from the mutant W570G were only temporarily formed, and then further degraded.

3.1.4 Time-courses of chitooligosaccharide degradation catalyzed by the D392N mutant

The D392N mutant produced $GlcNAc_2$ as a major product from $GlcNAc_4$ substrate, while a small amount of $GlcNAc_3$ was produced as shown in Figure 3.1.2G, probably through the mechanism shown in Figure 3.1.3. The $GlcNAc_3$ production was slightly enhanced in the D392N mutant, when compared with that in WT (Figure 3.1.2A). The D392N mutant hydrolyzed $GlcNAc_5$ substrate, yielding $GlcNAc_2$ and $GlcNAc_3$ as the major end products (Figure 3.1.2H). The enhanced formation of $GlcNAc_4$ was found in the reaction catalyzed by D392N. Since the $GlcNAc_4$ formation was not accompanied by GlcNAc formation, the tetramer was most likely derived from the mechanism shown in Figure 3.1.3, where the substrate and the acceptor molecules should be replaced with $GlcNAc_5$. With $GlcNAc_6$ substrate, $GlcNAc_2$ and $GlcNAc_4$ were the major hydrolytic products (Figure 3.1.2I),

while no other products was detected. These results suggested that mutation of Asp392, which is involved in sugar residue binding at subsites +1 and +2 (Figure 3.1.1), to asparagine enhanced the TG activity of *Vh*ChiA with the substrates GlcNAc$_4$ and GlcNAc$_5$, but not with the substrate GlcNAc$_6$.

3.1.5 Mutation of Asp313 is the most effective for obtaining chitooligosaccharides with longer chains

Asp313 is an essential residue located at the middle of the catalytic DxDxE motif (Asp311-x-Asp313-x-Glu315), and plays multiple roles in the catalytic cycle of chitin degradation by *Vh*ChiA (Suginta *et al*., 2012). Mutation of Asp313 to alanine (D313A) abolished the hydrolytic activity of the enzyme almost completely, while mutation of Asp313 to asparagine (D313N) retained slight hydrolytic activity. HPLC profiles of the products from incubation of the mutant D313A or D313N with GlcNAc$_4$ substrate indicated that a significant amount of GlcNAc$_6$ as the TG product was generated in addition to the major hydrolytic product GlcNAc$_2$ after 120 h of incubation, as shown in Figure 3.1.4B and 3.1.4C. In contrast, no GlcNAc$_6$ was found in the chromatogram for WT (Figure 3.1.4A). In the reactions catalyzed by D313A and D313N, the TG product GlcNAc$_6$ was not hydrolyzed into GlcNAc$_3$. Similarly, when GlcNAc$_6$ was incubated with the Asp313 mutants, a significant amount of GlcNAc$_8$, which was produced by the TG reaction between the donor GlcNAc$_2$ and the acceptor GlcNAc$_6$, was detected by HPLC (Figure 3.1.5B and 3.1.5C). WT did not produce GlcNAc$_8$ at all (Figure 3.1.5A). The chain length of the TG product, GlcNAc$_8$, was confirmed based on the theoretical retention time obtained by the simulation of the gel-filtration profile (Fukamizo *et al*., 1989). The donor for the TG

reaction appears to be GlcNAc$_2$, because *Vh*ChiA hydrolyzes most frequently the second β-1,4-glycosidic linkage from the non-reducing end of chitooligosaccharide substrates (Suginta, Pantoom, and Prinz, 2009). Thus, from the substrate GlcNAc$_5$, the Asp313 mutants may produce GlcNAc$_7$ by the TG reaction between the donor GlcNAc$_2$ and the acceptor GlcNAc$_5$.
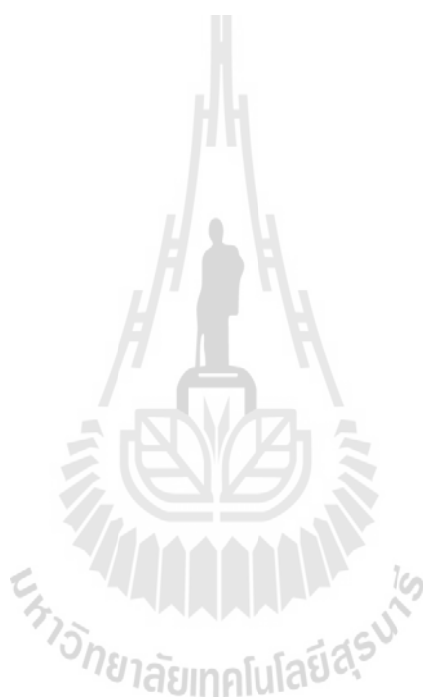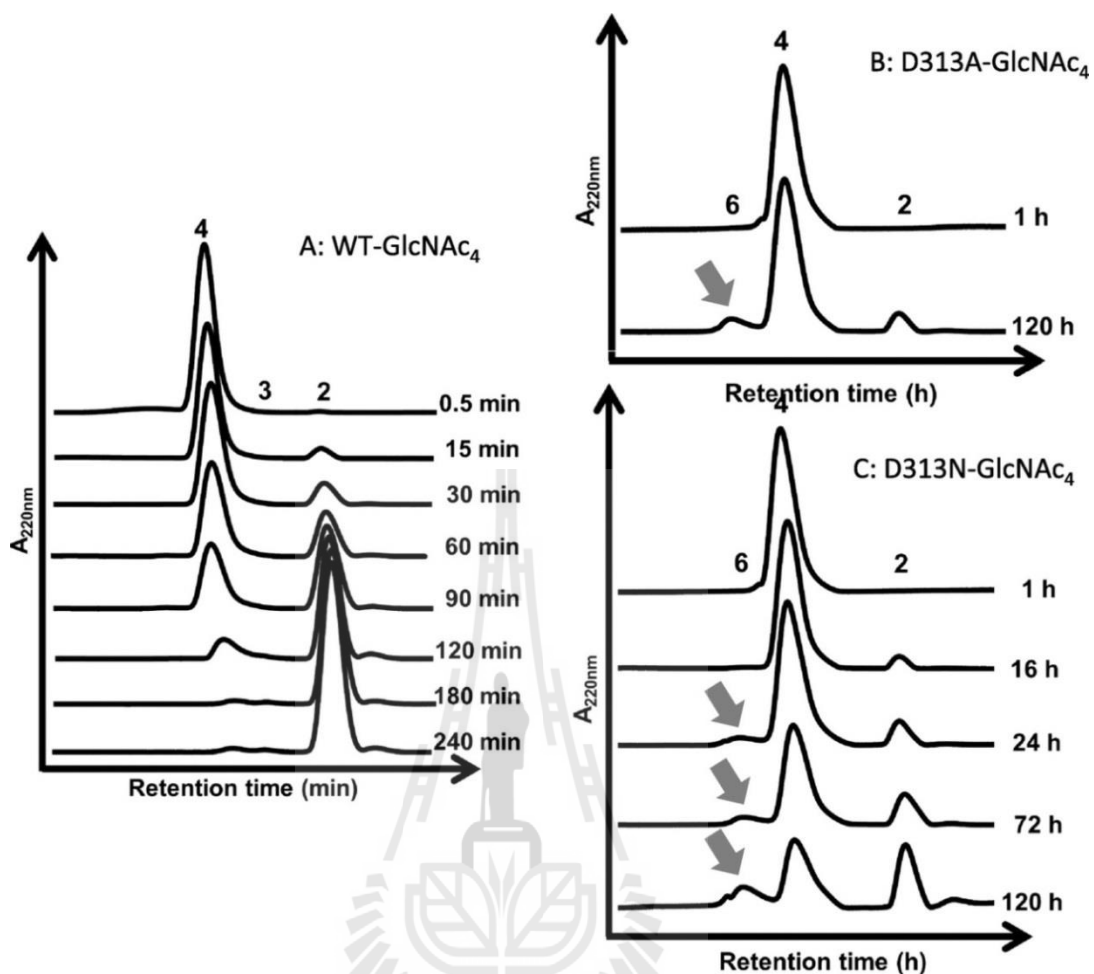
Figure 3.1.4 HPLC profiles showing the reaction of the wild type (A) and the mutants D313A (B) and D313N (C) *Vh*ChiA. A reaction mixture containing 6.8 mM GlcNAc$_4$ and the enzyme (5 μM wild type, 16 μM D313A, or 8 μM D313N) in 20 mM phosphate buffer, pH 7.0, was incubated at various times at 40 $^{\circ}$C. The reaction products were analyzed by gel-filtration HPLC. The TG product GlcNAc$_6$ is designated by arrow.
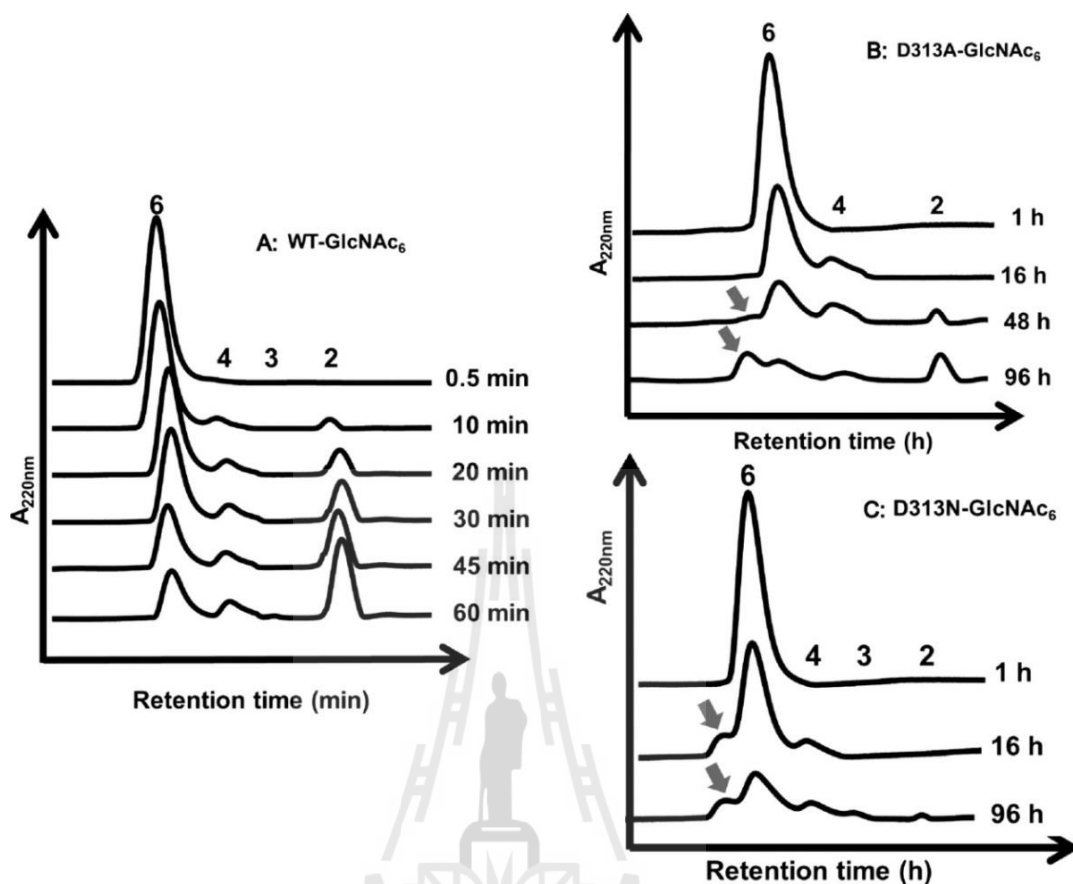
Figure 3.1.5 HPLC profiles showing the reaction of the wild type (A) and the mutants D313A (B) and D313N (C) *Vh*ChiA. A reaction mixture containing 4.6 mM GlcNAc$_6$ and the enzyme (5 μM wild type, 16 μM D313A, or 8 μM D313N) in 20 mM phosphate buffer, pH 7.0, was incubated at various times at 40 $^{\circ}$C. The reaction products were analyzed by gel-filtration HPLC. The TG product GlcNAc$_8$ is indicated by arrow.

3.2 Kinetics of inhibition of family-18 chitinase A from *Vibrio harveyi* by sodium azide

3.2.1 Effects of sodium salts on the hydrolytic activity of wild-type *Vh*ChiA

Sodium salts of azide, formate, acetate, nitrate, and chloride (Figure 3.2.1) were used to investigate the effects of sodium salts on the enzyme activity of WT *Vh*ChiA against pNP-GlcNAc$_2$ substrate at pH 5.5 and 7.5. The reactions were monitored at 37 $^{\circ}$C for 10 min. All sodium salts significantly decreased the specific activity of the enzyme, with the inhibitory effects being greater when the reaction was set at pH 7.5, compared to pH 5.5. At 5.5, sodium formate showed the greatest inhibition on the enzyme activity, while sodium azide the greatest inhibition at 7.5. Effects of sodium salts on chitinase activity are summarized in Table 3.2.1. For further study, we chose sodium azide at pH 7.5 to study the kinetics of inhibition on WT *Vh*ChiA, since sodium azide showed the most strong inhibition effect.

Na^+ $N^- = N^+ = N^-$ Sodium azide (NaN_3)

Sodium formate (HCOONa)

Sodium acetate (CH_3COONa)

Sodium nitrate ($NaNO_3$)

Sodium chloride (NaCl)
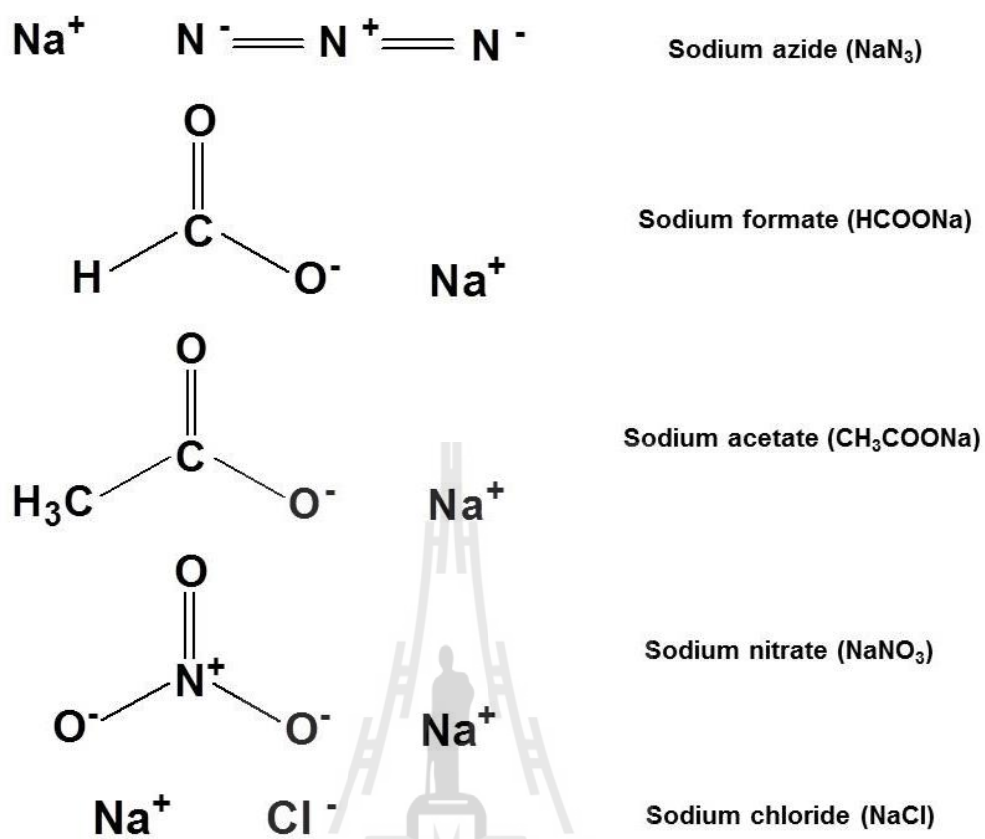
Figure 3.2.1 Chemical structures of sodium azide, sodium formate, sodium acetate, sodium nitrate, and sodium chloride.

Table 3.2.1 Specific activity of wild-type *Vh*ChiA with 2 M sodium salts against

pNP-GlcNAc$_2$ substrate

Sodium derivatives	Specific activity (nmol/min/µg)	
	pH 5.5	pH 7.5
No sodium salts	1.60 ± 0.03 (100)	1.60 ± 0.02 (100)
NaN$_3$	1.40 ± 0.02 (88)	0.50 ± 0.02 (31)
HCOONa	0.90 ± 0.03 (56)	0.80 ± 0.02 (50)
CH$_3$COONa	1.70 ± 0.06 (106)	1.10 ± 0.04 (69)
NaCl	1.30 ± 0.08 (81)	1.00 ± 0.06 (63)
NaNO$_3$	2.40 ± 0.09 (150)	1.30 ± 0.02 (81)

3.2.2 Effects of sodium and potassium cations on the hydrolytic activity of wild-type *Vh*ChiA

To investigate the effects of cations (Na$^+$ and K$^+$) of azide compounds on the hydrolytic activity of WT *Vh*ChiA, time courses of pNP-GlcNAc$_2$ hydrolysis with 2 M sodium azide, 2 M potassium azide, and without the azide compounds were performed in 100 mM potassium phosphate buffer, pH 7.5 (Figure 3.2.2). The hydrolytic activity of WT *Vh*ChiA was shown to be significantly decreased in the reactions, containing sodium azide and potassium azide, compared to the reaction without azide compounds. Potassium ion was shown to have slightly stronger inhibitory effect than sodium ion at 2 M.
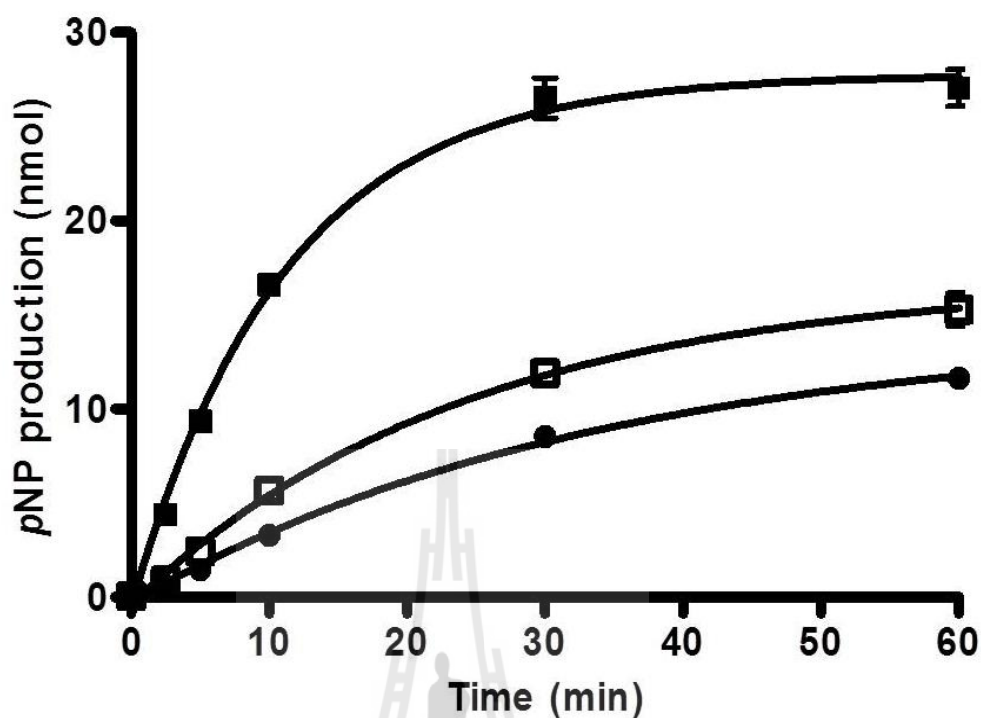
Figure 3.2.2 Time courses of wild-type *Vh*ChiA with and without sodium azide and potassium azide were investigated using *p*NP-GlcNAc$_2$ substrate. A reaction mixture (100 μl), containing 1 μg of *Vh*ChiA and 500 μM of *p*NP-GlcNAc$_2$ without sodium cation (filled squares), with 2 M sodium azide (open squares), or with 2 M potassium azide (filled circles) and 100 mM potassium phosphate buffer, pH 7.5, was incubated at 37 °C for 0, 2.5, 5, 10, 30, and 60 min. The reaction was terminated with 100 μl of 3 M Na$_2$CO$_3$. Release of *p*NP, monitored at A$_{405}$, was converted to molar quantities using a calibration curve of *p*NP (0-20 nmol).

3.2.3 Effects of sodium and potassium phosphate buffer, pH 7.5 on the hydrolytic activity of wild-type *Vh*ChiA

From the results of the previous section suggested that sodium and potassium cations inhibited the enzyme activity of WT *Vh*ChiA. In this experiment, we investigated the effects of rate of sodium and potassium phosphate buffer, pH 7.5 on the WT *Vh*ChiA activity against pNP-GlcNAc$_2$ substrate. The reactions were measured at 37 $^{\circ}$C for 10 min. The specific activity of the enzyme in sodium phosphate buffer was slightly higher than that in potassium phosphate buffer (Table 3.2.2). For the buffer concentrations, the reactions in 2 M phosphate buffer displayed lower specific activity of the enzyme than 0.1, 0.5, and 1.0 M phosphate buffer whereas the reactions in 0.1 M sodium and potassium phosphate buffers showed the highest activity of WT *Vh*ChiA (Table 3.2.2). The results suggested that 0.1 M sodium and potassium phosphate buffers, pH 7.5 showed the maximum activity. So, we chose this concentration to study the kinetics of inhibition on WT *Vh*ChiA.

Table 3.2.2 Specific activity of wild-type *Vh*ChiA against *p*NP-GlcNAc$_2$ substrate in various concentrations of sodium and potassium phosphate buffers, pH 7.5.

Concentration of phosphate buffer, pH 7.5 (M)	Specific activity (nmol/min/µg)	
	Sodium phosphate buffer, pH 7.5	Potassium phosphate buffer, pH 7.5
0.1	1.80 ± 0.04	1.60 ± 0.10
0.5	1.60 ± 0.10	1.40 ± 0.10
1.0	1.50 ± 0.04	1.40 ± 0.02
2.0	0.90 ± 0.04	0.60 ± 0.10

3.2.4 Effect of sodium azide on reversible inhibition of wild-type *Vh*ChiA

The effect of sodium azide on reversible inhibition of WT *Vh*ChiA was evaluated. After 2 M sodium azide was added to the reaction mixture, the remaining *Vh*ChiA activity was determined before dialysis and after dialysis. The results as shown in Figure 3.2.3, the chitinase activity was higher after dialysis than that before dialysis. In contrast, the enzyme without sodium azide that used as a control showed that the *p*NP product obtained from *p*NP-GlcNAc$_2$ degradation by *Vh*ChiA before and after dialysis were similar. The results suggested that dialysis did not cause a loss of the chitinase activity and sodium azide acted as reversible inhibitor (Figure 3.2.3).
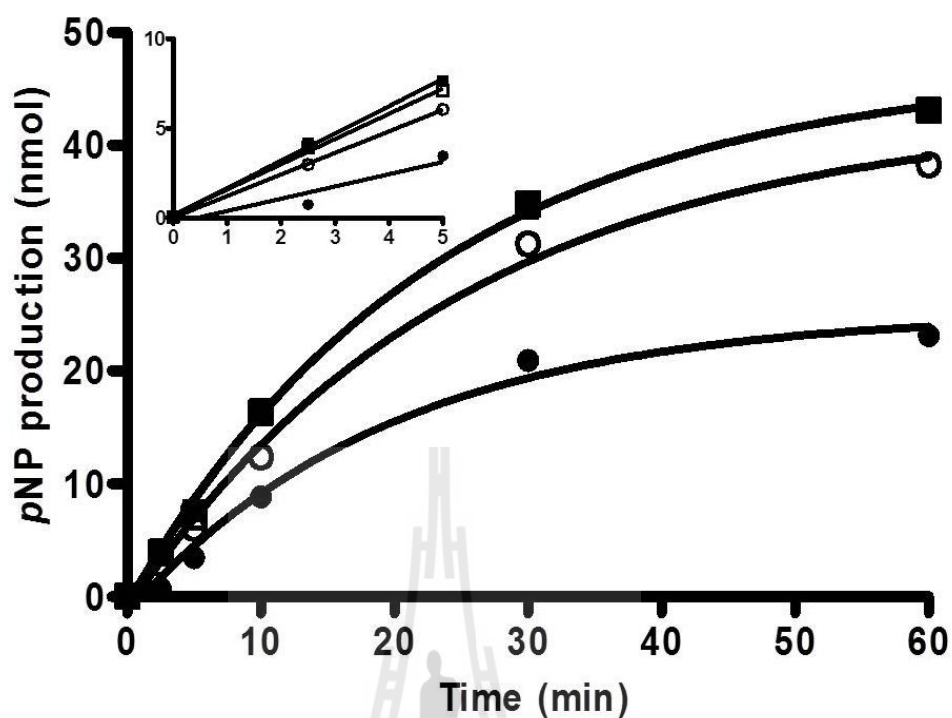
Figure 3.2.3 Reversible inhibition of wild-type *Vh*ChiA against *p*NP-GlcNAc$_2$ by sodium azide. Reaction time-courses of *Vh*ChiA without sodium azide before dialysis (black squares) and after dialysis (open squares) and *Vh*ChiA with 2 M sodium azide before dialysis (black circles) and after dialysis (open circles), a reaction mixture contained 1 μg *Vh*ChiA with or without sodium azide before and after dialysis, 500 μM *p*NP-GlcNAc$_2$ in 100 mM sodium phosphate buffer, pH 7.5. The initial rates (v_0) of the reactions were shown in an inset.

3.2.5 Effect of sodium azide on molecular structure of wild-type *Vh*ChiA

To investigate the effect of sodium azide on the molecular structure of WT *Vh*ChiA, fluorescence spectra were obtained in the presence of sodium azide, and the changes in the fluorescence intensity, as well as the shift in the maximum emission wavelength were monitored. The emission spectra were collected from 300-

500 nm upon excitation at 295 nm. The fluorescence intensity of *Vh*ChiA decreased with increasing concentrations of sodium azide from 0 to 3 M but no shift in the maximum emission wavelength were observed (Figure 3.2.4). On the other hand, the enzymes that were denatured by 8 M urea and heat at 100 ^{o}C for 10 min showed increases in fluorescence intensity, as compared to that of the non-denatured enzyme (Figure 3.2.4). The results suggested that sodium azide has effect to partially unfold the secondaly structure of *Vh*ChiA.
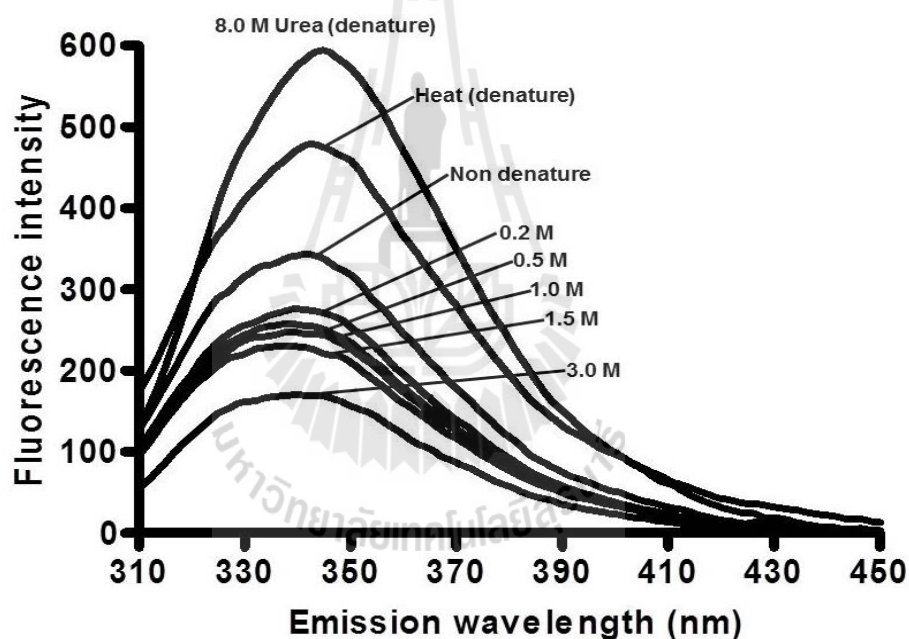
Figure 3.2.4 Effect of sodium azide on structural integrity of wild-type *Vh*ChiA. The *Vh*ChiA was investigated using fluorescence spectroscopy. The emission spectra were collected from 300-500 nm upon excitation at 295 nm.

3.2.6 Kinetics of inhibition of sodium azide on the hydrolytic activity of wild-type *Vh*ChiA

Kinetic experiments were carried out to define the inhibition type. *p*NP-GlcNAc$_2$ hydrolysis with or without 2 M sodium azide (Figure 3.2.5A) were performed to determine the initial rates (v_0) of WT *Vh*ChiA within the incubation period of 10 min. Figure 3.2.5B presents the non-linear (Michaelis-Menten) plots between v_0 and *p*NP-GlcNAc$_2$ concentrations. Different curve fits were obtained in various concentrations of sodium azide (0, 0.5, 1.0, 1.5 and 2.0 M), yielding the kinetic parameters, the apparant values of k_{cat}, K_m, and k_{cat}/K_m as presented in Table 3.2.3. The kinetic parameters were obtained by data-fitting based on the Michaelis-Menten equation or the substrate inhibition equation (Equation 3.2.1).

$$v_0 = \frac{V_{max}[S]}{K_m\left(1+\frac{[I]}{K_i}\right)+[S]\left(1+\frac{[I]}{\alpha K_i}\right)}$$

(3.2.1)

Where I is sodium azide and S is *p*NP-GlcNAc$_2$ substrate

The catalytic rate constant (k_{cat}) of the enzyme decreased with increase in the concentrations of sodium azide (2.4, 1.9, 1.2, 0.8 and 0.6 s^{-1} k_{cat} at 0, 0.5, 1.0, 1.5 and 2.0 M sodium azide, respectively). Likewise, the apparent K_m was found to be decrease from 196 to 83 μM, with increase in the concentration of sodium azide (Table 3.2.3). k_{cat} and K_m obtained from the data agrees with the mixed-type inhibition. This appears later.
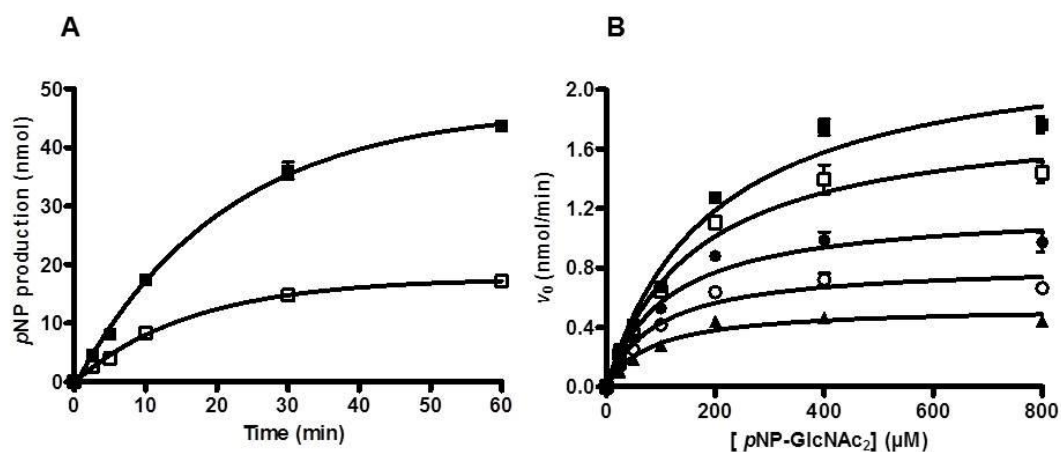
Figure 3.2.5 Kinetic properties of wild-type *Vh*ChiA were investigated using *p*NP-GlcNAc$_2$ substrate.

(A) Time-course of *p*NP-GlcNAc$_2$ hydrolysis by *Vh*ChiA. A reaction mixture (100 μl), containing 1 μg *Vh*ChiA and 500 μM *p*NP-GlcNAc$_2$ without sodium azide (filled squares) or with 2 M sodium azide (open squares) in 100 mM sodium phosphate buffer, pH 7.5, was incubated at 0, 2.5, 5, 10, 30 and 60 min at 37 $^{\circ}$C, and then the reaction was terminated with 100 μl of 3 M Na$_2$CO$_3$. Release of *p*NP, monitored at A$_{405}$, was converted to molar quantities using a calibration curve of *p*NP (0-20 nmol). The linear regression of the reactions was shown in an inset. (B) The Michaelis-Menten plots between v_0 and varied concentrations of *p*NP-GlcNAc$_2$ (0-800 μM) and sodium azide 0 M (filled squares), 0.5 M (open squares), 1 M (filled circles), 1.5 M (open circles), and 2 M (filled triangles).

Table 3.2.3 Effects of sodium azide on the kinetic parameters of wild-type *Vh*ChiA.

[NaN$_3$] (M)	K_m (µM)	k_{cat} (s^{-1})	k_{cat}/K_m (s^{-1} mM^{-1})
0	196 ± 25	2.40 ± 0.08	12.50 ± 0.30
0.5	164 ± 19	1.90 ± 0.08	11.70 ± 0.10
1.0	112 ± 15	1.20 ± 0.05	11.20 ± 0.70
1.5	92 ± 13	0.80 ± 0.02	9.20 ± 0.03
2.0	83 ± 12	0.60 ± 0.02	6.80 ± 0.20

To further confirm the inhibition type, a linear transformation of the non-linear progression curves (shown in Figure 3.2.5B) was performed using equation 3.2.2.

$$\frac{1}{v_0} = \frac{K_m}{V_{max}}\left(1 + \frac{[I]}{K_i}\right)\frac{1}{[S]} + \frac{\left(1 + \frac{[I]}{\alpha K_i}\right)}{V_{max}} \tag{3.2.2}$$

Where I is sodium azide and S is *p*NP-GlcNAc$_2$ substrate

Figure 3.2.6A is the Lineweaver-Burk plot between $1/v_0$ versus 1/[S]. As seen, all the double-reciprocal lines produced at different concentrations of sodium azide are found to intersect below the x and y axes, at negative values of 1/[S] and $1/v_0$. This pattern of lines indicated a typical mixed-type inhibition that sodium azide can bind reversibly to either free E or ES complex or both free E and ES complex. To obtain the values of K_i and αK_i, dixon plots (Copeland, 2000) were constructed

(Figures 3.2.6B and C). Figure 3.2.6B is the dixon plot of the slope of the primary plot (from the Lineweaver-Burk plot shown in Figure 3.2.6A) against sodium azide concentrations, while Figure 3.2.6C is the plot of $1/V_{max}^{app}$ at different sodium azide concentrations. The data showed that sodium azide inhibited the enzyme, with K_i for the EI complex of 1.50 ± 0.10 M (Figure 3.2.6B) and αK_i for the ESI complex of 0.40 ± 0.02 M (Figure 3.2.6C). The results suggested that sodium azide reacted more efficiently on the ES complex than the free E.
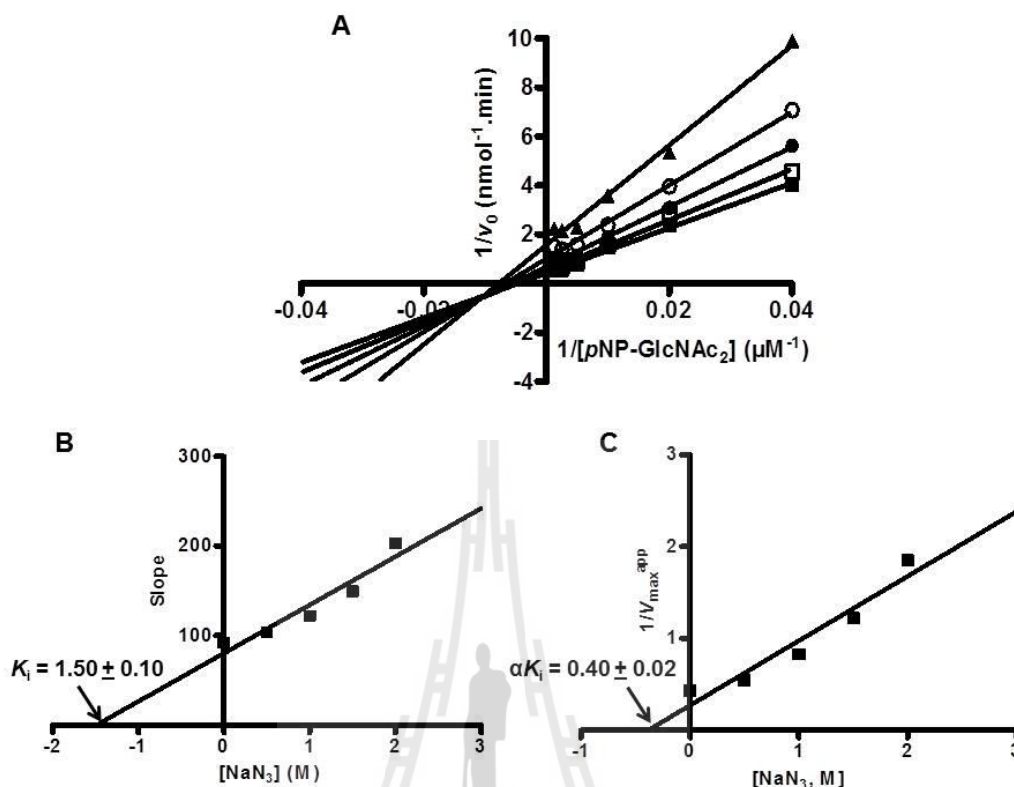
Figure 3.2.6 Determinaton of the inhibition constant for sodium azide acting on the wild-type *Vh*ChiA, using the linear transformation of the MM plot shown in Figure 3.2.5B. (A), sodium azide concentrations of 0, 0.5, 1.0, 1.5 and 2.0 M are shown as filled squares, open squares, filled circles, open circles, and filled triangles, respectively. K_i and αK_i values were derived from Dixon plots (B and C).

3.2.7 Dose-response of wild-type *Vh*ChiA on inhibition by sodium azide

The inhibitory effect of sodium azide on WT *Vh*ChiA activity was further examined. IC_{50} value of the enzyme was determined from the dose-response curve plotted between the fractional activity (v_i/v_0) versus a logarithmic scale of sodium azide concentrations (Figure 3.2.7). The plots showed sodium azide inhibitor

against WT *Vh*ChiA with IC_{50} of 0.40 ± 0.02 M. To confirm the accuracy of the Ki

value from Dixon plot ($K_i = 1.50 \pm 0.10$ M), the IC_{50} value was used to estimate the K_i

using Equation 3.2.3 (Cheng and Prusoff, 1973).

$$IC_{50} = \frac{[S] + K_m}{\frac{K_m}{K_i} + \frac{[S]}{\alpha K_i}} \qquad \textbf{(3.2.3)}$$

Where S is *p*NP-GlcNAc$_2$ substrate

The data showed K_i of sodium azide on the enzyme activity is $1.40 \pm$

0.07 M. The results suggest that the K_i values estimated from two methods are similar

to each other.
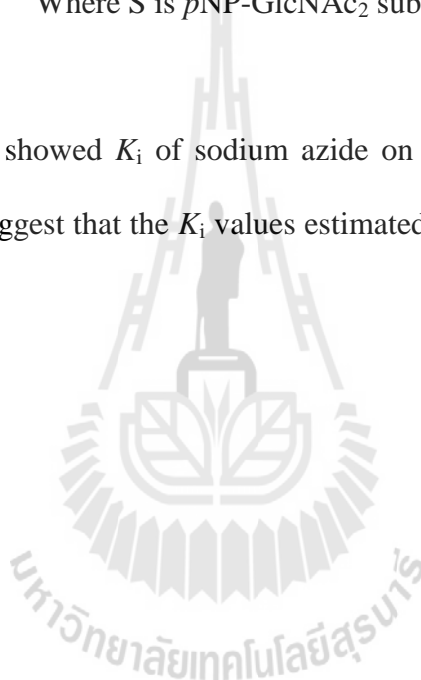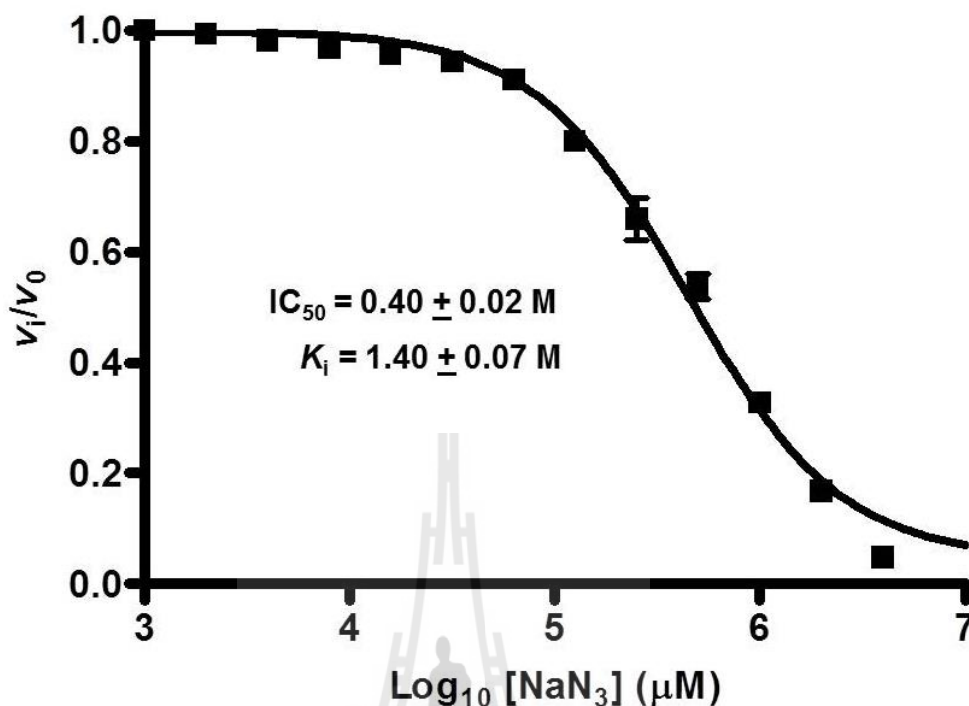
Figure 3.2.7 Dose-response plot of wild-type *Vh*ChiA fractional activity as a function of various sodium azide concentrations. The value of IC_{50} for sodium azide was determined from this graph. The mathematical equation used of logarithmic scale of sodium azide concentrations fit is $y = (y_{max}-y_{min}/1+[I]/IC_{50})+y_{min}$; where y is the fractional activity of the enzyme in the presence of inhibitor at concentration [I], y_{max} is the maximum value of y that is observed at zero inhibitor concentration (for fraction activity, this is 1.0), and y_{min} is the minimum value of y that can be obtained at high inhibitor concentration (Copeland, 2000). A reaction mixture (100 μl), containing 500 μM of *p*NP-GlcNAc₂, 1 μg of *Vh*ChiA and varied concentrations of sodium azide from 0-4 M in 100 mM sodium phosphate buffer, pH 7.5, was incubated at 37 °C for 10 min, and then the reaction was terminated as described elsewhere.

3.2.8 TLC analysis of the hydrolytic products of sodium azide inhibition on wild-type *Vh*ChiA

To confirm that sodium azide inhibited the hydrolytic activity of WT *Vh*ChiA, time courses of colloidal chitin hydrolysis were performed and the hydrolytic products analyzed on TLC. The hydrolysis of colloidal chitin produced $GlcNAc_{1-3}$ as the hydrolytic products (Figure 3.2.8A). When 2 M sodium azide was added in the same reaction, faint spots of the hydrolytic products ($GlcNAc_2$ and $GlcNAc_3$) were observed at longer incubation time (18 hr) (Figure 3.2.8B). Product analysis by TLC suggested that sodium azide significantly inhibited the enzyme activity of WT *Vh*ChiA with the natural substrates.
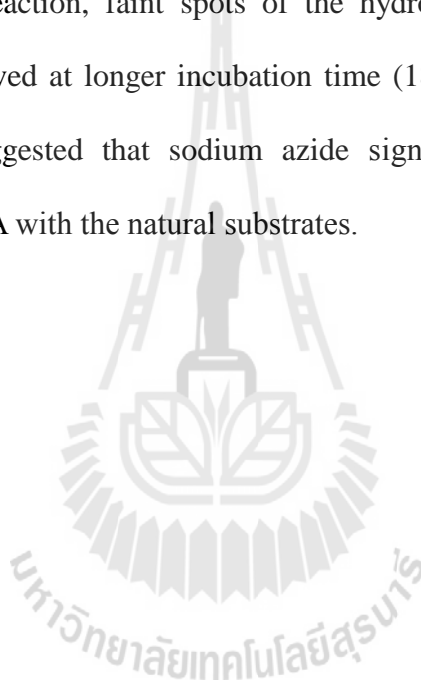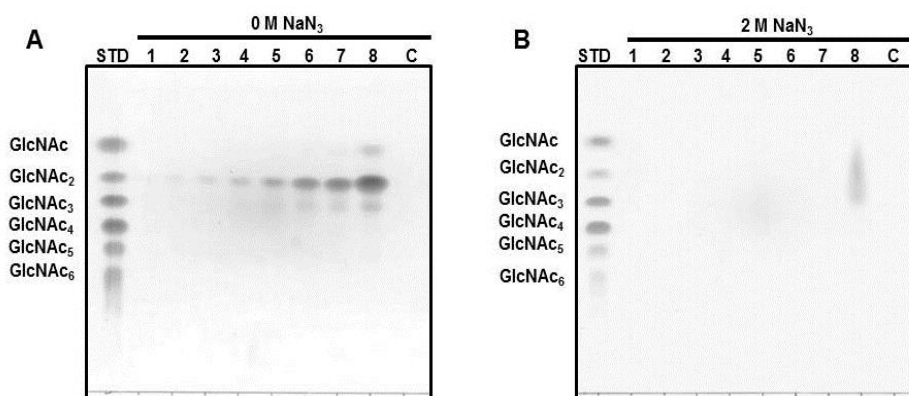
Figure 3.2.8 TLC analysis of colloidal chitin hydrolysis of wild-type *Vh*ChiA with 2 M sodium azide. Time-course of colloidal chitin hydrolysis by WT *Vh*ChiA, a reaction mixture (400 μl), containing 10 μg of *Vh*ChiA and 5% (w/v) colloidal chitin without sodium azide (A) or with 2 M sodium azide (B) in 100 mM phosphate buffer, pH 7.5, was incubated at various times at 37 ^{o}C, and then analyzed by TLC. Sugar products were detected with aniline-diphenylamine reagent. Lanes: std, a standard mix of GlcNAc$_{1-6}$; 1-8, incubation at 2, 5, 10, 15, 30, 60,180 and 1018 min, respectively; and C, substrate control.

3.2.9 Effect of sodium azide on the enzyme activity of wild-type and D313A and D313N mutants *Vh*ChiA

Sodium azide has been reported to act as an alternative nucleophile in the enzyme-catalyzed hydrolysis of various glycoside hydrolases (Cobucci-Ponzano *et al*., 2003; Fujita *et al*., 2007; MacLeod *et al*., 1994; Paal *et al*., 2004; Shallom *et al*., 2002; Vallmitjana *et al*., 1998; Viladot *et al*., 1998; Williams *et al*., 2002). Since we know that sodium azide presumably acts as a chemical rescue for the enzyme. Here, we set out the experiments to prove this hypothesis. The results showed that the

specific activity of WT and mutants D313A and D313N was decreased when sodium

azide (0-2 M) was added in the reaction mixture (Figure 3.2.9). However, when 2 M

sodium azide was added, the activity loss against pNP-GlcNAc$_2$ substrate was most

intensive in WT followed by the mutants D313N and D313A, respectively.
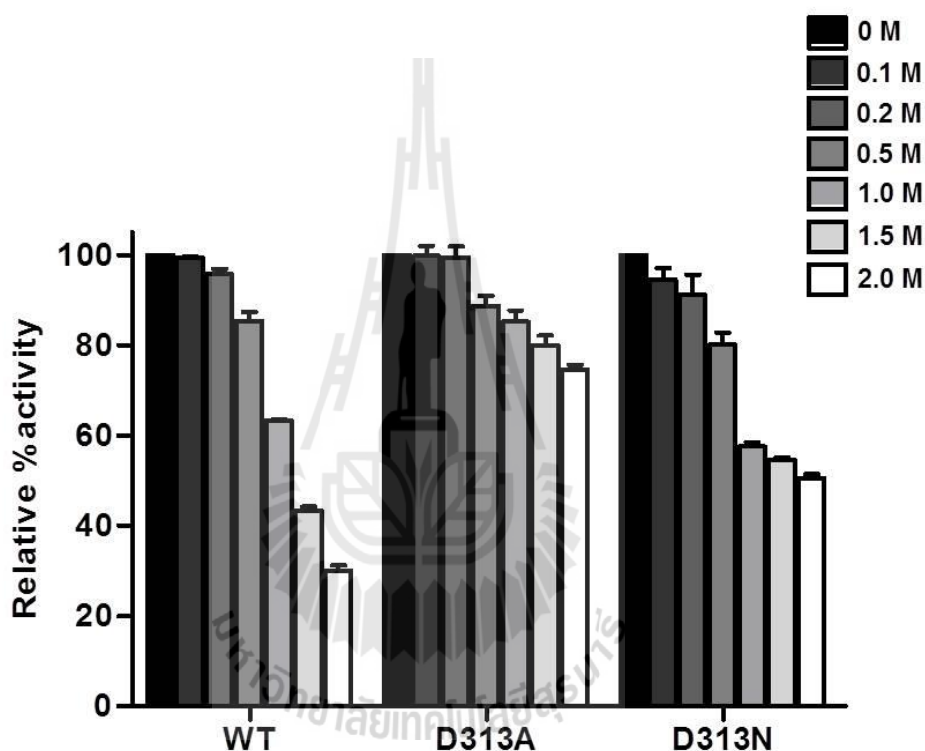
Figure 3.2.9 Specific activity of wild-type and mutants D313A and D313N *Vh*ChiA

with various concentrations of sodium azide against pNP-GlcNAc$_2$. Sodium azide (0-

2 M) was used to investigate the effect of sodium azide on the wild-type and both

mutants D313A and D313N in hydrolyzing pNP-GlcNAc$_2$ in 100 mM sodium

phosphate buffer, pH 7.5. The chitinase assay was carried out as described previously.

3.3 Kinetics of inhibition of sodium salts on a family-20 *β-N*-acetyl-glucosaminidase from *Vibrio harveyi*

3.3.1 Effects of sodium salts on the hydrolytic activity of wild-type *Vh*GlcNAcase

Sodium salts including sodium azide, sodium formate, sodium acetate, sodium nitrate and sodium chloride (Figure 3.2.1) were used to investigate the inhibitory activity toward the hydrolytic activity of WT *Vh*GlcNAcase against *p*NP-GlcNAc substrate at pH 5.5 and 7.5. The results showed that the enzyme activity was strongly inhibited by sodium azide and sodium nitrate at pH 7.5, while sodium formate, sodium acetate and sodium chloride decreased the enzyme activity with different values (Table 3.3.1). In addition, we found that the reaction mixtures with or without sodium salts at pH 5.5 showed the lower enzyme activity, since this pH value was not optimal for GlcNAcase acitivty. Therefore, we chose sodium azide and sodium nitrate for further kinetic studies of the inhibition of this enzyme at pH 7.5.

Table 3.3.1 Specific activity of wild-type *Vh*GlcNAcase against *p*NP-GlcNAc in the presence of 2 M sodium derivatives.

Sodium derivatives	Specific activity (nmol/min/µg)	
	pH 5.5	pH 7.5
No sodium derivative	0.040 ± 0.004 (100) [a]	0.400 ± 0.002 (100)
NaN₃	0.020 ± 0.002 (50)	0.020 ± 0.001 (5)
HCOONa	0.020 ± 0.001 (50)	0.200 ± 0.010 (50)
CH₃COONa	0.010 ± 0.001 (25)	0.200 ± 0.010 (50)
NaCl	0.020 ± 0.002 (50)	0.300 ± 0.002 (75)
NaNO₃	0.020 ± 0.002 (50)	0.030 ± 0.002 (8)

[a] Numbers in brackets reveal the % relative specific activities of *Vh*GlcNAcase with each sodium derivative concentration by comparing with *Vh*GlcNAcase without sodium derivative (set to 100).

3.3.2 Effects of sodium and potassium cations on the hydrolytic activity of wild-type *Vh*GlcNAcase

To investigate the effect of cations (Na$^+$ and K$^+$) of azide compounds on the hydrolytic activity of WT *Vh*GlcNAcase, time courses of *p*NP-GlcNAc hydrolysis with 2 M sodium azide, 2 M potassium azide, and without azides were performed in 100 mM potassium phosphate buffer, pH 7.5 (Figure 3.3.1). The initial rates (v_0) of the reactions were determined to be within 10 min as shown in an inset (Figure 3.3.1).

The results showed a strong inhibitory effect in the enzyme activity with sodium azide and potassium azide, compare to the reaction without azide compounds and the effects of both compounds were similar (Figure 3.3.1).
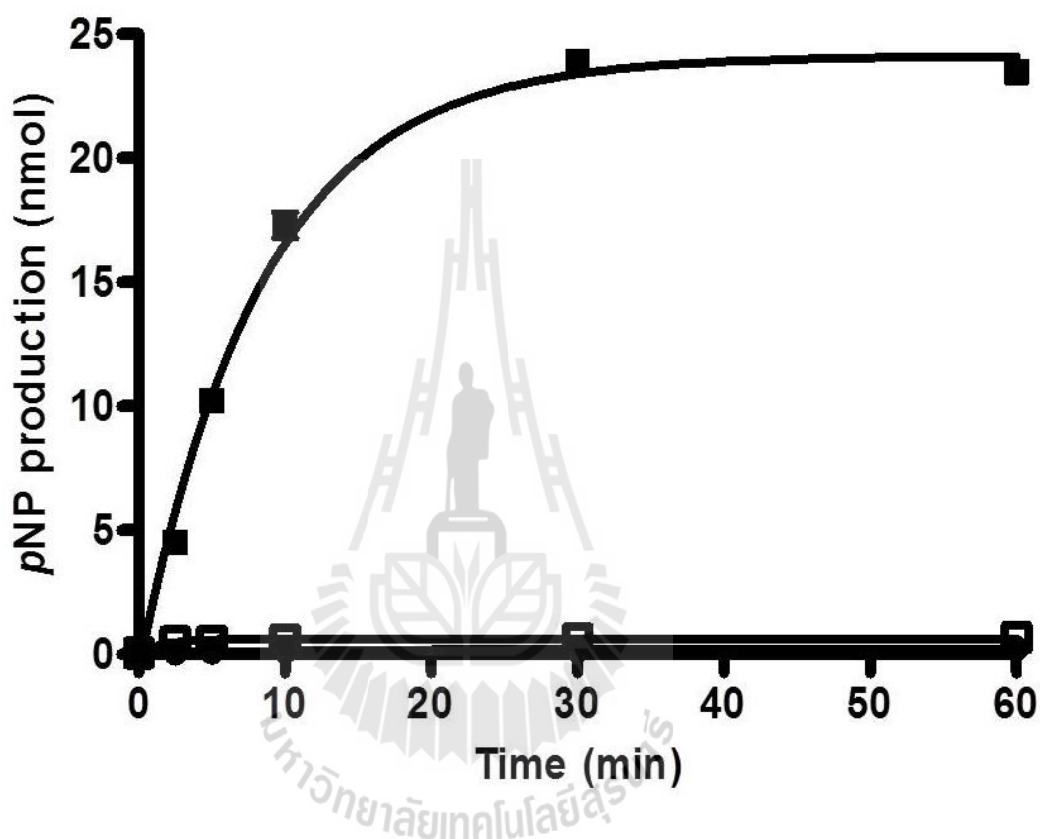
Figure 3.3.1 Time courses of wild-type *Vh*GlcNacase with and without sodium azide and potassium azide were investigated using *p*NP-GlcNAc substrate. A reaction mixture (100 µl), containing 3 µg of *Vh*GlcNAcase and 500 µM of *p*NP-GlcNAc without sodium compounds (filled squares), with 2 M sodium azide (open squares), or with 2 M potassium azide (filled circles) in 100 mM potassium phosphate buffer, pH 7.5, was incubated at 37 $^{\circ}$C for 0, 2.5, 5, 10, 30, and 60 min, and then the reaction was terminated.

3.3.3 Effects of sodium and potassium phosphate buffers, pH 7.5 on the hydrolytic activity of wild-type *Vh*GlcNAcase

From the results of the previous section suggested that sodium and potassium cations may inhibit the enzyme activity. In this experiment, we investigated the effects of sodium and potassium phosphate buffers, pH 7.5 on WT *Vh*GlcNAcase activity against *p*NP-GlcNAc substrate. As shown in Table 3.3.2, the specific activity of the enzyme in sodium phosphate buffer was slightly higher than that in potassium phosphate buffer. When concentrations of both buffers were varied, the reaction in 2.0 M phosphate buffer displayed lower specific activity than in 0.1, 0.5, and 1.0 M phosphate buffers. The reactions in 0.1, 0.5, and 1.0 M sodium and potassium phosphate buffers showed that the specific activity of WT *Vh*GlcNAcase was similar to each other (Table 3.3.2). The specific activity of the enzyme in the presence of 2 M sodium azide in 0.1 M potassium phosphate buffer, pH 7.5 (0.020 $\pm$ 0.001 nmol/min/μg) (Table 3.3.1), was much lower than that of the enzyme without sodium azide in 2 M potassium phosphate buffer, pH 7.5 (0.200 $\pm$ 0.001 nmol/min/μg) (Table 3.3.2). The results suggested that the azide anion displayed much higher inhibitory effect on the GlcNAcase activity than the sodium and potassium cations.

Table 3.3.2 Specific activity of wild-type *Vh*GlcNAcase against *p*NP-GlcNAc substrate in various concentrations of sodium and potassium phosphate buffers, pH 7.5.

Concentrations of phosphate buffer, pH 7.5 (M)	Specific activity (nmol/min/µg)	
	Sodium phosphate buffer, pH 7.5	Potassium phosphate buffer, pH 7.5
0.1	0.400 ± 0.010	0.400 ± 0.001
0.5	0.400 ± 0.010	0.400 ± 0.003
1.0	0.400 ± 0.004	0.400 ± 0.010
2.0	0.300 ± 0.010	0.200 ± 0.001

3.3.4 Effects of sodium azide and sodium nitrate on the molecular structure of wild-type *Vh*GlcNAcase

To investigate the effects of sodium azide and sodium nitrate on the molecular structure of WT *Vh*GlcNAcase, fluorescence spectra were obtained in the presence of sodium salts. The changes in the fluorescence intensity and the shift in the maximum emission wavelength that indicate the denaturation of the enzyme were monitored. The emission spectra were collected from 300-500 nm upon excitation at 295 nm. Although, the fluorescence intensity of the enzyme decreased with increasing sodium azide and sodium nitrate concentrations, the shifting in the maximum

emission wavelength were not observed. On the other hand, the enzyme that was denatured by 8.0 M urea and heat at 100 $^{\circ}$C for 10 min showed higher fluorescence intensity and shifting maximum emission wavelength, as compared to that of the non-denatured enzyme (Figure 3.3.3). In addition, we found that the fluorescence intensity of the enzyme with sodium nitrate (Figure 3.3.3B) was lower than the enzyme titrated with sodium azide (Figure 3.3.3A). The results suggested that sodium azide has effect to partially unfold the secondaly structure of *Vh*GlcNAcase whereas sodium nitrate strongly affect on the structural enzyme than sodium azide.
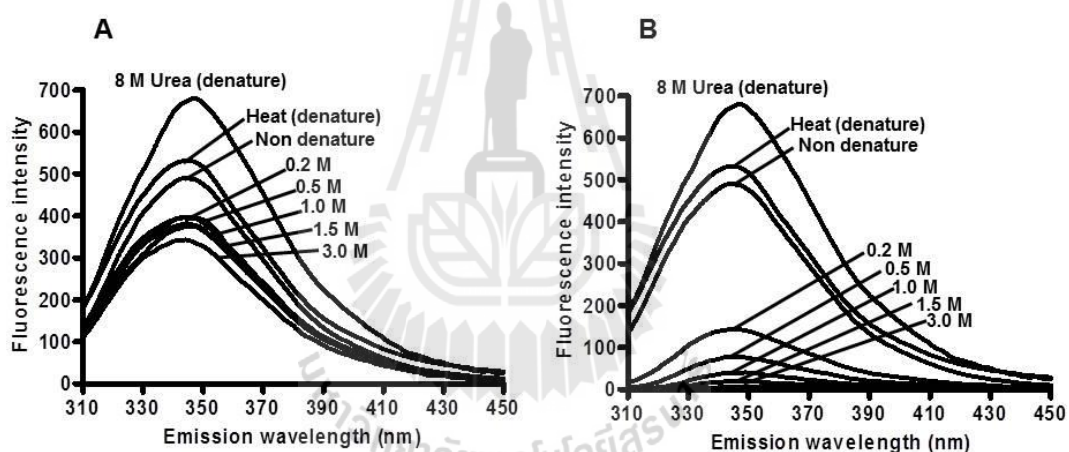
Figure 3.3.2 Effect of 0-3 M sodium azide (A) and sodium nitrate (B) on structural integrity of wild-type *Vh*GlcNAcase. The enzyme was investigated using fluorescence quenching spectroscopy. The emission spectra were collected from 300-500 nm upon excitation at 295 nm. Increasing the fluorescence intensity was resulted by enzyme denaturation.

3.3.5 Kinetics of inhibitions of sodium azide and sodium nitrate on the hydrolytic activity of wild-type *Vh*GlcNAcase

Kinetic experiments were carried out with the attempt to define the inhibition type. *p*NP-GlcNAc hydrolysis with and without 2.0 M sodium azide or sodium nitrate (Figure 3.3.3A) were performed to determine the initial rate (v_0) of the enzyme within the incubation period of 5 min. Figures 3.3.3B and C present the non-linear (Michaelis-Menten) plots between v_0 and the *p*NP-GlcNAc concentrations. Curve fittings were conducted for individual concentrations of sodium azide (Figure 3.3.3B) or sodium nitrate (Figure 3.3.3C) (0, 0.3, 0.4, 0.5 and 0.6 M), yielding the kinetic parameters k_{cat} and K_m as presented in Table 3.3.3. The kinetic parameters were obtained by data-fitting based on the Michaelis-Menten equation or the substrate inhibition equation (Equation 3.3.1). The catalytic rate constants (k_{cat}) of the enzyme at 0.3 M sodium azide and sodium nitrate (0.7 s^{-1}) are equal to k_{cat} without sodium azide or sodium nitrate. When higher concentrations of sodium azide or sodium nitrate were added, the value is slightly lower than that at 0 M sodium azide or sodium nitrate (0.6 s^{-1}). On the other hand, the apparent K_m was found to be elevating from 238 to 679 µM and 238 to 667 µM up with increasing sodium azide and sodium nitrate concentrations, respectively.

$$v_0 = \frac{V_{max}[S]}{K_m\left(1+\frac{[I]}{K_i}\right)+[S]} \tag{3.3.1}$$

Where I is sodium azide or sodium nitrate and S is *p*NP-GlcNAc substrate
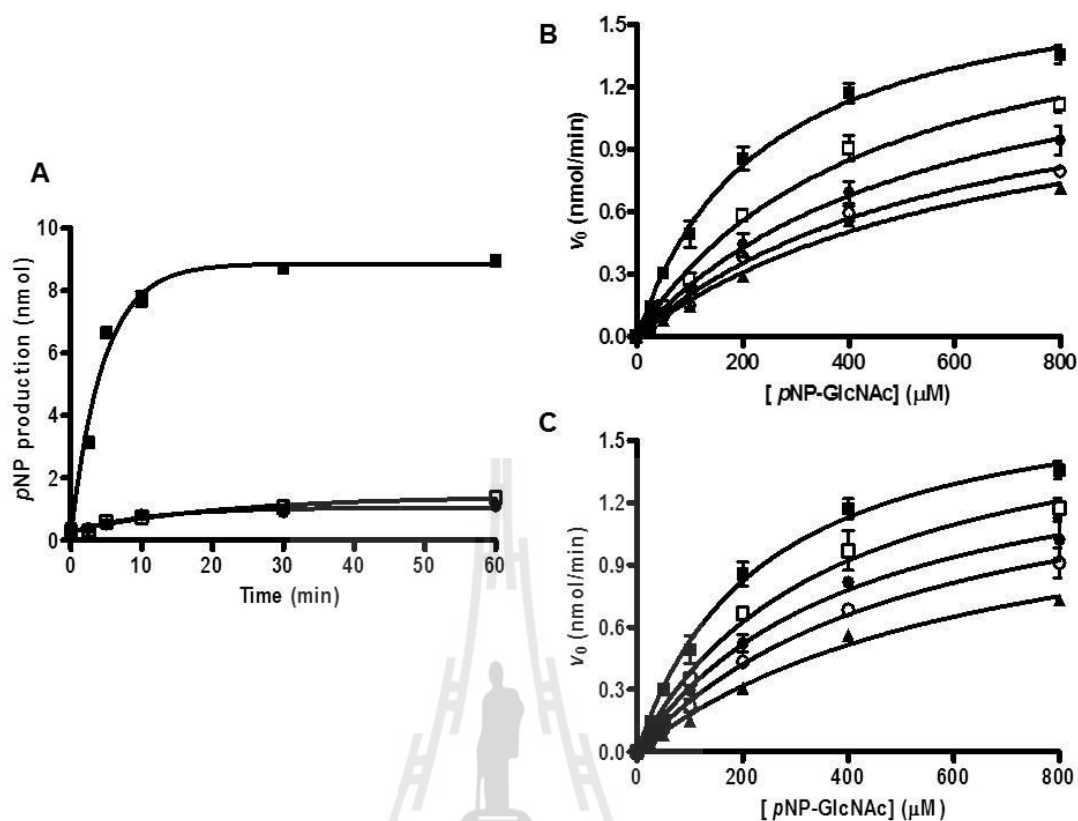
Figure 3.3.3 Kinetic properties of wild-type *Vh*GlcNAcase were investigated using *p*NP-GlcNAc as the substrate. A reaction time-course of *p*NP-GlcNAc hydrolysis by WT *Vh*GlcNAcase (A), Time course of *p*NP-GlcNAc hydrolysis by *Vh*GlcNAcase without sodium azide (filled squares), with 2 M sodium azide (open squares), or with 2 M sodium nitrate (filled circles). The enzyme assay was carried out as described in Section 2.7.1. The linear part of the reactions was shown in an inset. Kinetic parameters of the *Vh*GlcNAcase with sodium azide and sodium nitrate were obtained from Michaelis-Menten plots (B) and (C), respectively. A reaction was investigated using *p*NP-GlcNAc (0-800 μM) as the substrate, 3 μg of *Vh*GlcNAcase and 0 M (filled squares), 0.3 M (open squares), 0.4 M (filled circles), 0.5 M (open circles), or 0.6 M (filled triangles) sodium azide or sodium nitrate.

Table 3.3.3 Kinetic parameters of wild-type VhGlcNAcase with different NaN_3 and $NaNO_3$ concentrations.

	Kinetic parameters of inhibition of NaN_3 and $NaNO_3$ on the hydrolytic activity of wild-type VhGlcNAcase					
Concentration of NaN_3 or $NaNO_3$ (M)	NaN_3			$NaNO_3$		
	K_m (μM)	k_{cat} (s^{-1})	k_{cat}/K_m (s^{-1} mM^{-1})	K_m (μM)	k_{cat} (s^{-1})	k_{cat}/K_m (s^{-1} mM^{-1})
0	238 ± 19	0.70 ± 0.02	3.10 ± 0.10	238 ± 19	0.70 ± 0.02	3.10 ± 0.10
0.3	438 ± 51	0.70 ± 0.02	1.60 ± 0.04	362 ± 44	0.70 ± 0.03	2.00 ± 0.10
0.4	554 ± 67	0.60 ± 0.08	1.20 ± 0.10	411 ± 44	0.60 ± 0.02	1.60 ± 0.20
0.5	608 ± 76	0.60 ± 0.01	1.00 ± 0.02	528 ± 58	0.60 ± 0.04	1.20 ± 0.02
0.6	679 ± 92	0.60 ± 0.02	0.80 ± 0.02	667 ± 77	0.60 ± 0.01	0.80 ± 0.03

To further confirm the inhibition type, linear transformation of the non-linear regression function (shown in Figures 3.3.5B and C) was evaluated using equation 3.3.2.

$$\frac{1}{v_0} = \frac{K_m}{V_{max}}\left(1 + \frac{[I]}{K_i}\right)\frac{1}{[S]} + \frac{1}{V_{max}} \qquad \textbf{(3.3.2)}$$

Where I is sodium azide or sodium nitrate and S is pNP-GlcNAc substrate

Figures 3.3.4A and B were Lineweaver-Burk plots between $1/v_0$ versus $1/[S]$. As seen from the figure, all the double-reciprocal lines generated at different concentrations of sodium azide (Figure 3.3.4A) or sodium nitrate (Figure 3.3.4B) were found to meet the y-intercept at a value close to 0.3 ($nmol^{-1}.min$). Such pattern is a characteristic competitive inhibition that sodium azide and sodium nitrate bind only to free E. To obtain the values of K_i, Dixon plots were conducted as shown in Figures 3.3.4C and D, in which the slope of the primary plot (from the Lineweaver-Burk plots) were plotted against sodium azide and sodium nitrate concentrations, respectively. The data showed that sodium azide and sodium nitrate inhibited WT VhGlcNAcase with K_i of 0.20 ± 0.03 M and 0.20 ± 0.05 M, respectively (Figures 3.3.4C and 3.3.4D). The results suggested that sodium azide and sodium nitrate are not significantly different to inhibit the enzyme activity.
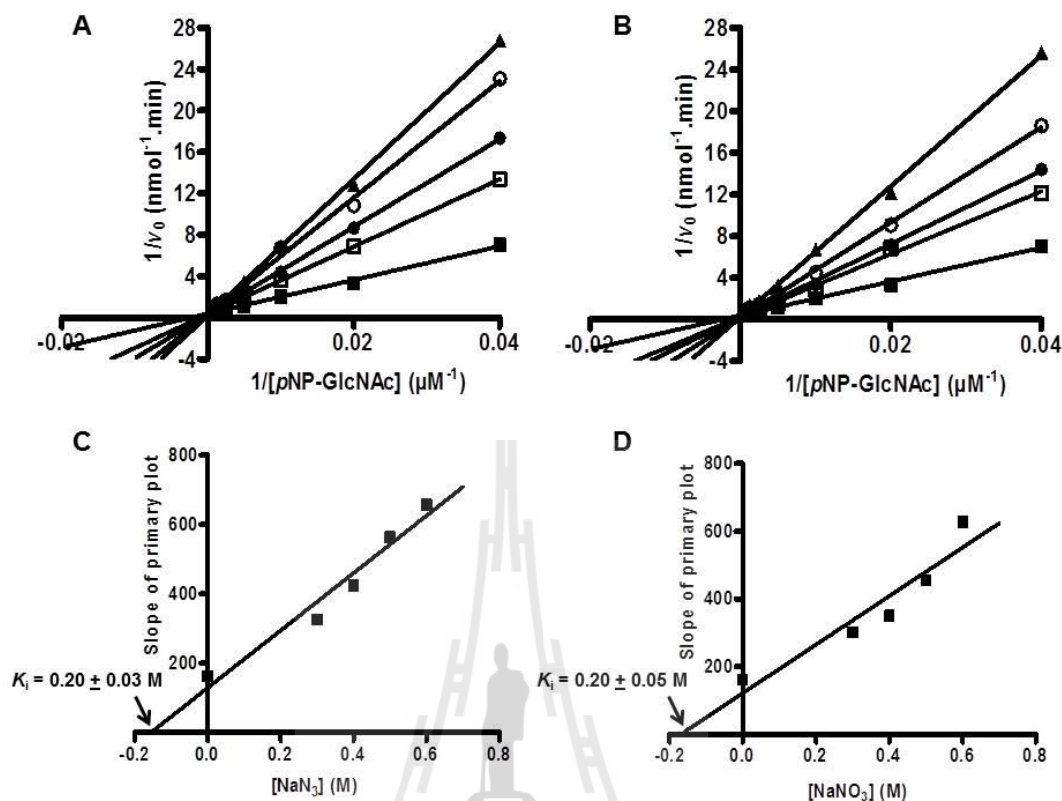
Figure 3.3.4 Kinetic properties of wild-type *Vh*GlcNAcase were investigated using *p*NP-GlcNAc (0-800 µM) as the substrate. The reaction containing 3 µg *Vh*GlcNAcase in 100 mM phosphate buffer, pH 7.5, was assayed at 37 °C for 10 min in the presence of various concentrations of sodium azide or sodium nitrate (0-0.6 M). Types of inhibition were assessed from Lineweaver-Burk plots (A) for sodium azide (B) for sodium nitrate. Sodium azide and sodium nitrate concentrations of 0, 0.3, 0.4, 0.5 and 0.6 M are shown as filled squares, open squares, filled circles, open circles and filled triangles, respectively. K_i values of sodium azide and sodium nitrate were derived from Dixon plots (B and C, respectively).

3.3.6 The inhibitory effects of sodium azide and sodium nitrate on the hydrolytic activity of wild-type *Vh*GlcNAcase

The inhibitory effects of sodium azide and sodium nitrate on *Vh*GlcNAcase activity were further accessed. IC_{50} values were determined from dose-response curve plotted between the fractional activity (v_i/v_0) versus the logarithmic scale of sodium azide or sodium nitrate concentration (Figure 3.3.5). The plots showed inhibition against WT *Vh*GlcNAcase with IC_{50} of 0.30 ± 0.03 M for sodium azide and 0.20 ± 0.02 M for sodium nitrate. To confirm the accuracy of the K_i values obtained from Dixon plots (K_i of sodium azide $= 0.20 \pm 0.03$ M and K_i of sodium nitrate $= 0.20 \pm 0.05$ M), the IC_{50} values were used to define the K_i using equation 3.3.3 (Cheng and Prusoff, 1973).

$$K_i = \frac{IC_{50}}{1 + \frac{[S]}{K_m}}$$

(3.3.3)

Where S is *p*NP-GlcNAc substrate

The data showed that K_i of sodium azide and sodium nitrate are equal to 0.10 ± 0.02 M and 0.10 ± 0.01 M, respectively. The results suggest that the K_i values estimated from the two equations are not significantly different.
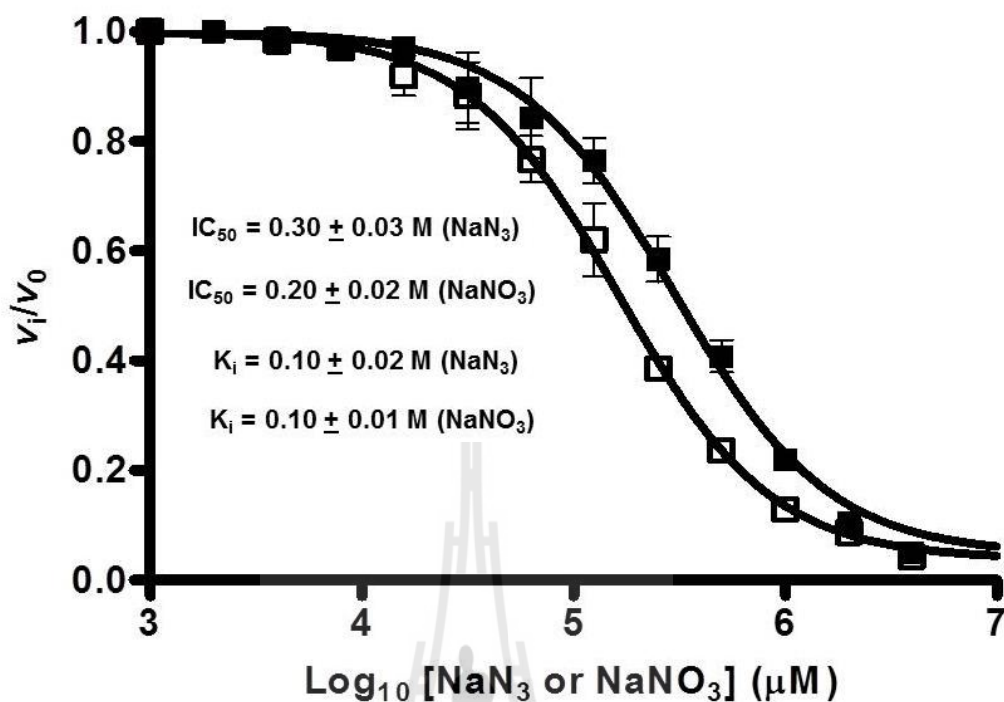
Figure 3.3.5 Dose-response plot of wild-type *Vh*GlcNAcase fractional activity as a function of sodium azide or sodium nitrate concentrations. The values of IC_{50} for sodium azide and sodium nitrate were determined from this graph. A reaction mixture (100 µl), contained 500 µM of *p*NP-GlcNAc, 3 µg of *Vh*GlcNAcase, and varied concentrations of sodium azide or sodium nitrate from 0-4 M. The assay was carried out as described in Materials and Methods (Section 2.7.1).

3.3.7 TLC analysis of the hydrolytic products of sodium azide and sodium nitrate inhibitions on wild-type *Vh*GlcNAcase

The effects of sodium azide and sodium nitrate on the inhibition of the hydrolytic activity of WT *Vh*GlcNAcase against the natural glycoside substrate: $GlcNAC_4$ was examined at various time points using TLC (Figure 3.3.6). Figure 3.3.6A showed that the enzyme without sodium salts sequentially hydrolyzed $GlcNAc_4$ to $GlcNAc_3$, $GlcNAc_2$, and GlcNAc as the final products. However, when the enzyme with sodium azide (Figure 3.3.6B) or sodium nitrate (Figure 3.3.6C) was incubated with $GlcNAc_4$, the TLC results showed no detectable hydrolytic products observed even after 18 h of incubation. The obtained results suggested that sodium azide and sodium nitrate strongly inhibited the enzyme activity.
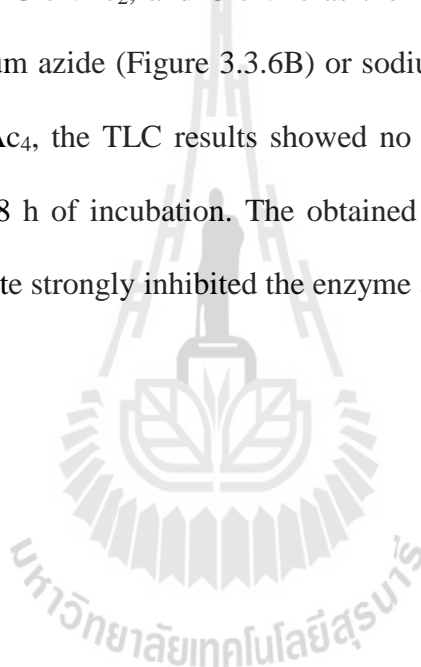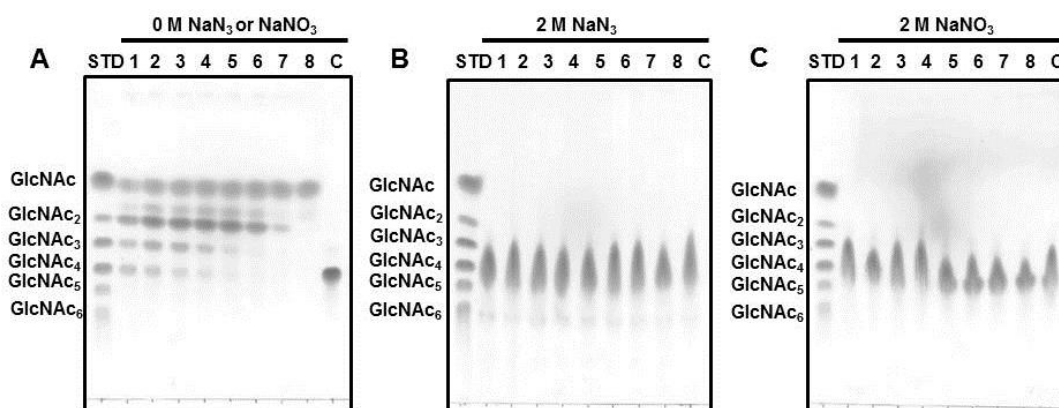
Figure 3.3.6 TLC analysis of the GlcNAc$_4$ hydrolysis by wild-type *Vh*GlcNAcase with 2 M sodium azide and sodium nitrate. Time-courses of the GlcNAc$_4$ hydrolysis by WT *Vh*GlcNAcase, a reaction mixture (20 µl), containing 1 µg of *Vh*GlcNAcase and 2.5 mM of GlcNAc$_4$ without sodium azide (A), with 2 M sodium azide (B), or with 2 M sodium nitrate (C) in 100 mM phosphate buffer, pH 7.5, was incubated at various times at 37 $^{\circ}$C, and then analyzed by TLC. Sugar products were detected with aniline-diphenylamine reagent. Lanes: std, a standard mix of GlcNAc$_{1-6}$; 1-8, incubation at 2, 5, 10, 15, 30, 60,180 and 1080 min, respectively; and C, substrate control.

CHAPTER IV

DISCUSSION

4.1 Mutation strategies for obtaining chitooligosaccharides with longer chains by transglycosylation reaction of a family GH18 chitinase A from *Vibrio harveyi*

Vibrio harveyi chitinase A (*Vh*ChiA) is a bacterial GH18 chitinase that cleaves a chitin chain into various chitooligosaccharide fragments. Based on our previous studies (Songsiriritthigul *et al*., 2008; Suginta *et al*., 2009), *Vh*ChiA has structure and function similar to those of *S. marcescens* chitinase A, and it degrades GlcNAc$_4$ substrate mostly to GlcNAc$_2$, GlcNAc$_5$ substrate to GlcNAc$_2$ and GlcNAc$_3$, and GlcNAc$_6$ to GlcNAc$_2$, GlcNAc$_3$ and GlcNAc$_4$. In this study, we investigated the transglycosylation activity of various mutated enzymes derived from *Vh*ChiA, including W570G, D392N, D313A, and D313N. Trp570 is responsible for the GlcNAc residue binding at subsites -2 and -1 (Figure 3.1.1), so that cleavage of the glycosidic bond between subsites -1 and +1 takes place most efficiently. Substitution of the Trp570 side chain with glycine completely removed the aromatic surface area, thereby causing a dramatic decrease in the hydrolytic activity to about 5% of the WT activity, and decreased the binding affinity (increased K_m) that affected sugar-enzyme interaction (Suginta *et al*., 2007). The reduction of the binding affinity

at these two subsites, on the other hand, may relatively enhance the affinity at the acceptor-binding site (positively-numbered subsites), resulting in the enhanced TG activity. However, all of the TG products immediately hydrolyzed again into oligosaccharides with shorter chains. Our previous kinetic data showed that the mutated enzymes, D392N, has greater affinity towards pNP-GlcNAc$_2$ and chitooligosaccharide substrates than those of WT (Songsiriritthigul et al., 2008). The greater affinity of D392N may facilitate the acceptor binding to subsites +1 and +2; hence, the TG reaction for the substrates GlcNAc$_4$ and GlcNAc$_5$ (Figures 3.1.2G and 3.1.2H). However, also in this mutant, the TG products were immediately hydrolyzed into oligosaccharides with shorter chains. Mutations of Trp570 and Asp392 are unlikely effective for obtaining chitooligosaccharides with longer chains, even though the mutant enzymes exhibit the enhanced TG activity.

GH18 chitinases have a catalytic motif specified by a sequence DxDxE, which correspond to Asp311-x-Asp313-x-Glu315 in VhChiA. Glu315 is a catalytic acid, which donates a proton to the β-1,4-glycosidic oxygen to cleave the linkage. Asp313 is located at the bottom of the substrate binding cleft (Figure 3.1.1). This aspartic acid plays multiple roles in the catalytic cycle of chitin hydrolysis (Suginta et al., 2012; Synstad, Ga$^\circ$ seidnes, van Aalten, Vriend, Nielsen, and Eijsink, 2004). It interacts with the 2-acetamido group of the sugar residue at subsite -1 (the cleavage site) and helps to lower the pKa value of the catalytic residue Glu315 so that bond cleavage can be achieved more easily. Moreover, it helps to orient the 2-acetamido group in the correct position to stabilize the oxazolinium ion intermediate in the substrate assisted mechanism. Mutations of Asp313 to Ala and Asn abolished the hydrolytic activity almost completely by disrupting hydrogen-bond interactions with the sugar residue.

Instead, the mutations enhanced the TG activity. We tried to compare the efficiencies of TG reaction obtained by our D313A/N mutants with those obtained by the corresponding mutants of the two *Serratia* enzymes, *Sm*ChiA and *Sm*ChiB (Zakariassen *et al*., 2011). In the *Serratia* enzymes, the mutations of the middle Asp of the DxDxE motif to Asn were reported to enhance the TG reaction more strongly than the mutations to Ala. In our *Vh*ChiA mutants, however, no significant difference was found in the highest yields of the TG products (GlcNAc$_6$ from the initial substrate GlcNAc$_4$, Figure 3.1.4; or GlcNAc$_8$ from the initial substrate GlcNAc$_6$, Figure 3.1.5) between D313A and D313N. The TG efficiencies in the mutants from *Serratia* enzymes were evaluated from the GlcNAc$_3$ production from the initial substrate GlcNAc$_4$, indicating that the TG product GlcNAc$_6$ was decomposed into GlcNAc$_3$ as shown in Figure 3.1.3 (Zakariassen *et al*., 2011). The evaluation of TG efficiency based on the yield of GlcNAc$_n$ with longer chains (TG products) may be more informative for practical use of the transglycosylating chitinases. Thus, the mutants of the middle Asp of the DxDxE motif from *Vh*ChiA are likely more effective for obtaining GlcNAc$_n$ with longer chains than the corresponding mutants from the *Serratia* enzymes, *Sm*ChiA and *Sm*ChiB (Zakariassen *et al*., 2011). In the Asp313 mutants from *Vh*ChiA, the K_m values toward GlcNAc$_6$ were 4-(D313N) or 6-fold (D313A) higher than that of the wild type (Suginta *et al*., 2012). The lower affinity may result in the spontaneous release of the TG product from the enzyme without relocation to the productive binding mode (process IV in Figure 3.1.3). This situation may bring about the accumulation of the TG products in the Asp313 mutants. In the other mutants W570G and D392N, however, the TG products may be immediately relocated to the productive binding mode spanning the catalytic center, due to the

affinity with Asp313, and subsequently broken down by the hydrolytic action of the enzyme. Zakariassen *et al.*, 2011 who reported the hypertransglycosylating mutants obtained from the *Serratia* enzymes, explained that the mutation of Asp313 changes the electrostatics around the catalytic center, decreasing the probability of nucleophilic attack of a water molecule to the oxazolinium ion intermediate. Similar situation may possibly take place in the *Vh*ChiA mutants, D313A and D313N. Aronson *et al.*, 2006 reported that the mutation of Trp167 of *Sm*ChiA to alanine (W167A) significantly enhances the TG reaction. In W167A, the side chain of Asp313 is oriented only toward Glu315, whereas in the wild type, the Asp313 side chain is equally distributed between two orientations, toward Asp311 or toward Glu315. They explained that the orientation of Asp313 toward Glu315 may interfere with the attack of a water molecule to the oxazolinium ion intermediate. Thus, the state of the side chain of Asp313 appears to be related to the efficiency of TG reaction. Crystal structure analysis of *Vh*ChiA D313N or D313A will afford valuable information on the structural factor for enhancing the TG reaction in *Vh*ChiA.

4.2 Kinetics of inhibition of family-18 chitinase A from *Vibrio harveyi* by sodium azide

Vibrio harveyi chitinase (*Vh*ChiA) is a member of family-18 chitinases that catalyzes chitin degradation via the substrate-assisted retaining mechanism (Songsiriritthigul *et al.*, 2008; Suginta *et al.*, 2005; Suginta *et al.*, 2009). Like other family-18 chitinases, the catalytic cycle of *Vh*ChiA has been proposed to involve a concerted action of three acidic residues in the DXDXE sequence motif (Synstad *et al.*, 2004; Tews, van Scheltinga, Perrakis, Wilson, and Dijkstra, 1997; van Aalten *et*

al., 2001). In *Vh*ChiA (Songsiriritthigul *et al*., 2008) and its close homolog *Sm*ChiA (Perrakis *et al*., 1994), such residues are identified as Asp311-Asp313-Glu315. Asp313, which is located at the center of this motif, has been suggested to play multiple essential roles for catalysis. One of its roles is to support the 2-acetamido group to act as a powerful, primary nucleophile that helps stabilization of the oxazolinium ion intermediate, which further undergoes the second nucleophilic attack by neighboring water, yielding the retention of the *β*-configuration of the anomeric products (Synstad *et al*., 2004; van Aalten *et al*., 2001).

Sodium azide has been routinely used to identify the catalytic nucleophile of several glycoside hydrolases that employ acid-base catalysis in the retaining mechanism (Cobucci-Ponzano *et al*., 2003; Fujita *et al*., 2007; MacLeod *et al*., 1994; Paal *et al*., 2004; Shallom *et al*., 2002; Vallmitjana *et al*., 1998; Viladot *et al*., 1998; Williams *et al*., 2002). For example, activity of *Arthrobacter protophormiae* endo-*β*-N-acetylglucosaminidase (Endo A) inactive mutant E173A was increased by 127-fold when 2 M sodium azide was added in the assayed reaction (Fujita *et al*., 2007). The most relevant case to family-18 chitinases is a report on *Streptomyces plicatus* hexosaminidase (*Sp*Hex) (Williams *et al*., 2002). *Sp*Hex is a family-20 exoglycosidase that removes GlcNAc moiety from the non-reducing end of glycoconjugates, oligosaccharides and polysaccharides. An acidic pair (Asp313-Glu314) is identified to be most essential resides in catalysis. Functional roles of Asp313 are predicted to aid the 2-acetamido group of (-1)GlcNAc to act as a powerful nucleophile and to stabilize the oxazolinium ion intermediate. On the other hand, Glu314 acts as the catalytic residue that directly attacks the *β*-1,4-glycosidic bond at the cleavage site. Single mutation of Asp313 of *Sp*Hex to Ala or Asn (mutant D313A

or D313N) almost abolished the hydrolytic activity of *Sp*Hex. However, rate of reaction of the D313A variant was enhanced up to 16 fold of the original rate when sodium azide was added. It has been concluded that the azide ion acts as an alternative nucleophile to water and open the oxazolinium ion intermediate formed after acid catalysis by Glu314.

To examine the effect of sodium salts on wide-type *Vh*ChiA, we applied various sodium salts (sodium azide, sodium formate, sodium acetate, sodium nitrate, and sodium chloride) into the hydrolytic activity assay of WT *Vh*ChiA at pH 5.5 and 7.5. All sodium salts should be in the ionized forms at both pH values (Cobucci-Ponzano *et al*., 2003; Comfort, Bobrov, Ivanen, Shabalin, Harris, Kulminskaya, Brumer, and Kelly, 2007; Viladot *et al*., 1998; Williams *et al*., 2002). After we screened the effect of several salts, we found that all salts showed less effect at lower pH than higher pH. Since, lower pH (pH value below 7) means higher concentration of proton (H^+) in the solution, so it may interfere the binding of the salts to chitinase by forming hydrogen bond with the derivative anions. Whereas, higher pH (pH value above 7) means lower concentration of proton in the solution, so the derivative anions are able to easily compete with the substrate to interact with the hydrogen atom of the catalytic carboxyl group of the enzyme and inhibit the enzyme activity. Moreover, the result showed that sodium azide is the strongest inhibitor for this enzyme that may be because the negatively charged azide ion (N_3^-) is more powerful nucleophile so that it could to compete with the substrate to react with the carboxyl group of the catalytic amino acid than the other derivatives.

Since we know that sodium azide is the strongest inhibitor for WT *Vh*ChiA, so we chose this molecule to investigate the kinetics of inhibition on this enzyme.

However, the result of the effects of sodium derivatives on WT *Vh*ChiA showed the different inhibitory effects on the enzyme activity when several derivatives were added in the reactions (Figure 3.2.2). Therefore, we could not conclude that only azide anion or both azide anion and sodium cation affect to inhibit the enzyme activity, so we tried to investigate the effect of cations from sodium azide and potassium azide on the hydrolytic activity of WT *Vh*ChiA at pH 7.5. A time course study displayed a decrease in the enzyme activity with sodium azide and potassium azide, respectively, when compared to the enzyme without both compounds (Figure 3.2.3). The results obtained from this assay showed that potassium azide having larger effects inhibit the enzyme activity than sodium azide, but the difference was not so much when compare to the difference of the inhibitory effects of sodium derivatives on the enzyme activity (Figure 3.2.2), suggested that sodium cation may slightly also affect to inhibit the enzyme activity but the inhibitory effect on the enzyme activity was predominately derived from azide anion.

The inhibition effect of cation may occur from sodium ion reacts with the deprotonated side chain of the carboxylate of Asp313, which is sharing the proton with the protonated side chain of the carboxyl group of Asp311 (Suginta *et al*., 2012) (Figure 4.1). If sodium ion was able to compete with the proton of the carboxyl group of Asp311 to interact with the carboxylate of Asp313, the Asp313 will be blocked and cannot be rotate to form H-bond with the side chain of the catalytic carboxyl group of Glu315, then preventing the glycosidic bond of the chitin substrate to be hydrolyzed by this residue.
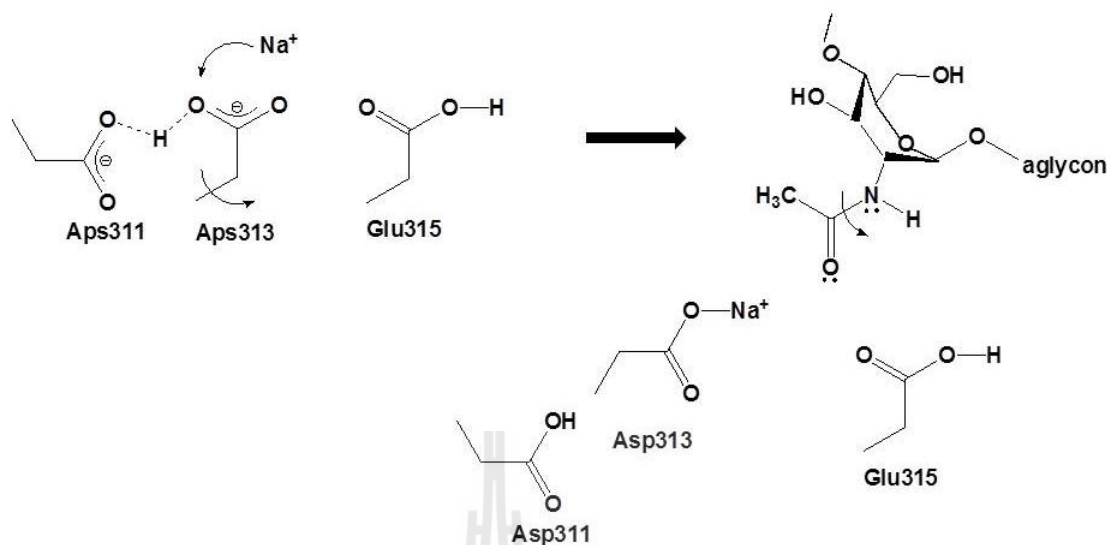
Figure 4.1 Proposed mechanism of sodium cation inhibiting the activity of the wild-type *Vh*ChiA (modified from Suginta *et al*., 2012).

To confirm that sodium or potassium ion from 0.1 M phosphate buffer, pH 7.5 that we used for this experiment will not interrupt the sodium azide inhibition study, the concentrations of sodium and potassium phosphate buffers (0.1, 0.5, 1.0, and 2.0 M) were varies. From the enzyme activity assay, we found that 0.1 M sodium and potassium phosphate buffers showed high specific activity, when compared to other concentrations, whereas 2.0 M sodium and potassium phosphate buffers displayed a decrease in the specific activity. The results suggested that sodium or potassium phosphate buffer at high concentration (2.0 M) affected the enzyme activity, but 0.1 M phosphate buffer did not interfere the kinetic study of enzyme inhibition (Figure 3.2.4).

The kinetic analysis showed that sodium azide acted as a reversible inhibitor for WT *Vh*ChiA, with the pattern of mixed-type inhibition. The mechanism displayed lower αK_i of ESI complex than K_i of EI complex, indicating that sodium azide acted more effectively on ES complex than on free E (Scheme 4.1).

Scheme 4.1 (Copeland, 2000)
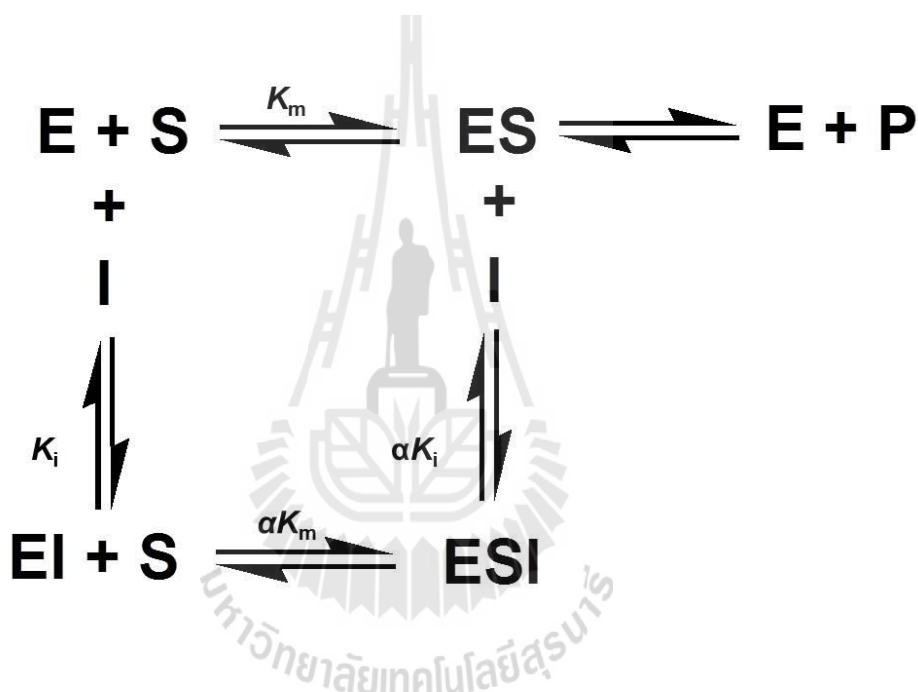
Where K_m, K_i, αK_m and αKi represent the various equilibrium constants for enzyme-substrate (ES), enzyme-inhibitor (EI), enzyme-substrate-inhibitor (ESI, forms when substrate binds to EI) and (ESI, forms when inhibitor binds to ES)

The inhibitory effect of sodium azide on WT *Vh*ChiA was also confirmed by IC_{50} using *p*NP-GlcNAc$_2$ as substrate and TLC using GlcNAc$_6$ and colloidal chitin as substrates. The dose-response curve displayed IC_{50} of 0.40 ± 0.02 M. This IC_{50} value was used to convert to K_i value using Equation 3.2.3 (Cheng and Prusoff, 1973), and

the K_i value estimated from dose response curve was compared with the value obtained from Dixon plot. The results showed K_i obtained from IC_{50} and Dixon plot are similar, which are around 1.50 M. Time-courses of hydrolysis of chitooligosaccharides were investigated by TLC. The results showed that the reactions with sodium azide increased as longer time of incubation, comparing with the reaction without sodium azide. The results suggested that sodium azide, indeed, inhibited the chitinase activity of WT *Vh*ChiA towards its natural substrates.

We postulate that the azide anion interacts with the protonated side chain of the catalytic carboxyl group of Glu315, subsequently preventing the incoming substrate to be accessed by this residue. Figure 4.2 shows how sodium azide interrupts the catalytic cycle at the cleavage step of WT *Vh*ChiA. This simplified mechanism demonstrates that the azide anion competes with the chitin substrate by simply abstracting a proton from the γ-COOH group of Glu315. The products of this reaction are hydrogen azide (HN_3) and the deprotonated form (γ-COO⁻) of Glu315, which is inactive to attack the glycosidic bond at the cleavage site. Basically, the azide anion might diminish the proportion of the effective proton essentially required for bond cleavage.
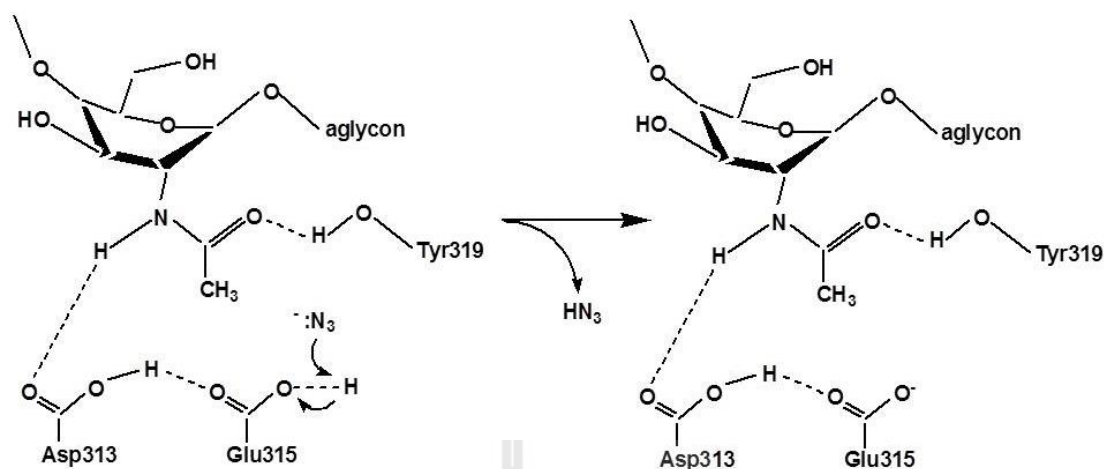
Figure 4.2 Proposed mechanism of azide anion inhibiting the hydrolytic activity of the wild-type *Vh*ChiA.

Since *Streptomyces plicatus* hexosaminidase (*Sp*Hex) adopts the substrated-assisted mechanism like all family-18 chitinases, sodium azide presumably acts as a chemical rescue for this enzyme. Here, we set out the kinetic experiments to see the effect of sodium azide on the hydrolytic activity of mutants D313A and D313N and also WT *Vh*ChiA. The results obtained in this study showed that sodium azide inhibited the activity of the three chitinase variants, instead (Figure 3.2.12). The activity loss against pNP-GlcNAc$_2$ substrate is most seen with WT, followed by mutants D313N and D313A, comparing to the activity without sodium azide.

4.3 Kinetics of inhibition of family-20 *β-N*-acetyl-glucosaminidase from *Vibrio harveyi* by sodium azide and sodium nitrate

*Vh*GlcNAcase is a bacterial GH-20 *β-N*-acetylglucosaminidase or GlcNAcase that cleaves chitooligosaccharide fragments via the substrate-assisted retaining mechanism (Kim *et al*., 2007; Vocadlo *et al*., 2005). The catalytic mechanism usually takes place through two steps. In the first step, the glycosidic oxygen is protonated by a catalytic acid to cleave the *β*-(1,4)-glycosidic linkage and to form the oxazolinium ion intermediate, in which the C1 carbon of the -1 sugar is stabilized by anchimeric assistance of the sugar *N*-acetamido group. In the second step, the oxazolinium ion intermediate is attacked by a water molecule from the *β*-side, leading to hydrolysis with net retention of anomeric form (Aronson *et al*., 2006; Zakariassen *et al*., 2011).

Here, we set out kinetic experiments to investigate the effects of sodium azide, formate, acetate, nitrate, and chloride (Figure 3.2.1) on the hydrolytic activity of WT *Vh*GlcNAcase at pH 5.5 and pH 7.5. All sodium salts were found to decrease the specific activity of the enzyme, compared to the hydrolytic reaction without several salts. At higher pH value, especially sodium azide and sodium nitrate displayed the strongest inhibitory effect for this enzyme. However, we found that the GlcNAcase activity with and without sodium salts was decreased at lower pH value, suggesting that the optimal activity of WT *Vh*GlcNAcase is approximately pH 7.5 (Suginta *et al*., 2010), and also at this pH, all sodium salts should be in ionized form (Cobucci-Ponzano *et al*., 2003; Comfort, Bobrov, Ivanen, Shabalin, Harris, Kulminskaya, Brumer, and Kelly, 2007; Viladot *et al*., 1998; Williams *et al*., 2002). In addition, the stronger effects of azide and nitrate anions on WT *Vh*GlcNAcase activity than the other anions may be caused by the negatively charged azide and nitrate ions acting as

a more effective nucleophile to compete with the substrate to interact with the catalytic carboxyl group to inhibit the enzyme (Figure 3.2.1).

To confirm that cation from sodium salts does not affect to WT *Vh*GlcNAcase activity, time courses of the hydrolytic activity of the enzyme with and without cations from sodium azide and potassium azide were investigated at pH 7.5. The strong inhibitory effects of both compounds were observed from the first period of reaction time, compared to the enzyme activity without cation. In addition, sodium azide and potassium azide did not show significantly different into inhibiting the GlcNAcase activity (Figure 3.3.2). The result obtained from this assay suggested that sodium and potassium cations slightly affected the enzyme activity. As such, the inhibitory effects of of the enzyme activity were assumed to be predominated by the presence of the azide or nitrate anion.

We additionally investigated the effect of sodium and potassium phosphate buffer concentrations (0.1, 0.5, 1.0, and 2.0 M) at pH7.5 on the hydrolytic activity of WT *Vh*GlcNAcase. From these results, we found that 0.1 M sodium and potassium phosphate buffers showed the highest specific activity of the enzyme, when compared to the other concentration buffers, whereas 2.0 M sodium and potassium phosphate buffers showed a decrease in the specific activity. The results suggested that 0.1 M sodium and potassium phosphate buffer that we used in this experiment did not interfere the kinetic study of enzyme inhibition.

The kinetic inhibitions on WT *Vh*GlcNAcase activity showed that of sodium azide and sodium nitrate inhibited the enzyme against *p*NP-GlcNAc substrate by competitive inhibition. The mechanism displaying the inhibitor-enzyme complex (EI) is shown in scheme 4.2.

Scheme 4.2

$$E + S \; \underset{}{\overset{K_m}{\rightleftharpoons}} \; ES \; \rightleftharpoons \; E + P$$

$$+$$

$$I$$

$$K_i \; \updownarrow$$

$$EI$$
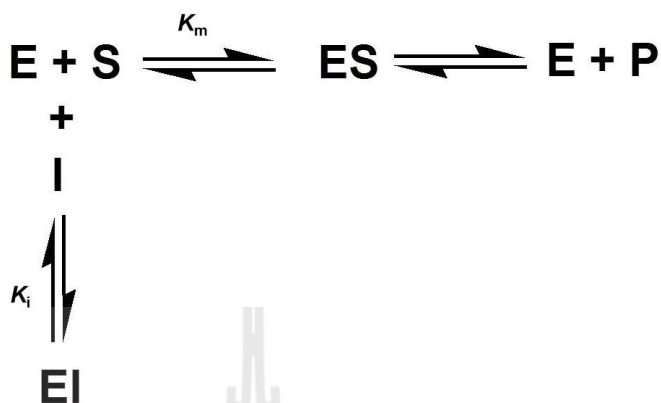
Where K_m and K_i represent the equilibrium constants for enzyme-substrate (ES) and enzyme-inhibitor (EI) complexes.

The inhibitory effects of sodium azide and sodium nitrate on WT *Vh*GlcNAcase were also confirmed by IC_{50} values using *p*NP-GlcNAc as substrate and TLC using $GlcNAc_2$ and $GlcNAc_4$ as substrates. The dose-response curve displayed IC_{50} for sodium azide of 0.30 ± 0.03 M, whereas sodium nitrate showed slightly stronger effect with IC_{50} of 0.20 ± 0.02 M against the activity of WT *Vh*GlcNAcase. The IC_{50} values were used to convert to K_i values using Equation 3.3.3 (Cheng and Prusoff, 1973) to compare with K_i values from Dixon plot and the values are not significantly different. Then, the time-courses of $GlcNAc_2$ and $GlcNAc_4$ hydrolysis were investigated by TLC. The results confirmed that both sodium azide and sodium nitrate are strong inhibitors for this enzyme because no hydrolytic product was detected in the reactions with both compounds.

We postulate that azide and nitrate anions interact with the protonated side chain of the catalytic residue that acts as a catalytic acid in the catalytic mechanism, subsequently preventing the incoming substrate to be accessed by this residue. Figure 4.3 shows how sodium azide/nitrate may interrupt the catalytic cycle at the cleavage step of *Vh*GlcNAcase. This simplified mechanism demonstrates that azide/nitrate anion competes with the chitooligosaccharide substrate by simply abstracting a proton from the β-COOH group of Asp303 that acts as the catalytic residue (Meekrathok, unpublished data). The product of this reaction is the hydrogen azide (HN_3) or the hydrogen nitrate (HNO_3) and the deprotonated form (β-COO$^-$) of Asp303, which is inactive to attack the glycosidic bond at the cleavage site. Basically, the azide and nitrate anions diminish the proportion of the effective proton essentially required for bond cleavage.
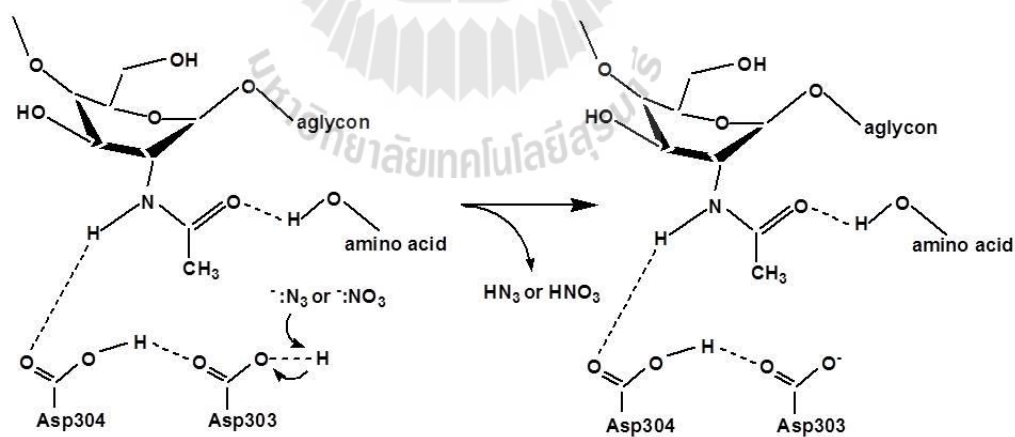
Figure 4.3 Proposed mechanism of azide or nitrate anion inhibits the activity of the wild-type *Vh*GlcNAcase (Meekrathok, unpublished data).

4.4 Comparison of kinetics of inhibition for GH-18 *Vh*ChiA and GH-20 *Vh*GlcNAcase

Vibrio harveyi initially secretes chitinase A (*Vh*ChiA) to degrade chitin polymer, yielding chitooligosaccharide fragments, which can be taken up by the cell through chitoporin. In the periplasm, GlcNAcase (*Vh*GlcNAcase) is sequentially degrades the transported chitooligosaccharides into GlcNAc monomers that are further metabolized inside the cells (Figure 4.4) (Suginta, Chumjan, Mahendran, Janning, Schulte, and Winterhalter, 2013).
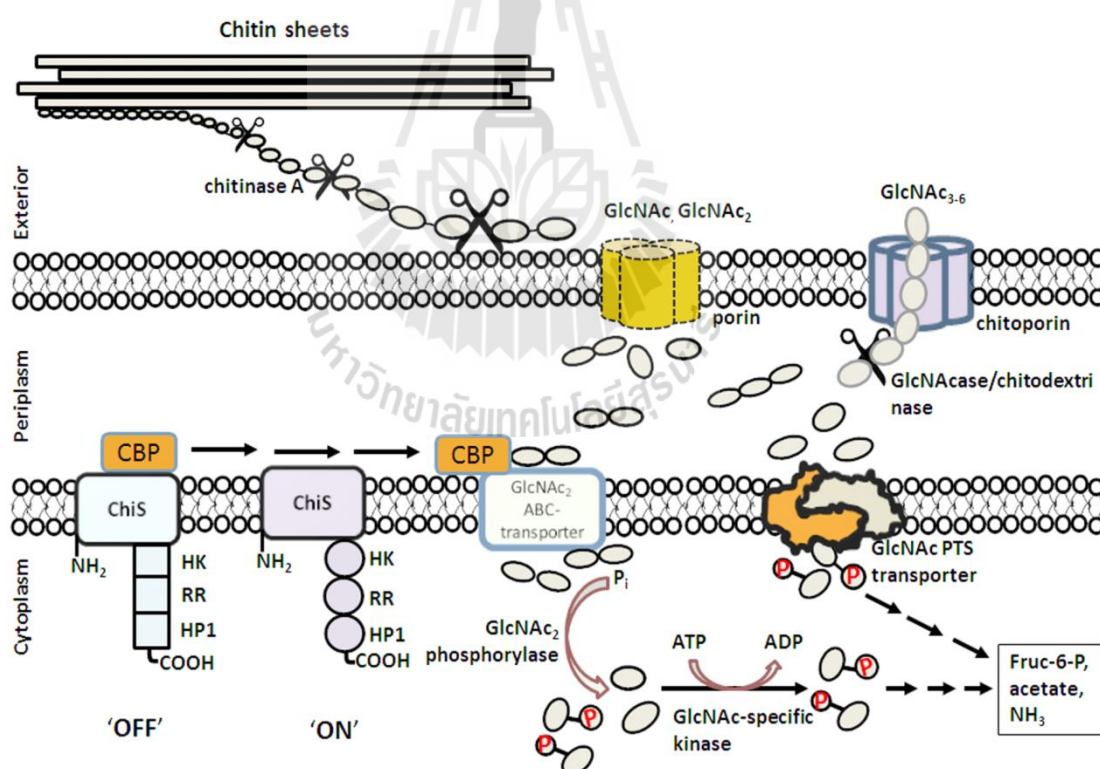
Figure 4.4 Model of the chitin degradation cascade of the marine bacterium *Vibrio harveyi* (Suginta *et al*., 2013).

Although *Vh*ChiA and *Vh*GlcNAcase are different classes of glycoside hydrolases, both catalyze the hydrolytic reaction through the substrate-assisted retaining mechanism (Suginta *et al*., 2005; Suginta *et al*., 2010; Vocadlo *et al*., 2005; Williams *et al*., 2002). In this study, we investigated the effects of sodium salts on the hydrolytic activity of *Vh*ChiA and *Vh*GlcNAcase against *p*NP-glycosides. The results showed that the specific activity of *Vh*ChiA was significantly decreased by sodium azide, whereas *Vh*GlcNAcase was found to be considerably inhibited by sodium azide and sodium nitrate. In addition, the inhibitory effects of sodium azide and sodium nitrate on *Vh*GlcNAcase activity were much effective than *Vh*ChiA. Especially, sodium azide that displayed the most effective inhibitor for both enzymes, it may be because the size and shape of this compound is suitable for the structure of the active site of *Vh*ChiA and *Vh*GlcNAcase.

The binding cleft of *Vh*ChiA has a long, deep groove, which contains six chitooligosaccharide ring-binding subsites (-4)(-3)(-2)(-1)(+1)(+2) (Songsiriritthigul *et al*., 2008). The kinetics of inhibition showed that sodium azide was found to more inhibit the enzyme activity in term of ES complex than the free enzyme that may be because azide anion not only able to react with the catalytic carboxyl group of the enzyme but also the substrate binding residues that located around the active site. In contrast, the binding pocket of *Vh*GlcNAcase contains four substrate binding subsites, designated (-1)(+1)(+2)(+3) (Suginta *et al*., 2010), so it may allow azide or nitrate anion to react with the hydrogen of the catalytic carboxyl group to inhibit the free enzyme activity easily.

Kinetics of inhibition were further investigated using *p*NP-glycosides as substrates and the data showed that sodium azide inhibited *Vh*ChiA employing the mixed-type mode, whereas sodium azide and sodium nitrate were found to inhibit *Vh*GlcNAcase activity using the competitive mode. The inhibitory effects of sodium derivatives on *Vh*ChiA and *Vh*GlcNAcase suggested that both enzymes may adopt the substrate-assisted retaining mechanism in chitin degradation, but the mechanistic details of the catalysis (as accessed by the inhibition study) are not the same, owing to the dissimilar features in shape and molecular arrangement of the binding/catalytic residues that form the binding cleft of the two enzyme species.
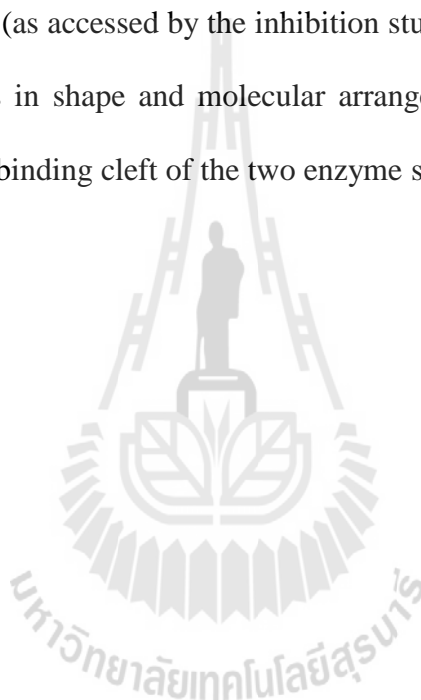
CHAPTER IV

CONCLUSION

This research described transglycosylation reaction and kinetics of inhibitions of sodium salts of small nucleophiles on family-18 chitinase A and family-20 β-N-acetylglucosaminidase from *Vibrio harveyi*. The studies are divided into three parts. The first part was focused on mutation strategies for obtaining chitooligosaccharides with longer chains by transglycosylation reactions. Mutations of Trp570 to Gly and Asp392 to Asn of *Vh*ChiA significantly enhanced the TG reaction, but the TG products were immediately hydrolyzed into chitooligosaccharides with shorter chains. In contrast, mutations of Asp313 to Ala and Asn strongly enhanced the TG reaction, and the products, chitooligosaccharides with longer chains, were not hydrolyzed but accumulated in the reaction mixture. The results obtained from this study may suggest a convenient, strategic design for new chitinase molecules with suitable property for producing the biologically-active chitooligosaccharides required for pharmaceutical and industrial uses.

The second part of this study involved investigation of kinetics of inhibition of family-18 chitinase from *Vibrio harveyi* by sodium azide. *Vh*ChiA degrades chitin employing the substrate-assisted mechanism. Three acidic residues Asp311-Asp313-Glu315 that align linearly at the bottom of the substrate binding cleft have been proposed to play a concerted role in chitin hydrolysis. In particular, Asp313 is thought

to participate in various stages in the catalytic cycle of the *Vh*ChiA. This study investigates the effects of sodium azide, which is known to chemically rescue retaining glycoside hydrolases, on the chitinase activity of the wild-type, as well as the D313A and D313N mutants. The results obtained from this study consistently demonstrate that sodium azide did not recover the activity of the mutants but slightly inhibited the mutants D313A and D313N, respectively, compared to the wild-type, when 2 M sodium azide was added. Decreases in the apparent K_m and k_{cat} at increasing sodium azide concentrations suggest that sodium azide displays mixed-type inhibition with the *p*NP-glycoside substrate. The mixed-type inhibition was further confirmed by the pattern of the lines in Lineweaver-Burk double-reciprocal plots. The mechanism describing the enzyme-azide ion interaction has proposed to involve proton withdrawal from of the side chain of Glu315, thereby preventing bond cleavage.

The third part involved investigation of the kinetics of inhibition of a family-20 *β*-N-acetylglucosaminidase from *Vibrio harveyi* by sodium azide and sodium nitrate. This study investigated the effects of sodium salts on the enzyme activity of GH-20 *Vh*GlcNAcase. The results obtained from this study consistently demonstrate that *Vh*GlcNAcase was strongly inhibited by sodium azide and sodium nitrate. An increase in the apparent K_m and a fairly steady k_{cat} at increasing sodium azide and sodium nitrate concentrations suggest that the two compounds react competitively towards *Vh*GlcNAcase. The competitive inhibition was further confirmed by the pattern of the double-reciprocal lines in Lineweaver-Burk plots. The mechanism describing the enzyme-azide anion or the enzyme-nitrate anion interaction was

proposed to involve proton abstraction of the side chain of the catalytic residue, thereby preventing bond cleavage.

GH-18 *Vh*ChiA and GH-20 *Vh*GlcNAcase were inhibited strongly by sodium azide or sodium nitrate. Sodium azide inhibited *Vh*ChiA in a mixed type manner, whereas the two compounds reacted competitively towards *Vh*GlcNAcase. The resulted suggested that the catalytic mechanisms of both enzymes are not identical, owing to the dissimilar features in shape and molecular arrangement within the enzyme's binding clefts. It is proposed that azide or nitrate anion may abstract the proton from the carboxyl group of the glutamic acid that acts as a catalytic residue in the catalytic mechanism.

The inhibitory effects of both compounds on both enzyme activities were also confirmed by the determination of IC_{50} values and the time courses of the hydrolytic products by TLC that supported the conclusion that azide and nitrate anions are more effective to inhibit the activity of *Vh*GlcNAcase than *Vh*ChiA.

REFERENCES

REFERENCES

Aly, M.R.E., Ibrahim, E-SI., Ashry, E.S.H.E., and Schmidt, R.R. (2001) Synthesis of chitotetraose and chitohexaose based on dimethylmaleoyl protection. **Carbohydr. Res.** 331: 129-142.

Armand, S., Tomita, H., Heyraud, A., Gey, C., Watanabe, T., and Henrissat, B. (1994). Stereochemical course of the hydrolysis reaction catalyzed by chitinases A1 and D from *Bacillus circulans* WL-12. **FEBS Lett.** 343: 177-180.

Aronson, N.N. Jr., Halloran, B.A., Alexyev, M.F., Amable, L., Madura, J.D., Pasupulati, L., Worth, C., and Van Roey, P. (2003). Family 18 chitinaseoligosaccharide substrate interaction: subsite preference and anomer selectivity of *Serratia marcescens* chitinase A. **Biochem. J.** 376: 87-95.

Aronson, N.N., Halloran, B.A., Alexeyev, M.F., Zhou, X.E., Wang, Y., Meehan, E.J., and Chen, L. (2006) Mutation of a conserved tryptophan in the chitin-binding cleft of *Serratia marcescens* chitinase A enhances transglycosylation. **Biosci. Biotechnol. Biochem.** 70: 243-251.

Brameld, K.A. and Goddard III, W.A. (1998). Substrate distortion to a boat conformation at subsite -1 is critical in the mechanism of family 18 chitinases. **J. Am. Chem. Soc.** 120: 3571-3580.

Brameld, K.A. and Goddard, W.A. III. (1998). The role of enzyme distortion in the single displacement mechanism of family 19 chitinases. **Proc. Nat. Acad. Sci.** 95: 4276-4281.

Centinbas, N., Macauley, M.S., Stubbs, K.A., Drapala, R., and Vocadlo, D.J. (2006). Identificationof Asp174 and Asp175 as the key catalytic residues of human O-GlcNAcase by functional analysis of site-directed mutants. **J. Am. Chem. Soc.** 45: 3835-3844.

Cheng, Y.C. and Prusoff, W.H. (1973). Relationship between the inhibition constant (K1) and the concentration of inhibitor which causes 50 per cent inhibition (I50) of an enzymatic reaction. **Biochem. Pharmacol.** 22: 3099-3108.

Chen, J.K., Shen, C-R., and Liu, C-L. (2010). *N*-acetylglucosamine: production and applications. **Mar. Drugs.** 8: 2493-2516.

Chitlaru, E. and Roseman, S. (1996). Molecular cloning and characterization of a novel *β-N*-acetyl-D-glucosaminidase from *Vibrio furnissii*. **J. Mol. Biol.** 271: 33433-33439.

Choi, K-H., Seo, J.Y., Park, K-M., Park, C-S., and Cha, J. (2009). Characterization of glycosyl hydrolase family 3 β-*N*-acetylglucosaminidases from *Thermotoga maritima* and *Thermotoga neapolitana*. **J. Biosci. Bioeng.** 108: 455-459.

Cobucci-Ponzano, B., Trincone, A., Giordano, A., Rossi, M., and Moracci, M. (2003). Identification of the catalytic nucleophile of the family 29 alpha-L-fucosidase from *Sulfolobus solfataricus* via chemical rescue of an inactive mutant. **Biochemistry.** 42: 9525-9531.

Cohen-Kupiec, R. and Chet, I. (1998). The molecular biology of chitin digestion. **Curr. Opin. Biotechnol.** 9: 270-277.

Comfort, D.A., Bobrov, K.S., Ivanen, D.R., Shabalin, K.A., Harris, J.M., Kulminskaya, A.A., Brumer, H., and Kelly, R.M. (2007). Biochemical analysis of *Thermotoga maritima* GH36 α-Galactosidase (*Tm*GalA) confirms the mechanistic commonality of clan GH-D glycoside hydrolases. **Biochemistry.** 46: 3319-3330.

Copeland, R. A., (2000). Enzymes: a practical introduction to structure, mechanism, and data analysis. John Wiley and Sons, Inc., New York, USA.

Davies, G. and Henrissat B. (1995). Structures and mechanisms of glycosyl hydrolases. **Structure.** 3: 853-859.

Davies, G.J., Wilson, K.S., and Henrissat, B. (1997). Nomenclature for sugar-binding subsites in glycosyl hydrolases. **Biochem. J.** 321: 557-559.

Dı́ez, B., Rodrı́guez-Saı́z, M., de la Fuente, J.L., Moreno, M.A´., and Barredo, J.L. (2005). The nagA gene of *Penicillium chrysogenum* encoding β-*N*-acetylglucosaminidase, **FEMS Microbiol. Lett.** 242: 257-264.

Di Rosa, M., Malaguarnera, G., De Gregorio, C., Drago, F., and Malaguarnera, L. (2012). Evaluation of CHI3L-1 and CHIT-1 expression in differentiated and polarized macrophages. **Inflammation.** 36: 482-492.

Donnelly, L.E. and Barnes, P.J. (2004). Acidic mammalian chitinase - a potential target for asthma therapy. **Trends Pharmacol. Sci.** 25: 509-511.

Fujita, K., Sato, R., Toma, K., Kitahara, K., Suganuma, T., Yamamoto, K., and Takegawa, K. (2007). Identification of the catalytic acid base residue of arthrobacter endo-beta-*N*-acetylglucosaminidase by chemical rescue of an inactive mutant, **J. Biochem.** 142: 301-306.

Fukamizo, T., Goto, S., Torikata, T., and Araki, T. (1989). Enhancement of transglycosylation activity of lysozyme by chemical modification. **Agric. Biol. Chem.** 53: 2641-2651.

Fukamizo, T., Koga, D., and Goto, S. (1995). Comparative Biochemistry of chitinases-anomeric form of the reaction Products. **Biosci. Biotech. Biochem.** 59: 311-313.

Fukamizo, T., Sasaki, C., Schelp, E., Bortone, K., and Robertus, J.D. (2001). Kinetic properties of chitinase-1 from the fungal pathogen *Coccidioides immitis*. **Biochemistry.** 40: 2448-2454.

Fukamizo, T., Miyake, R., Tamura, A., Ohnuma, T., Skriver, K., Pursiainenc, N.V., and Juffer, A.H. (2009). A flexible loop controlling the enzymatic activity and specificity in a glycosyl hydrolase family 19 endochitinase from barley seeds (*Hordeum vulgare L.*). **BBA-Proteins and Proteomics.** 1794: 1159-1167.

Funkhouser, J.D. and Aronson, N.N. (2007). Chitinase family GH18: evolutionary insights from the genomic history of a diverse protein family. **BMC. Evol. Biol.** 7: 96.

Hart, P.J., Pfluger, H.D., Monzingo, A.F., Hollis, T., and Robertus, J.D. (1995). The refined crystal structure of an endochitinase from *Hordeum vulgare* L. seeds at 1.8 Å resolution. **J. Mol. Biol.** 248: 402-413.

Harvey, A.J., Hrmova, M., De Gori, R., Varghese, J.N., and Fincher, G.B. (2000). Comparative modeling of the three-dimensional structures of family 3 glycoside hydrolases. **Proteins.** 2: 257-269.

Henrissat, B. and Bairoch, A. (1993). New families in the classification of glycosyl hydrolases based on amino acid sequence similarities. **Biochem. J.** 293: 781-788.

Henrissat, B. and Davies, G.J. (2000). Glycoside hydrolases and glycosyltransferases. families, modules, and implications for genomics. **Plant. Physiol.** 124: 1515-1519.

Henrissat, B. and Daviest, G. (1997). Structural and sequence-based classification of glycoside hydrolases. **J. Struct. Biol.** 7: 637-644.

Hoell, I.A., Dalhus, B., Heggset, E.B., Aspmo, S.I., and Eijsink, V.G.H. (2006). Crystal structure and enzymatic properties of a bacterial family 19 chitinase reveal differences from plant enzymes. **FEBS J.** 273: 4889-4900.

Hollis, T., Honda, Y., Fukamizo, T., Marcotte, E., Day, P.J., and Robertus, J.D. (1997). Kinetic analysis of barley chitinase. **Arch. Biochem. Biophys.** 344: 335-342.

Hurtado-Guerrero, R., Schuttelkopf, A.W., Mouyna, I., Ibrahim, A.F., Shepherd, S., Fontaine, T., Latge, J.P., and van Aalten, D.M. (2009) Molecular mechanisms of yeast cell wall glucan remodeling. **J. Biol. Chem.** 284: 8461-8469.

Ikegami, T., Okada, T., Hashimoto, M., Seino, S., Watanabe, T., and Shirakawa, M. (2000). Solution structure of the chitin-binding domain of *Bacillus circulans* WL-12 Chitinase A1. **J. Biol. Chem.** 275: 13654-13661.

Ilankovan, P., Hein, S., Ng, C-H., Trung, T.S., and Stevens, W.F. (2006). Production of N-acetyl chitobiose from various chitin substrates using commercial enzymes. **Carbohydr. Polym.** 63: 245-250.

Iseli, B., Armand, S., Boller, T., Neuhaus, Jean-Marc, and Henrissat, B. (1996). Plant chitinases use two different hydrolytic mechanisms. **FEBS Lett.** 382: 186-188.

Kadokura, K., Sakamoto, Y., Saito, K., Ikegami, T., Hirano, T., Hakamata, W., Oku, T., and Nishio, T. (2007). Production of a recombinant chitin oligosaccharide deacetylase from *Vibrio parahaemolyticus* in the culture medium of *Escherichia coli* cells. **Biotechnol. Lett.** 29: 1209-1215.

Kanneganti, M., Kamba, A., and Mizoguchi, E. (2013). Role of chitotriosidase (chitinase 1) under normal and disease conditions. **J. Epithel. Biol. Pharmacol.** 5: 1-9.

Kaku, H., Nishizawa, Y., Ishii-Minami, N., Akimoto-Tomiyama, C., Dohmae, N., Takio, K., Minami, E., and Shibuya, N. (2006). Plant cells recognize chitin fragments for defense signaling through a plasma membrane receptor. **Proc. Nat. Acad. Sci.** 103: 11086-11091.

Kanie, O., Ito, Y., and Ogawa, T. (1994). Orthogonal glycosylation strategy in oligosaccharide synthesis. **J. Am. Chem. Soc.** 116: 12073-12074.

Kawase, T., Saito, A., Sato, T., Kanai, R., Fujii, T., Nikaidou, N., Miyashita, K., and Watanabe, T. (2004). Distribution and phylogenetic analysis of family 19 chitinases in actinobacteria. **Appl. Environ. Microbiol.** 70: 1135-1144.

Kim, S., Matsuo, I., Ajisaka, K., Nakajima, H., and Kitamoto, K. (2002). Cloning and characterization of the *nag A* gene that encodes *β-N*-acetylglucosaminidases from *Aspergillus nidulans* and its expression in *Aspergillus oryzae*. **Biosci. Biotechnol. Biochem.** 10: 2168-2175.

Koide, S.S. (1998). Chitin-chitosan: properties, benefits and risks. **Nutr. Res.** 18: 1091 1101.

Kubota, T., Miyamoto, K., Yasuda, M., Inamori, Y., and Tsujibo, H. (2004). Molecular characterization of an intracellular *β-N*-acetylglucosaminidase involved in the chitin degradation system of *Streptomyces thermoviolaceus* OPC-520. **Biosci. Biotechnol. Biochem.** 68: 1306-1314.

Kumar, A.B.V., Varadaraj, M.C., Gowda, L.R., and Tharanathan, R.N. (2005). Characterization of chito-oligosaccharides prepared by chitosanolysis with the aid of papain and pronase, and their bactericidal action against *Bacillus cereus* and *Escherichia coli*. **Biochem. J.** 391: 167-175.

Kzhyshkowska, J., Gratchev, A., and Goerdt, S. (2007). Human chitinases and chitinase-like proteins as indicators for inflammation and cancer. **Biomark. Insights.** 2: 128-146.

Langley, D.B., Harty, D.W.S., Jacques, N.A., Hunter, N., Guss, J.M., and Collyer, C.A. (2008). Structure of *N*-acetyl-*β*-D-glucosaminidase (GcnA) from the Endocarditis Pathogen *Streptococcus gordonii* and its Complex with the Mechanism-based Inhibitor NAG-Thiazoline. **J. Mol. Biol.** 377: 104-116.

Li, H., Morimoto, K., Katagiri, N., Kimura, T., Sakka, K., Lun, S., and Ohmiya, K. (2002). A novel *β-N*-acetylglucosaminidase of *Clostridium paraputrificum* M-21 with high activity on chitobiose. **Appl. Microbiol. Biotechnol.** 60: 420-427.

MacLeod, A.M., Lindhorst, T., Withers, S.G., and Warren, R.A. (1994). The acid/base catalyst in the exoglucanase/xylanase from *Cellulomonas fimi* is glutamic acid 127: evidence from detailed kinetic studies of mutants. **Biochemistry.** 33: 6371-6376.

Madhuprakash, J., Tanneeru, K., Purushotham, P., Guruprasad, L., and Podile, A.R. (2012). Transglycosylation by chitinase D from *Serratia proteamaculans* improved through altered substrate interactions. **J. Biol. Chem.** 287: 44619-44627.

Mark, B.L., Wasney, G.A., Salo, T.J.S., Khan, A.R., Cao, Z., Robbins, P.W., James, M.N.G., and Triggs-Raine B.L. (1998). Structural and functional characterization of *Streptomyces plicatus* *β-N*-acetylhexosaminidase by comparative molecular modeling and site-directed mutagenesis. **J. Biol. Chem.** 273: 19618-19624.

Mark, B.L., Vocadlo, D.J., Knapp, S., Triggs-Raine B.L., Withers S.G., and James, M.N.G. (2001). Crystallographic evidence for substrate-assisted catalysis in a bacterial *β*-hexosaminidase. **J. Biol. Chem.** 276: 10330-10337.

Martinez, E.A., Boer, H., Koivula, A., Samain, E., Driguez, H., Armand, S., and Cottaz, S. (2012). Engineering chitinases for the synthesis of chitin oligosaccharides: Catalytic amino acid mutations convert the GH-18 family glycoside hydrolases into transglycosylases. **J. Mol. Catal. B: Enzym.** 74: 89-96.

Matsuo, Y., Kurita, M., Park, J.K., Tanaka, K., Nakagawa, T., Kawamukai, M., and Matsuda, H. (1999). Purification, characterization and gene analysis of *N*-acetylglucosaminidase from *Enterobacter* sp. G-1. **Biosci. Biotechnol. Biochem.** 63: 1261-1268.

Mayer, C., Vocadlo, D.J., Mah, M., Rupitz, K., Stoll, D., Warren, R.A., and Withers, S.G. (2006). Characterization of a beta-*N*-acetylhexosaminidase and a beta-*N*-acetylglucosaminidase/beta-glucosidase from *Cellulomonas fimi*. **FEBS. J.** 13: 2929-2941.

Miya, A., Albert, P., Shinya, T., Desaki, Y., Ichimura, K., Shirasu, K., Narusaka, Y., Kawakami, N., Kaku, H., and Shibuya, N. (2007). CERK1, a LysM receptor kinase, is essential for chitin elicitor signaling in Arabidopsis. **Proc. Nat. Acad. Sci.** 104: 19613-19618.

Nanjo, F., Sakai, K., Ishikawa, M., Isobe, K., and Usui, T. (1989). Properties and transglycosylation reaction of a chitinase from *Nocardia orientalis*. **Agric. Biol. Chem.** 53: 2189-2195.

Nogawa, M., Takahashi, H., Kashiwagi, A., Ohshima, K., Okada, H., and Morikawa Y. (1998). Purification and characterization of exo-*β*-D-glucosaminidase from a cellulolytic fungus, *Trichoderma reesei* PC-3-7. **Appl. Environ. Microbiol.** 64: 890-895.

Paal, K., Ito, M., and Withers, S.G. (2004). *Paenibacillus* sp. TS12 glucosylceramidase: kinetic studies of a novel sub-family of family 3 glycosidases and identification of the catalytic residues. **Biochem. J.** 378: 141-149.

Papanikolau, Y., Prag, G., Tavlas, G., Vorgias, C.E., and Petratos, K. (2003). De novo purification scheme and crystallization conditions yield high-resolution structures of chitinase A and its complex with the inhibitor allosamidin. **Acta. Cryst.** D59: 400-403.

Papanikolau, Y., Prag, G., Tavlas, G., Vorgias, C.E., Oppenheim, A.B., and Petratos, K. (2001). High resolution structural analyses of mutant chitinase A complexes with substrates provide new insight into the mechanism of catalysis. **Biochemistry.** 40: 11338-11343.

Park, J.K., Kim, W.J., and Park, Y.I. (2010). Purification and characterization of an exo-type *β-N*-acetylglucosaminidase from *Pseudomonas fluorescens* JK-0412. **J. Appl. Microbiol.** 1364-5072: 1-10.

Patil, R.S., Ghormade, V. and Deshpande, M.V. (2000). Chitinolytic enzymes: an exploration. **Enzyme. Microbial. Technol.** 26: 473-483.

Perrakis, A., Tews, I., Dauter, Z., Oppenheim, A.B., Chet, I., Wilson, K.S., and Vorgias, C.E. (1994). Crystal structure of a bacterial chitinase at 2.3 A resolution. **Structure.** 2: 1169-1180.

Petutschnig, E.K., Jones, A.M., Serazetdinova, L., Lipka, U., and Lipka, V. (2010). The lysin motif receptor-like kinase (LysM-RLK) CERK1 is a major chitin-binding protein in Arabidopsis thaliana and subject to chitin-induced phosphorylation. **J. Biol. Chem.** 285: 28902-28911.

Purushotham, P. and Podile, A.R. (2012). Synthesis of long-chain chitooligosaccharides by a hypertransglycosylating processive endochitinase of *Serratia proteamaculans* 568. **J. Bacteriol.** 194: 4260-4271.

Qin, C., Li, H., Xiao, Q., Liu, Y., Zhu, J., and Du, Y. (2006). Water-solubility of chitosan and its antimicrobial activity. **Carbohydr. Polym.** 63: 367-374.

Ramasubbu, N., Thomas, L.M., Ragunath, C., and Kaplan, J.B. (2005). Structural analysis of dispersin B, a biofilm-releasing glycoside hydrolase from the periodontopathogen *Actinobacillus actinomycetemcomitans*. **J. Mol. Biol.** 349: 475-486.

Rinaudo, M. (2006). Chitin and chitosan: properties and applications. **Prog. Polym. Sci.** 31: 603-632.

Rosa, M.D., Malaguarnera, G., De Gregorio, C., Drago, F., and Malaguarnera, L. (2012). Evaluation of CHI3L-1 and CHIT-1 expression in differentiated and polarized macrophages. **Inflammation.** 36: 482-492.

Sasaki, C., Yokoyama, A., Itoh, Y., Hashimoto, M., Watanabe, T., and Fukamizo, T. (2002). Comparative study of the reaction mechanism of family 18 chitinases from plants and microbes. **J. Biochem.** 131: 557-564.

Sashiwa, H., Fujishima, S., Yamano, N., Kawasaki, N., Nakayama, A., Muraki, E., Sukwattanasinitt, M., Pichyangkurac, R., and Aiba, S. (2003). Enzymatic production of *N*-acetyl-D-glucosamine from chitin. Degradation study of *N*-acetyl chitooligosaccharide and the effect of mixing of crude enzymes. **Carbohydr. Polym.** 51: 391-395.

Shallom, D., Belakhov, V., Solomon, D., Shoham, G., Baasov, T., and Shoham, Y. (2002). Detailed kinetic analysis and identification of the nucleophile in α-L-arabinofuranosidase from *Geobacillus stearothermophilus* T-6, a Family 51 glycoside hydrolase. **J. Biol. Chem.** 277: 43667-43673.

Songsiriritthigul, C., Pantoom, S., Aguda, A.H., Robinson, R.C., and Suginta, W. (2008). Crystal structures of *Vibrio harveyi* chitinase A complexed with chitooligosaccharides: Implications for the catalytic mechanism. **J. Struct. Biol.** 162: 491-499.

Suginta, W., Robertson, P.A., Austin, B., Fry, S.C., and Fothergill-Gilmore, L.A. (2000). Chitinases from *Vibrio*: activity screening and purification of chiA from *Vibrio carchariae*. **J. Appl. Microbiol.** 89: 76-84.

Suginta, W., Vongsuwan, A., Songsiriritthigul C., Prinz, H., Estibeiro, P., Duncan, R. R., Svasti, J., and Fothergill-Gilmore, L.A. (2004). An endochitinase A from *Vibrio carchariae*: cloning, expression, mass and sequence analyses, and chitin hydrolysis. **Arch. Biochem. Biophys.** 424: 171-180.

Suginta, W., Vongsuwan, A., Songsiriritthigul, C., Svasti, J., and Prinz, H. (2005). Enzymatic properties of wild-type and active site mutants of chitinase A from *Vibrio carchariae*, as revealed by HPLC-MS. **FEBS J.** 272: 3376-3386.

Suginta, W., Songsiriritthigul, C., Kobdaj, A., Opassiri, R., and Svasti, J. (2007). Mutations of Trp275 and Trp397 altered the binding selectivity of *Vibrio carchariae* chitinase A. **Biochim. Biophys. Acta.** 1770: 1151-1160.

Suginta, W., Pantoom, S., and Prinz, H. (2009). Substrate binding modes and anomer selectivity of chitinase A from *Vibrio harveyi*. **J. Chem. Biol.** 2: 191-202.

Suginta, W., Chuenark, D., Mizuhara, M., and Fukamizo, T. (2010). Novel *β-N*-acetylglucosaminidases from *Vibrio harveyi* 650: cloning, expression, enzymatic properties, and subsite identification. **BMC. Biochem.** 11: 1-12.

Suginta, W. and Sritho, N. (2012). Multiple roles of Asp313 in the refined catalytic cycle of chitin degradation by *Vibrio harveyi* chitinase A. **Biosci., Biotechnol. Biochem.** 76: 2275-2281.

Suginta, W., Chumjan, W., Mahendran, K.R., Janning, P., Schulte, A., and Winterhalter, M. (2013). Molecular uptake of chitooligosaccharides through chitoporin from the marine bacterium *Vibrio harveyi*. **PLoS ONE.** 8: e55126.

Sumida, T., Ishii, R., Yanagisawa, T., Yokoyama, S., and Ito, M. (2009). Molecular cloning and crystal structural analysis of a novel *β-N*-acetylhexosaminidase from *Paenibacillus* sp. TS12 capable of degrading glycosphingolipids. **J. Mol. Biol.** 392: 87-99.

Synstad, B., Gaseidnes, S., van Aalten, D.M., Vriend, G., Nielsen, J.E., and Eijsink, V.G. (2004). Mutational and computational analysis of the role of conserved residues in the active site of a family 18 chitinase. **Eur. J. Biochem.** 271: 253-262.

Taira, T., Fujiwara, M., Dennhart, N., Hayashi, H., Onaga, S., Ohnuma, T., Letzel, T., Sakuda, S., and Fukamizo, T. (2010). Transglycosylation reaction catalyzed by a class V chitinase from cycad, *Cycas revoluta*: A study involving site-directed mutagenesis, HPLC, and real-time ESI-MS. **Biochim. Biophys. Acta.** 1804: 668-675.

Tews, I., Perrakis, A., Oppenheim, A., Dauter, Z., Wilson, K.S., and Vorgias, C.E. (1996). Bacterial chitobiase structure provides insight into catalytic mechanism and the basis of Tay-Sachs disease. **Nature. Structural. Biol.** 3: 638-648.

Tews, I., Terwisscha van Scheltinga, A.C., Perrakis, A., Wilson, K.S., and Dijkstra, B.W. (1997). Substrate-assisted catalysis unifies two families of chitinolytic enzymes. **J. Am. Chem. Soc.** 119: 7954-7959.

Ueda, M., Fujita, Y., Kawaguchi, T., and Araai, M. (2000). Cloning, nucleotide sequence and expression of the *β-N*-acetyl-glucosaminidase gene from *Aeromonas* sp. No. 10S-24. **J. Biosci. Bioeng.** 89: 164-169.

Ueda, M., Kojima, M., Yoshikawa, T., Mitsuda, N., Araki, K., Kawaguchi, T., Miyatake, K., Arai, M., and Fukamizo, T. (2003). A novel type of family 19 chitinase from *Aeromonas* sp. No. 10S-24. Cloning, sequence, expression, and the enzymatic properties. **Eur. J. Biochem.** 270: 2513-2520.

Umemoto, N., Ohnuma, T., Mizuhara, M., Sato, H., Skriver, K., and Fukamizo, T. (2013). Introduction of a tryptophan side chain into subsite +1 enhances transglycosylation activity of a GH-18 chitinase from *Arabidopsis thaliana*, *At*ChiC. **Glycobiology.** 23: 81-90.

Vallmitjana, M., Ferrer-Navarro, M., Planell, R., Abel, M., Ausín, C., Querol, E., Planas, A., and Pérez-Pons, J.A. (2001). Mechanism of the family 1 beta-glucosidase from *Streptomyces* sp: catalytic residues and kinetic studies. **Biochemistry.** 40: 5975-5982.

van Aalten, D., Komander, D., Synstad, B., Gaseidnes, S., Peter, M., and Eijsink, V. (2001). Structural insights into the catalytic mechanism of a family 18 exo-chitinase. **Proc. Nat. Acad. Sci.** 98: 8979-8984.

van Scheltinga, A.C.T., Hennig, M., and Dijkstra, B.W. (1996). The 1.8 Å Resolution structure of hevamine, a plant chitinase/lysozyme, and analysis of the conserved sequence and structure motifs of glycosyl hydrolase family 18. **J. Mol. Biol.** 262: 243-257.

Viladot, J.L., de Ramon, E., Durany, O., and Planas, A. (1998). Probing the mechanism of *Bacillus* 1,3-1,4-*β*-D-glucan 4-glucanohydrolases by chemical rescue of inactive mutants at catalytically essential residues. **Biochemistry.** 37: 11332-11342.

Vocadlo, D.J. and Withers, S.G. (2005). Detailed comparative analysis of the catalytic mechanisms of *β-N*-acetylglucosaminidases from families 3 and 20 of glycoside hydrolases. **Biochemistry.** 44: 12809-12818.

Vuong, T.V. and Wilson, D.B. (2010). Glycoside hydrolases: catalytic base/nucleophile diversity. **Biotechnol. Bioeng.** 107: 195-205.

Williams, S.J., Mark, B.L., Vocadlo, D.J., James, M.N.G., and Withers, S.G. (2002). Aspartate 313 in the *Streptomyces plicatus* hexosaminidase plays a critical role in substrate-assisted catalysis by orienting the 2-acetamido group and stabilizing the transition state. **J. Biol. Chem.** 277: 40055-40065.

Wills-Karp, M. and Karp, C.L. (2004). Chitin checking: novel insights into asthma. **N. Engl. J. Med.** 351: 1455-1457.

Yamaguchi, K., Yamada, K., Ishikawa, K., Yoshimura, S., Hayashi, N., Uchihashi, K., Ishihama, N., Kishi-Kaboshi, M., Takahashi, A., Tsuge, S., Ochiai, H., Tada, Y., Shimamoto, K., Yoshioka, H., and Kawasaki, T. (2013). A receptor-like cytoplasmic kinase targeted by a plant pathogen effector is directly phosphorylated by the chitin receptor and mediates rice immunity. **Cell. Host. Microbe.** 13: 347-357.

Zakariassen, H., Hansen, M.C., Jøranli, M., Eijsink, V.G., and Sørlie, M. (2011). Mutational effects on transglycosylating activity of family 18 chitinases and construction of a hypertransglycosylating mutant. **Biochemistry.** 50: 5693-5703.

Zhu, Z., Zheng, T., Homer, R.J., Kim, Y.K., Chen, N.Y., Cohn, L., Hamid, Q., and Elias, J.A. (2004). Acidic mammalian chitinase in asthmatic Th2 inflammation and IL-13 pathway activation. **Science.** 304: 678-1682.
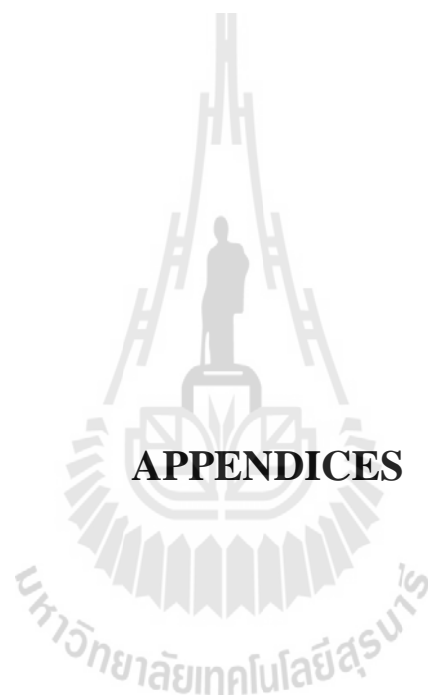
APPENDICES

APPENDIX A

STANDARD CURVES

1. Stand curve of BSA by Bradford's method

Plot showing Absorbance of 540 nm versus BSA (µg/ml) with equation y = 0.0025x + 0.0104 and R² = 0.9952.
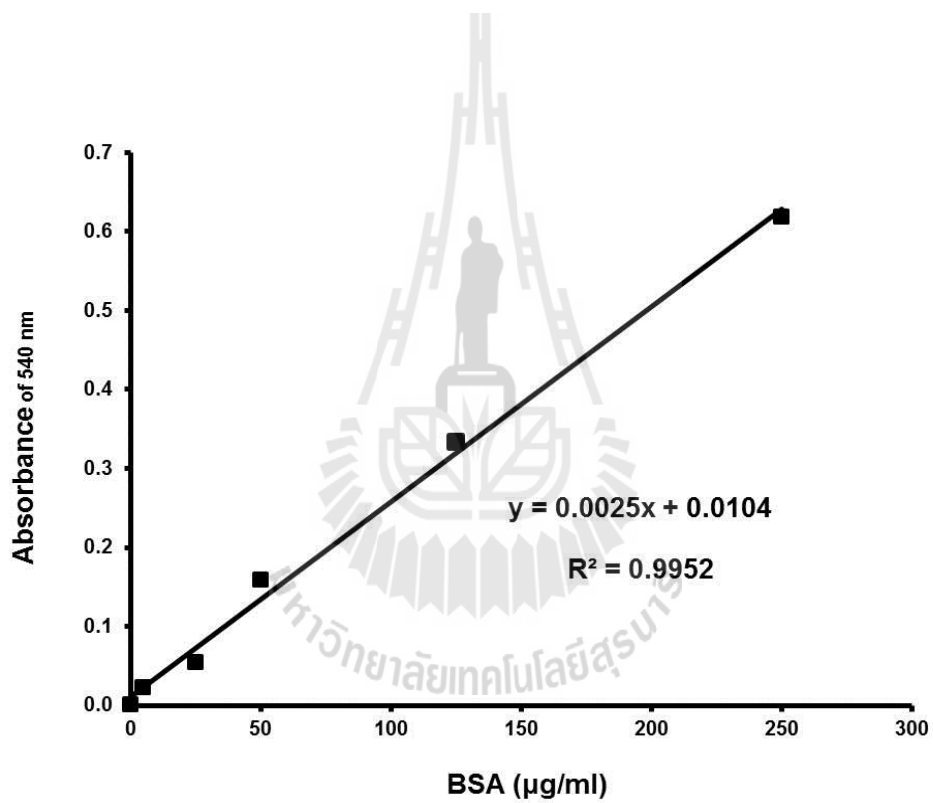
2. Standard curve of p-nitrophenol

$$y = 0.0462x + 0.0036$$

$$R^2 = 0.9997$$
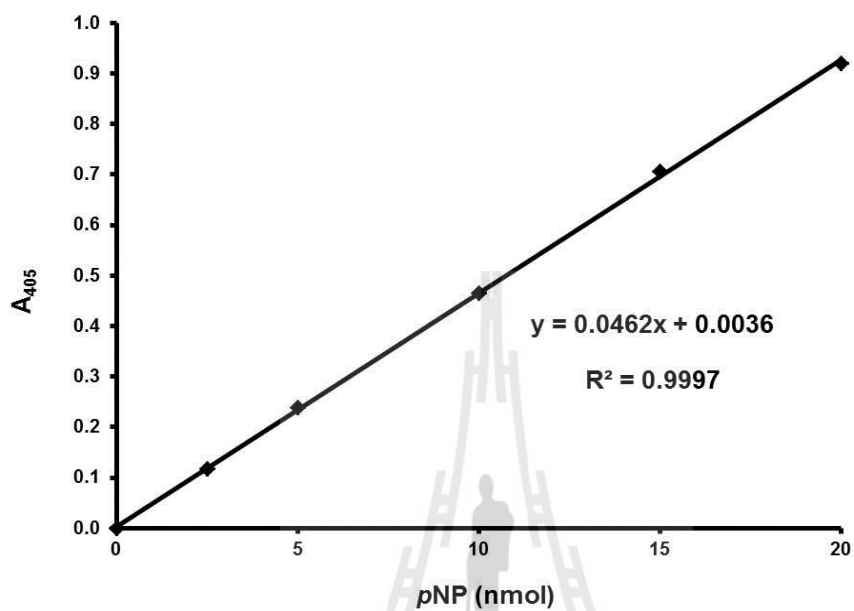
APPENDIX B

PUBLICATIONS

Sirimontree, P., Suginta, W., Sritho, N., Kanda, Y., Shinya, S., Ohnuma, T., and Fukamizo, T. (2014). Mutation strategies for obtaining chitooligosaccharides with longer chains by transglycosylation reaction of family GH18 chitinase. **Biosci. Biotechnol. Biochem.** 1-9.
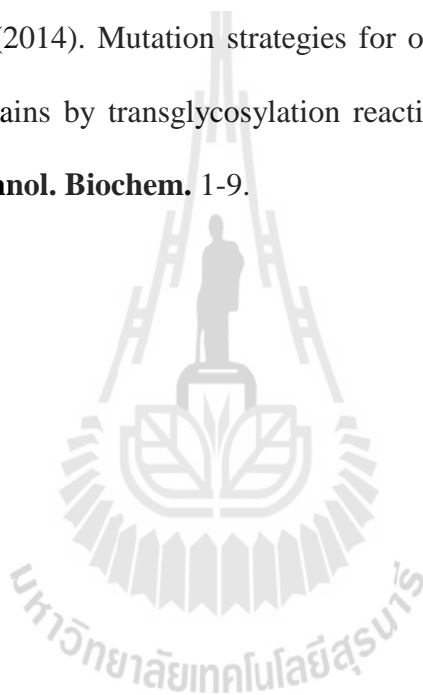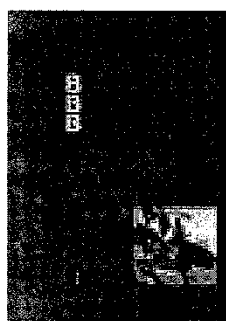
Bioscience, Biotechnology, and Biochemistry

Mutation strategies for obtaining chitooligosaccharides with longer chains by transglycosylation reaction of family GH18 chitinase

Paknisa Sirimontree[a], Wipa Suginta[a], Natchanok Sritho[a], Yuka Kanda[b], Shoko Shinya[b], Takayuki Ohnuma[b] & Tamo Fukamizo[b]

[a] Biochemistry-Electrochemistry Research Unit, Schools of Chemistry and Biochemistry, Suranaree University of Technology, Nakhon Ratchasima, Thailand

[b] Department of Advanced Biosciences, Kinki University, Nara, Japan
Published online: 15 Aug 2014.

PLEASE SCROLL DOWN FOR ARTICLE

JSBA

Mutation strategies for obtaining chitooligosaccharides with longer chains by transglycosylation reaction of family GH18 chitinase

Paknisa Sirimontree[1], Wipa Suginta[1,*], Natchanok Sritho[1], Yuka Kanda[2], Shoko Shinya[2], Takayuki Ohnuma[2] and Tamo Fukamizo[2,*]

[1]*Biochemistry-Electrochemistry Research Unit, Schools of Chemistry and Biochemistry, Suranaree University of Technology, Nakhon Ratchasima, Thailand;* [2]*Department of Advanced Biosciences, Kinki University, Nara, Japan*

Enhancing the transglycosylation (TG) activity of glycoside hydrolases does not always result in the production of oligosaccharides with longer chains, because the TG products are often decomposed into shorter oligosaccharides. Here, we investigated the mutation strategies for obtaining chitooligosaccharides with longer chains by means of TG reaction catalyzed by family GH18 chitinase A from *Vibrio harveyi* (*Vh*ChiA). HPLC analysis of the TG products from incubation of chitooligosaccharide substrates, $GlcNAc_n$, with several mutant *Vh*ChiAs suggested that mutant W570G (mutation of Trp570 to Gly) and mutant D392N (mutation of Asp392 to Asn) significantly enhanced TG activity, but the TG products were immediately hydrolyzed into shorter $GlcNAc_n$. On the other hand, the TG products obtained from mutants D313A and D313N (mutations of Asp313 to Ala and Asn, respectively) were not further hydrolyzed, leading to the accumulation of oligosaccharides with longer chains. The data obtained from the mutant *Vh*ChiAs suggested that mutations of Asp313, the middle aspartic acid residue of the DxDxE catalytic motif, to Ala and Asn are most effective for obtaining chitooligosaccharides with longer chains.

Key words: chitooligosaccharides; *Vibrio harveyi*; family GH18 chitinase; site-directed mutagenesis; transglycosylation

Chitinases (EC 3.2.1.14) are enzymes that hydrolyze chitin, an insoluble polysaccharide consisting of β-(1,4)-linked *N*-acetylglucosamine (GlcNAc) units and a major component of the shells of crustaceans, the exoskeletons of insects, and the cell walls of fungi.[1–3] Chitinases are classified into glycoside hydrolase family 18 (GH18) and family 19 (GH19), depending on the amino acid sequence identity of their catalytic domains and the mode of enzyme action.[4–9] In nature,

degradation of insoluble chitin polymer by chitinases generates water-soluble chitooligosaccharide fragments.[10] Chitooligosaccharides, $GlcNAc_n$ (*n*, degree of polymerization or chain length), have various biological functions; for example, they can stimulate the plant immune system to respond to microbial infections[11–13] and can be used as antimicrobial agents.[14] However, the biological activities of chitooligosaccharides are most efficient, when the chain lengths are more than five or six.[14,15] Usually, chemical synthesis of chitooligosaccharides with such longer chains is cumbersome and costly due to the selective protection and subsequent manipulation of various monosaccharide donors and acceptors.[16,17] Therefore, enzymatic synthesis employing the transglycosylation (TG) activity of chitinases may serve as a better biological tool for a large-scale production of such biologically active compounds.

TG reaction catalyzed by GH18 chitinases usually takes place through two steps.[18–20] In the first step, the glycosidic oxygen is protonated by a catalytic acid to cleave the β-1,4-glycosidic linkage and to form the oxazolinium ion intermediate, in which the C1 carbon of the −1 sugar is stabilized by anchimeric assistance of the sugar *N*-acetamido group. In the second step, the oxazolinium ion intermediate is attacked by a water molecule from the β-side, leading to hydrolysis with net retention of anomeric form. When a water molecule is outcompeted by another acceptor, such as carbohydrates, TG reaction takes place, resulting in the formation of a glycosidic linkage and yielding longer chain chitooligosaccharides instead. Chitinases from various sources have been reported to potentially catalyze TG reaction. For examples, a chitinase from *Nocardia orientalis* was reported to convert $GlcNAc_4$ substrate to $GlcNAc_6$ under high ammonium sulfate concentration.[21] Recently, *Serratia proteamaculans* chitinase D (*Sp*ChiD) showed high TG activity with $GlcNAc_{3–6}$ substrates generating $GlcNAc_{7–13}$ products, which were hydrolyzed into smaller $GlcNAc_n$ after 90 min of the

---

2   *P. Sirimontree et al.*

reaction.[22] Mutations of some amino acids located close to the catalytic cleft were found to enhance TG activity in various GH18 chitinases, such as *Serratia marcescens* chitinase A and chitinase B.[19,20] Similar enhancement of TG activity was reported for the mutants of *Bacillus circulans* WL-12 chitinase A1, those of *Trichoderma harzanium* chitinase 42,[23] and those of *S. proteamaculans* chitinase D (*Sp*ChiD).[24] Such mutants displayed higher TG activity, whereas their hydrolytic activity was dramatically diminished. From those studies on the TG reaction catalyzed by family GH18 chitinases, it is obvious that enhancing the TG activity of chitinases does not always result in the production of chitooligosaccharides with longer chains, because the TG products are often decomposed into shorter oligosaccharides. In this study, we investigated the mutation strategies for obtaining chitooligosaccharides with longer chains by means of enzymatic TG reaction using family GH18 chitinase A from *Vibrio harveyi* (*Vh*ChiA). Mutations were introduced into Asp313, Asp392, and Trp570, each of which is responsible for sugar residue binding at subsites −2, −1, +1, and +2, as seen from the crystal structure of *Vh*ChiA shown in Fig. 1. We found that mutations of Asp313, the middle aspartic acid residue of the catalytic motif DxDxE, to Ala and Asn are most effective for obtaining chitooligosaccharides with longer chains.

Materials and methods

Materials. Chitooligosaccharides, GlcNAc$_{2-6}$, were produced by acid hydrolysis of chitin,[25] and purified by gel-filtration column of Gel-25 m (JNC Co., Tokyo). Colloidal chitin was prepared from crab chitin by the method of Hsu and Lockwood.[26] Ni-NTA agarose resin was purchased from Bio-Rad Laboratories (Hercules, USA), and HiPrep 16/60 Sephacryl S-100 resin was from GE Healthcare. Other reagents were of analytical grade and commercially available.
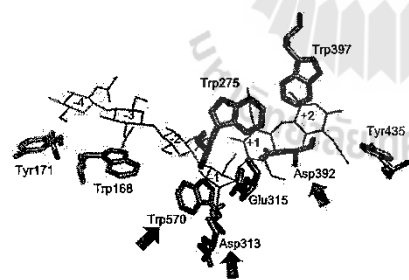
Fig. 1. Superimposition of the active site structure of ligand-free wild-type *Vh*ChiA and *Vh*ChiA E315M mutant complexed with GlcNAc$_6$ (only GlcNAc$_6$ shown as green; PDB code, 3B9A).

Notes: GlcNAc-binding subsites are indicated by integers based on the nomenclature suggested by Davies et al.[39]. The amino acid residues presented as the stick model are important for chitooligosaccharide binding. The structure of ligand-free wild-type *Vh*ChiA was obtained from the PDB database (PDB code, 3B8S)[30] and displayed by the program PyMol (www.pymol.org/). The arrows indicate the mutation targets.

Mutation targets. To enhance the TG activity, two strategies were proposed: (1) enhancing the acceptor-binding ability[27] and (2) suppressing the attack of a nucleophilic water molecule to the transition state.[20,28] Since the acceptor-binding site (+1 and +2) of wild-type enzymes are evolutionarily optimized for efficiently accepting their natural substrates, the mutations introduced into the acceptor-binding site usually reduce the acceptor-binding ability. Thus, mutations for enhancing the binding ability are quite difficult. In the former studies,[19,29] mutations were introduced into the glycon-binding site (−2 and −1) to suppress the sugar-binding ability of the negatively numbered subsites. The suppression of the sugar-binding to the negatively numbered subsites relatively enhances the binding ability toward the positively numbered subsites (acceptor-binding site). In fact, mutation of Trp167 (subsite −3) of *S. marcescens* chitinase A enhanced the TG activity.[19] Here, we tried to mutate Trp570, which is responsible for the sugar-residue binding at subsites −1 and −2 (Fig. 1),[30,31] to glycine. Asp392, which is supposed to be responsible for the acceptor-binding at subsites+1 and+2,[30] was also mutated to asparagine, which may facilitate hydrogen bonding interaction with the sugar residue. In addition to these mutations, we mutated the middle aspartic acid residue (Asp313) in the DxDxE catalytic motif, because this mutation was reported to significantly enhance the TG activity of *S. marcescens* chitinases.[20,23]

Production and purification of the wild type and mutates Vh*ChiA.* Four *Vh*ChiA mutants W570G, D392N, D313A, and D313N were generated by PCR-based site-directed mutagenesis as described previously.[31,32] The recombinant wild-type *Vh*ChiA and its mutants were highly expressed in *E. coli* M15 cells as described by Pantoom et al.[33] For purification, the IPTG-induced cells were collected by centrifugation, re-suspended in 40 mL of 20 mM Tris-HCl buffer, pH 8.0, containing 150 mM NaCl, and then lysed on ice using an Ultrasonic disruptor with a 1.5 cm-diameter probe. The supernatant obtained after centrifugation at 12,000 rpm for 40 min was applied to a Ni-NTA agarose affinity column (Bio-Rad Laboratories, Hercules, CA, USA), washed thoroughly with 5 and 20 mM imidazole, and then eluted with 250 mM imidazole prepared in 20 mM Tris-HCl, pH 8.0, and 150 mM NaCl. The eluted fractions were further purified by gel filtration chromatography on a HiPrep 16/60 Sephacryl S-100 HR column connected to an FPLC purifier system (GE Healthcare). After SDS-PAGE analysis, the chitinase-containing fractions were pooled, then dialyzed with 20 mM phosphate buffer at pH 7.0, and concentrated using the Vivaspin-20 ultrafiltration membrane concentrator (M_r 10,000 cutoff, Vivascience AG, Hannover, Germany). A final protein concentration was determined by UV absorbance at 280 nm, using the extinction coefficient obtained from the equation proposed by Pace et al.[34]

Time-course study of TG reaction by quantitative HPLC. A reaction mixture (100 μL) contained chitooligosaccharide substrate (6.8 mM GlcNAc$_4$, 5.5 mM

GlcNAc$_5$, or 4.6 mM GlcNAc$_6$), VhChiA (5 μM of wild-type, W570G, or D392N, 16 μM of D313A, or 8 μM of D313N), and 20 mM phosphate buffer, pH 7.0. The reaction mixture was incubated at 40 °C, and then an aliquot of (10 μL) was transferred to a new microcentrifuge tube containing 10 μL of 0.1 M NaOH to terminate the enzymatic reaction at various times of incubation. To determine the enzymatic products, the resultant solution was immediately applied onto a gel filtration column of TSK-GEL G2000PW (7.5 mm × 600 mm) connected with a Hitachi L-7000 HPLC system (Hitachi Koki Co., Ltd, Tokyo, Japan). Elution was conducted with a Milli-Q water at a constant flow rate of 0.3 mL min^{-1}. The oligosaccharide products in the effluent were monitored by UV absorption at 220 nm. Peak area of each GlcNAc$_n$ obtained from the elution profile was then converted into molar concentration using the standard calibration curve of the GlcNAc$_n$ mixture with known concentrations.

Results and discussion

Time courses of chitooligosaccharide degradation catalyzed by wild-type VhChiA

We first evaluated TG activity of the wild-type VhChiA (WT). Incubation of WT with the GlcNAc$_4$ substrate produced GlcNAc$_2$ as the major hydrolytic product after 3 h of reaction (Fig. 2(A)). A small but

detectable amount of GlcNAc$_3$ was also produced after 3 h, but no GlcNAc was detected at all. From the GlcNAc$_5$ substrate, GlcNAc$_2$ and GlcNAc$_3$ were formed as the major hydrolytic products, and a trivial amount of GlcNAc$_4$ was also formed at 2 h (Fig. 2(B)). The GlcNAc$_4$ formation from GlcNAc$_5$ was not accompanied by GlcNAc formation. The GlcNAc$_3$ product from GlcNAc$_4$ and the GlcNAc$_4$ product from GlcNAc$_5$ were not derived from a simple hydrolysis of the initial substrates. Aronson et al.[19] reported a similar hydrolytic profile obtained by S. marcescens chitinase A. Plant class V chitinase from cycad also exhibited a similar reaction profile.[35] Both reports explained that GlcNAc$_3$ is produced from initial substrate GlcNAc$_4$ through the TG product GlcNAc$_6$, as shown in Fig. 3. GlcNAc$_4$ was first hydrolyzed into GlcNAc$_2$ + GlcNAc$_2$ (Step I). After the latter GlcNAc$_2$ is released from the enzyme, the acceptor GlcNAc$_4$ binds to the acceptor-binding site (the positively numbered subsites) (Step IIb), and then attacks the oxazolinium ion intermediate at subsite −1, producing GlcNAc$_6$ as the TG product (Step III). The GlcNAc$_6$ produced is relocated to the more stable binding mode (−3, −2, −1, +1, +2) (Step IV), and hydrolyzed into GlcNAc$_3$ + GlcNAc$_3$ (Step V). In the case of the initial substrate GlcNAc$_5$, WT produced a small amount of GlcNAc$_4$ at 2 h in addition to GlcNAc$_2$ and GlcNAc$_3$ (Fig. 2(B)). Since GlcNAc$_5$ is assumed to act as an
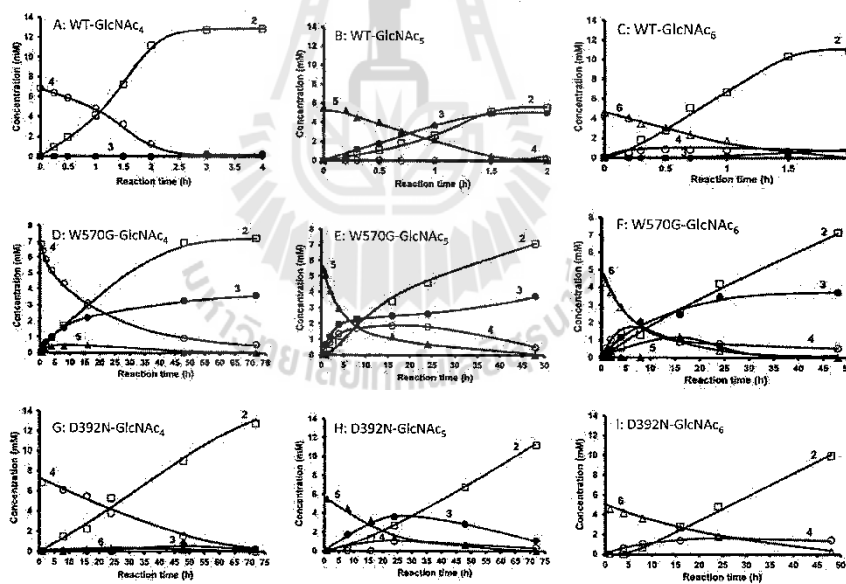
Fig. 2. Reaction time courses of the wild-type and mutated VhChiA toward chitooligosaccharide substrates GlcNAc$_{4-6}$.

Notes: The wild-type VhChiA (5 μM) was incubated with 6.8 mM GlcNAc$_4$ (A), 5.5 mM GlcNAc$_5$ (B), or 4.6 mM GlcNAc$_6$ (C), W570G VhChiA (5 μM) was incubated with 6.8 mM GlcNAc$_4$ (D), 5.5 mM GlcNAc$_5$ (E), or 4.6 mM GlcNAc$_6$ (F). D392N VhChiA (5 μM) was incubated with 6.8 mM GlcNAc$_4$ (G), 5.5 mM GlcNAc$_5$ (H), or 4.6 mM GlcNAc$_6$ (I). Individual reactions were conducted in 20 mM phosphate buffer, pH 7.0 at 40 °C. The products were analyzed by gel-filtration HPLC at various times of incubation. Numbers represent the degree of polymerization. Symbols are □, GlcNAc$_2$; ●, GlcNAc$_3$; O, GlcNAc$_4$; ▲, GlcNAc$_5$; Δ, GlcNAc$_6$.

4 P. Sirimontree *et al.*
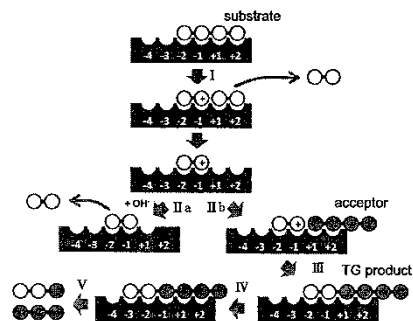
substrate

Fig. 3. The reaction scheme for hydrolysis/TG catalyzed by *Vh*ChiA with GlcNAc$_4$ substrate.

Notes: Step I: Bond cleavage; GlcNAc$_4$ binds to the −2 to +2 subsites and the glycosidic linkage located between the −1 and +1 subsites is cleaved by the action of Glu315 to form GlcNAc$_2$ with an oxazolinium ion intermediate at subsites −2 and −1 and the intact GlcNAc$_2$ product at subsites +1 and +2, which will diffuse away. Step IIa: Hydration; a water molecule attacks the C1 carbon of the oxazolinium ion intermediate to release the product of GlcNAc$_2$. Steps IIb and III: Acceptor binding and formation of glycosidic linkage; an incoming GlcNAc$_4$ attacks the intermediate instead of a water molecule to form a new glycosidic linkage, producing the TG product of GlcNAc$_6$. Step IV: Shifting the binding mode of GlcNAc$_6$ to subsites −3 to +2. Step V: the newly formed GlcNAc$_6$ is then hydrolyzed to form two molecules of GlcNAc$_3$. GlcNAc residues are represented by open circles, an incoming GlcNAc$_4$ molecule is represented by grey circles, the oxazolinium ion intermediate is represented by positive signs in open circles and the binding subsites of the enzyme given as integers based on the nomenclature suggested by Davies et al.[39] Formation of the TG products by the mutants *Vh*ChiA D313A and D313N is represented from Step I to Step III, while the additional steps (Step IV and Step V) should be introduced for the reactions catalyzed by the mutants W570G and D392N.

acceptor molecule as well as a substrate in the mechanism shown in Fig. 3, GlcNAc$_4$ is most likely produced through the TG product GlcNAc$_7$. Thus, we concluded that the WT enzyme has a very low TG activity. From the initial substrate GlcNAc$_6$, WT produced GlcNAc$_2$, GlcNAc$_3$, and GlcNAc$_4$ (Fig. 2(C)). No evidence for TG reaction was obtained from the reaction toward GlcNAc$_6$. The result suggested that WT not only catalyzes the hydrolysis of the chitooligosaccharide substrates, but also catalyzes TG reaction much less efficiently with the substrates GlcNAc$_4$ and GlcNAc$_5$.

Time courses of chitooligosaccharide degradation catalyzed by W570G

The hydrolytic activities of mutant W570G toward the substrates GlcNAc$_{4-6}$ were much less than those of WT (Fig. 2(D), (E), and (F)), and the results were consistent with the specific activity data reported previously.[31] However, a considerable amount of GlcNAc$_3$ was produced in addition to GlcNAc$_2$ from the initial substrate GlcNAc$_4$ (Fig. 2(D)). The GlcNAc$_3$ produced was clearly derived from the mechanism shown in Fig. 3, because no GlcNAc was found in the products. GlcNAc$_5$, which may be derived from the TG reaction

between the donor GlcNAc$_2$ and the acceptor GlcNAc$_3$, was also detected in the early stage of the reaction. The productions of GlcNAc$_3$ and GlcNAc$_5$ indicate that TG activity was significantly enhanced in W570G. The time-course profiles of mutant W570G with GlcNAc$_5$ substrate (Fig. 2(E)) showed that GlcNAc$_2$ and GlcNAc$_3$ were the major hydrolytic products. GlcNAc$_4$ was also produced without the formation of GlcNAc, and the maximum level of GlcNAc$_4$ was approximately 2 mM at 16 h of incubation. GlcNAc$_4$ was then gradually degraded to GlcNAc$_2$, and only 0.5 mM remained at 48 h. The GlcNAc$_4$ product may be derived from the mechanism shown in Fig. 3, where the substrate and the acceptor molecules should be replaced with GlcNAc$_5$. Mutant W570G hydrolyzed GlcNAc$_6$ substrate to GlcNAc$_2$, along with GlcNAc$_3$ and GlcNAc$_4$ (Fig. 2(F)). GlcNAc$_5$ was also detected, but GlcNAc was not. Thus, the GlcNAc$_5$ product may be produced through the TG product GlcNAc$_8$ as shown in Fig. 3, where the substrate and the acceptor molecules should be replaced with GlcNAc$_6$. The results obtained from this set of experiments suggested that the mutation of Trp570 located in between subsites −2 and −1 strongly enhanced TG activity, but the TG products obtained from the mutant W570G were only temporarily formed, and then further degraded. Trp570 is responsible for the GlcNAc residue binding at subsites −2 and −1 (Fig. 1), so that cleavage of the glycosidic bond between subsites −1 and +1 takes place most efficiently. Substitution of the Trp570 side chain with glycine completely removed the aromatic surface area, thereby causing a dramatic decrease in the hydrolytic activity to about 5% of the WT activity, and decreased the binding affinity (increased K_m) that affected sugar–enzyme interaction.[31] The reduction of the binding affinity at these two subsites, on the other hand, may relatively enhance the affinity at the acceptor-binding site (positively numbered subsites), resulting in the enhanced TG activity. However, all of the TG products immediately hydrolyzed again into oligosaccharides with shorter chains.

Time courses of chitooligosaccharide degradation catalyzed by D392N

The D392N mutant produced GlcNAc$_2$ as a major product from GlcNAc$_4$ substrate, while a small amount of GlcNAc$_3$ was produced as shown in Fig. 2(G), probably through the mechanism shown in Fig. 3. The GlcNAc$_3$ production was slightly enhanced in the D392N mutant, when compared with that in WT (Fig. 2(A)). The D392N mutant hydrolyzed GlcNAc$_5$ substrate, yielding GlcNAc$_2$ and GlcNAc$_3$ as the major end products (Fig. 2(H)). The enhanced formation of GlcNAc$_4$ was found in the reaction catalyzed by D392N. Since the GlcNAc$_4$ formation was not accompanied by GlcNAc formation, the tetramer was most likely derived from the mechanism shown in Fig. 3, where the substrate and the acceptor molecules should be replaced with GlcNAc$_5$. With GlcNAc$_6$ substrate, GlcNAc$_2$ and GlcNAc$_4$ were the major hydrolytic products (Fig. 2(I)), while no other products were detected. These results suggested that mutation of Asp392, which is involved in sugar residue binding at subsites +1 and

133

+2 (Fig. 1), to asparagine enhanced the TG activity of VhChiA with the substrates GlcNAc$_4$ and GlcNAc$_5$, but not with the substrate GlcNAc$_6$. Our previous kinetic data showed that D392N has greater affinity towards pNP-GlcNAc$_2$ and chitooligosaccharide substrates than those of WT.[31] The greater affinity of D392N may facilitate the acceptor binding to subsites +1 and +2; hence, the TG reaction for the substrates GlcNAc$_4$ and GlcNAc$_5$ (Fig. 2(G) and (H)). However, also in this mutant, the TG products were immediately hydrolyzed into oligosaccharides with shorter chains. Mutations of Trp570 and Asp392 are unlikely effective for obtaining chitooligosaccharides with longer chains, even though the mutant enzymes exhibit the enhanced TG activity.

Mutation of Asp313 is the most effective for obtaining chitooligosaccharides with longer chains

Asp313 is an essential residue located at the middle of the catalytic DxDxE motif (Asp311-x-Asp313-x-Glu315), and plays multiple roles in the catalytic cycle of chitin degradation by VhChiA[32]. Mutation of Asp313 to alanine (D313A) abolished the hydrolytic activity of the enzyme almost completely, while mutation of Asp313 to asparagine (D313N) retained slight hydrolytic activity. HPLC profiles of the products from incubation of the mutant D313A or D313N with Glc-NAc$_4$ substrate indicated that a significant amount of GlcNAc$_6$ as the TG product was generated in addition to the major hydrolytic product GlcNAc$_2$ after 120 h of incubation, as shown in Fig. 4(B) and (C). In contrast,

no GlcNAc$_6$ was found in the chromatogram for WT (Fig. 4(A)). In the reactions catalyzed by D313A and D313N, the TG product GlcNAc$_6$ was not hydrolyzed into GlcNAc$_3$. Similarly, when GlcNAc$_6$ was incubated with the Asp313 mutants, a significant amount of GlcNAc$_8$, which was produced by the TG reaction between the donor GlcNAc$_2$ and the acceptor GlcNAc$_6$, was detected by HPLC (Fig. 5(B) and (C)). WT did not produce GlcNAc$_8$ at all (Fig. 5(A)). The chain length of the TG product, GlcNAc$_8$, was confirmed based on the theoretical retention time obtained by the simulation of the gel-filtration profile.[29] The donor for the TG reaction appears to be GlcNAc$_2$, because VhChiA hydrolyzes most frequently the second β-1,4-glycosidic linkage from the nonreducing end of chitooligosaccharide substrates.[36] Thus, from the substrate GlcNAc$_5$, the Asp313 mutants may produce GlcNAc$_7$ by the TG reaction between the donor GlcNAc$_2$ and the acceptor GlcNAc$_5$.

VhChiA is a bacterial GH18 chitinase that cleaves a chitin chain into various chitooligosaccharide fragments.[37] Based on our previous studies,[30,36] VhChiA has structure and function similar to those of S. marcescens chitinase A, and it degrades GlcNAc$_4$ substrate mostly to GlcNAc$_2$, GlcNAc$_5$ substrate to GlcNAc, GlcNAc$_2$, and GlcNAc$_3$, while GlcNAc$_6$ is degraded to GlcNAc$_2$, GlcNAc$_3$, and GlcNAc$_4$. GH18 chitinases have a catalytic motif specified by a sequence DxDxE, which correspond to Asp311-x-Asp313-x-Glu315 in VhChiA. Glu315 is a catalytic acid, which donates a proton to the β-1,4-glycosidic oxygen to cleave the linkage. Asp313 is located at the bottom of the
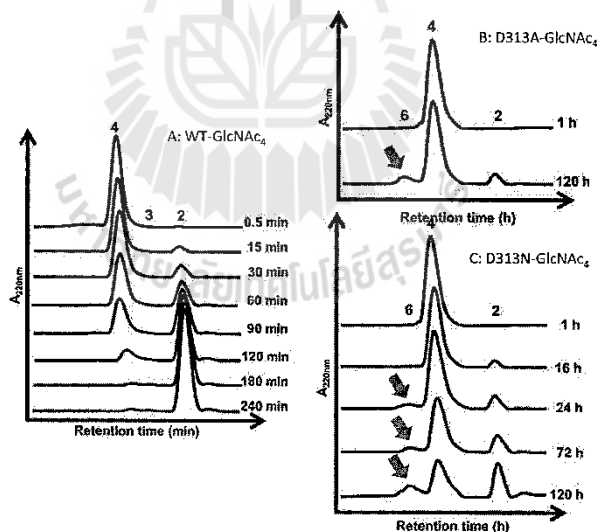
Fig. 4. HPLC profiles showing the reaction of the wild type (A) and the mutants D313A (B) and D313N (C) VhChiA.

Notes: A reaction mixture containing 6.8 mM GlcNAc$_4$ and the enzyme (5 μM wild type, 16 μM D313A, or 8 μM D313N) in 20 mM phosphate buffer, pH 7.0, was incubated at various times at 40 °C. The reaction products were analyzed by gel-filtration HPLC. The TG product GlcNAc$_6$ is designated by arrow.

6   P. Sirimontree *et al.*
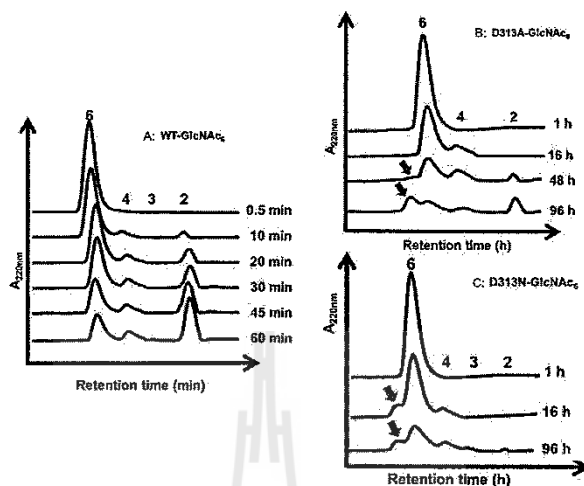
Fig. 5. HPLC profiles showing the reaction of the wild type (A) and the mutants D313A (B) and D313N (C) *Vh*ChiA.

Notes: A reaction mixture containing 4.6 mM GlcNAc$_6$ and the enzyme (5 μM wild type, 16 μM D313A, or 8 μM D313N) in 20 mM phosphate buffer, pH 7.0, was incubated at various times at 40 °C. The reaction products were analyzed by gel-filtration HPLC. The TG product GlcNAc$_8$ is indicated by arrow.

substrate binding cleft (Fig. 1). This aspartic acid plays multiple roles in the catalytic cycle of chitin hydrolysis.[32,38] It interacts with the 2-acetamido group of the sugar residue at subsite −1 (the cleavage site) and helps to lower the pKa value of the catalytic residue Glu315, so that bond cleavage can be achieved more easily. Moreover, it helps to orient the 2-acetamido group in the correct position to stabilize the oxazolinium ion intermediate in the substrate-assisted mechanism. Mutations of Asp313 to Ala and Asn abolished the hydrolytic activity almost completely by disrupting hydrogen-bond interactions with the sugar residue. Instead, the mutations enhanced the TG activity. We tried to compare the efficiencies of TG reaction obtained by our D313A/N mutants with those obtained by the corresponding mutants of the two *Serratia* enzymes, *Sm*ChiA and *Sm*ChiB.[20] In the *Serratia* enzymes, the mutations of the middle Asp of the DxDxE motif to Asn were reported to enhance the TG reaction more strongly than the mutations to Ala. In our *Vh*ChiA mutants, however, no significant difference was found in the highest yields of the TG products (GlcNAc$_6$ from the initial substrate GlcNAc$_4$, Fig. 4; or GlcNAc$_8$ from the initial substrate GlcNAc$_6$, Fig. 5) between D313A and D313N. The TG efficiencies in the mutants from *Serratia* enzymes were evaluated from the GlcNAc$_3$ production from the initial substrate GlcNAc$_4$, indicating that the TG product GlcNAc$_6$ was decomposed into GlcNAc$_3$ as shown in Fig. 3.[20] The evaluation of TG efficiency based on the yield of GlcNAc$_n$ with longer chains (TG products) may be more informative for practical use of the transglycosylating chitinases. Thus, the mutants of the middle Asp of the DxDxE motif from *Vh*ChiA are likely more effective

for obtaining GlcNAc$_n$ with longer chains than the corresponding mutants from the *Serratia* enzymes, *Sm*ChiA and *Sm*ChiB.[20]

In the Asp313 mutants from *Vh*ChiA, the K_m values toward GlcNAc$_6$ were four- (D313N) or six-fold (D313A) higher than that of the wild type.[32] The lower affinity may result in the spontaneous release of the TG product from the enzyme without relocation to the productive binding mode (process IV in Fig. 3). This situation may bring about the accumulation of the TG products in the Asp313 mutants. In the other mutants W570G and D392N, however, the TG products may be immediately relocated to the productive binding mode spanning the catalytic center, due to the affinity with Asp313, and subsequently broken down by the hydrolytic action of the enzyme. Zakariassen et al.[20] who reported a hypertransglycosylating mutants obtained from the *Serratia* enzymes, explained that the mutation of Asp313 changes the electrostatics around the catalytic center, decreasing the probability of nucleophilic attack of a water molecule to the oxazolinium ion intermediate. Similar situation may possibly take place in the *Vh*ChiA mutants, D313A and D313N. Aronson et al. reported that the mutation of Trp167 of *Sm*ChiA to alanine (W167A) significantly enhances the TG reaction.[19] In W167A, the side chain of Asp313 is oriented only toward Glu315, whereas in the wild type, the Asp313 side chain is equally distributed between two orientations, toward Asp311 or toward Glu315. They explained that the orientation of Asp313 toward Glu315 may interfere with the attack of a water molecule to the oxazolinium ion intermediate. Thus, the state of the side chain of Asp313 appears to be related to the efficiency of TG reaction. Crystal structure

135

analysis of *Vh*ChiA D313N or D313A will afford valuable information on the structural factor for enhancing the TG reaction in *Vh*ChiA.

In conclusion, mutations of Trp570 and Asp392 of *Vh*ChiA significantly enhanced the TG reaction, but the TG products were immediately hydrolyzed into chitooligosaccharides with shorter chains. In contrast, mutations of Asp313 strongly enhanced the TG reaction, and the products, chitooligosaccharides with longer chains, were not hydrolyzed but accumulated in the reaction mixture. The results obtained from this study may suggest a convenient, strategic design for new chitinase molecules with suitable property for producing the biologically active chitooligosaccharides required for pharmaceutical and industrial uses.

Acknowledgments

Funding

References

[1] Arbia W, Arbia L, Adour L, Amrane A. Chitin recovery from crustacean shells by biological methods—A review. Food Technol. Biotechnol. 2013;51:12–25.

[2] Merzendorfer H, Zimoch L. Chitin metabolism in insects: Structure, function and regulation of chitin synthases and chitinases. J. Exp. Biol. 2003;206:4393–4412.

[3] Free SJ. Fungal cell wall organization and biosynthesis. Adv. Genet. 2013;81:33–82.

[4] Funkhouser JD, Aronson NN. Chitinase family GH18: Evolutionary insights from the genomic history of a diverse protein family. BMC Evol. Biol. 2007;7:96.

[5] Kawase T, Saito A, Sato T, Kanai R, Fujii T, Nikaidou N, Miyashita K, Watanabe T. Distribution and phylogenetic analysis of family 19 chitinases in actinobacteria. Appl. Environ. Microbiol. 2004;70:1135–1144.

[6] van Aalten D, Komander D, Synstad B, Gaseidnes S, Peter M, Eijsink V. Structural insights into the catalytic mechanism of a family 18 exo-chitinase. Proc. Nat. Acad. Sci. 2001;98:8979–8984.

[7] Terwisscha van Scheltinga AC, Hennig M, Dijkstra BW. The 1.8 Å resolution structure of hevamine, a plant chitinase/lysozyme, and analysis of the conserved sequence and structure motifs of glycosyl hydrolase family 18. J. Mol. Biol. 1996;262:243–257.

[8] Brameld KA, Goddard WA III. The role of enzyme distortion in the single displacement mechanism of family 19 chitinases. Proc. Nat. Acad. Sci. 1998;95:4276–4281.

[9] Hoell IA, Dalhus B, Heggset EB, Aspmo SI, Eijsink VGH. Crystal structure and enzymatic properties of a bacterial family 19 chitinase reveal differences from plant enzymes. FEBS J. 2006;273:4889–4900.

[10] Rinaudo M. Chitin and chitosan: Properties and applications. Prog. Polym. Sci. 2006;31:603–632.

[11] Kaku H, Nishizawa Y, Ishii-Minami N, Akimoto-Tomiyama C, Dohmae N, Takio K, Minami E, Shibuya N. Plant cells recognize chitin fragments for defense signaling through a plasma membrane receptor. Proc. Nat. Acad. Sci. 2006;103:11086–11091.

[12] Miya A, Albert P, Shinya T, Desaki Y, Ichimura K, Shirasu K, Narusaka Y, Kawakami N, Kaku H, Shibuya N. CERK1, a LysM receptor kinase, is essential for chitin elicitor signaling in *Arabidopsis*. Proc. Nat. Acad. Sci. 2007;104:19613–19618.

[13] Yamaguchi K, Yamada K, Ishikawa K, Yoshimura S, Hayashi N, Uchihashi K, Ishihama N, Kishi-Kaboshi M, Takahashi A, Tsuge S, Ochiai H, Tada Y, Shimamoto K, Yoshioka H, Kawasaki T. A receptor-like cytoplasmic kinase targeted by a plant pathogen effector is directly phosphorylated by the chitin receptor and mediates rice immunity. Cell Host Microbe. 2013;13:347–357.

[14] VishuKumar AB, Varadaraj MC, Gowda LR, Tharanathan RN. Characterization of chito-oligosaccharides prepared by chitosanolysis with the aid of papain and Pronase, and their bactericidal action against *Bacillus cereus* and *Escherichia coli*. Biochem. J. 2005;391:167–175.

[15] Petutschnig EK, Jones AM, Serazetdinova L, Lipka U, Lipka V. The lysin motif receptor-like kinase (LysM-RLK) CERK1 is a major chitin-binding protein in *Arabidopsis thaliana* and subject to chitin-induced phosphorylation. J. Biol. Chem. 2010;285:28902–28911.

[16] Kanie O, Ito Y, Ogawa T. Orthogonal glycosylation strategy in oligosaccharide synthesis. J. Am. Chem. Soc. 1994;116:12073–12074.

[17] Aly MRE, Ibrahim E-SI, Ashry ESHE, Schmidt RR. Synthesis of chitotetraose and chitohexaose based on dimethylmaleoyl protection. Carbohydr. Res. 2001;331:129–142.

[18] Fukamizo T, Sasaki C, Schelp E, Bortone K, Robertus JD. Kinetic properties of chitinase-1 from the fungal pathogen *Coccidioides immitis*. Biochemistry. 2001;40:2448–2454.

[19] Aronson NN, Halloran BA, Alexeyev MF, Zhou XE, Wang Y, Meehan EJ, Chen L. Mutation of a conserved tryptophan in the chitin-binding cleft of *Serratia marcescens* chitinase a enhances transglycosylation. Biosci., Biotechnol. Biochem. 2006;70:243–251.

[20] Zakariassen H, Hansen MC, Jøranli M, Eijsink VG, Sørlie M. Mutational effects on transglycosylating activity of family 18 chitinases and construction of a hypertransglycosylating mutant. Biochemistry. 2011;50:5693–5703.

[21] Nanjo F, Sakai K, Ishikawa M, Isobe K, Usui T. Properties and transglycosylation reaction of a chitinase from *Nocardia orientalis*. Agric. Biol. Chem. 1989;53:2189–2195.

[22] Purushotham P, Podile AR. Synthesis of long-chain chitooligosaccharides by a hypertransglycosylating processive endochitinase of *Serratia proteamaculans* 568. J. Bacteriol. 2012;194:4260–4271.

[23] Martinez EA, Boer H, Koivula A, Samain E, Driguez H, Armand S, Cottaz S. Engineering chitinases for the synthesis of chitin oligosaccharides: Catalytic amino acid mutations convert the GH-18 family glycoside hydrolases into transglycosylases. J. Mol. Catal. B: Enzym. 2012;74:89–96.

[24] Madhuprakash J, Tanneeru K, Purushotham P, Guruprasad L, Podile AR. Transglycosylation by chitinase D from *Serratia proteamaculans* improved through altered substrate interactions. J. Biol. Chem. 2012;287:44619–44627.

[25] Rupley JA. The hydrolysis of chitin by concentrated hydrochloric acid, and the preparation of low-molecular-weight substrate for lysozyme. Biochim. Biophys. Acta. 1964;83:245–255.

[26] Hsu SC, Lockwood JL. Powdered chitin agar as a selective medium for enumeration of actinomycetes from water and soil. Appl. Microbiol. 1975;29:422–426.

[27] Umemoto N, Ohnuma T, Mizuhara M, Sato H, Skriver K, Fukamizo T. Introduction of a tryptophan side chain into subsite +1 enhances transglycosylation activity of a GH-18 chitinase from Arabidopsis thaliana, AtChiC. Glycobiology. 2013;23:81–90.

[28] Hurtado-Guerrero R, Schuttelkopf AW, Mouyna I, Ibrahim AF, Shepherd S, Fontaine T, Latge JP, van Aalten DM. Molecular mechanisms of yeast cell wall glucan remodeling. J. Biol. Chem. 2009;284:8461–8469.

[29] Fukamizo T, Goto S, Torikata T, Araki T. Enhancement of transglycosylation activity of lysozyme by chemical modification. Agric. Biol. Chem. 1989;53:2641–2651.

8   P. Sirimontree *et al.*

[30] Songsiririthigul C, Pantoom S, Aguda AH, Robinson RC, Suginta W. Crystal structures of *Vibrio harveyi* chitinase a complexed with chitooligosaccharides: Implications for the catalytic mechanism. J. Struct. Biol. 2008;162:491–499.

[31] Suginta W, Songsiririthigul C, Kobdaj A, Opassiri R, Svasti J. Mutations of Trp275 and Trp397 altered the binding selectivity of *Vibrio carchariae* chitinase A. Biochim. Biophys. Acta. 2007;1770:1151–1160.

[32] Suginta W, Sritho N. Multiple roles of Asp313 in the refined catalytic cycle of chitin degradation by *Vibrio harveyi* chitinase A. Biosci., Biotechnol. Biochem. 2012;76:2275–2281.

[33] Pantoom S, Songsiririthigul C, Suginta W. The effects of the surface-exposed residues on the binding and hydrolytic activities of *Vibrio carchariae* chitinase A. BMC Biochem. 2008;9:2.

[34] Pace CN, Vajdos F, Fee L, Grimsley G, Gray T. How to measure and predict the molar absorption coefficient of a protein. Protein Sci. 1995;4:2411–2423.

[35] Taira T, Fujiwara M, Dennhart N, Hayashi H, Onaga S, Ohnuma T, Letzel T, Sakuda S, Fukamizo T. Transglycosylation reaction catalyzed by a class V chitinase from cycad, *Cycas revoluta*: A study involving site-directed mutagenesis, HPLC, and real-time ESI-MS. Biochim. Biophys. Acta. 2010;1804:668–675.

[36] Suginta W, Pantoom S, Prinz H. Substrate binding modes and anomer selectivity of chitinase A from *Vibrio harveyi*. J. Chem. Biol. 2009;2:191–202.

[37] Suginta W, Vongsuwan A, Songsiririthigul C, Prinz H, Estibeiro P, Duncan RR, Svasti J, Fothergill-Gilmore LA. An endochitinase A from *Vibrio carchariae*: Cloning, expression, mass and sequence analyses, and chitin hydrolysis. Arch. Biochem. Biophys. 2004;424:171–180.

[38] Synstad B, Gaseidnes S, van Aalten DM, Vriend G, Nielsen JE, Eijsink VG. Mutational and computational analysis of the role of conserved residues in the active site of a family 18 chitinase. Eur. J. Biochem. 2004;271:253–262.

[39] Davies GJ, Wilson KS, Henrissat B. Nomenclature for sugar-binding subsites in glycosyl hydrolases. Biochem. J. 1997;321:557–559.
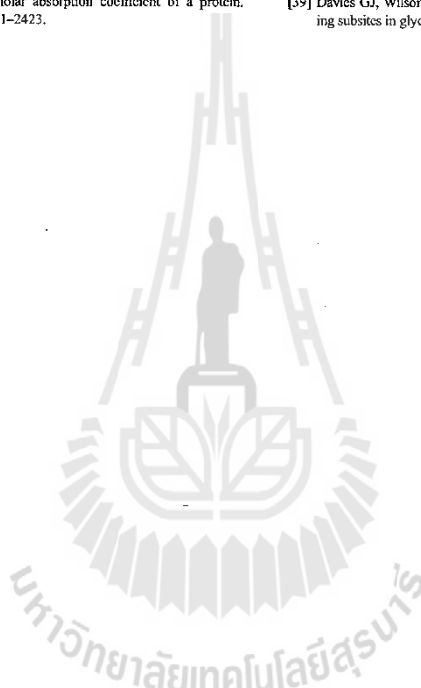
CURRICULUM VITAE

NAME   Miss Paknisa Sirimontree

DATE OF BIRTH   6 February 1983

PLACE OF BIRTH   Buriram, Thailand

INSTITUTION ATTENDED

Khon Kaen University, Khon Kaen, Thailand,

2001-2005, Bachelor of Science (Microbiology)

Suranaree University of Technology, Nakhon

Ratchasima, Thailand, 2008-2014, Doctor of

Philosophy (Biochemistry)

AWARDS AND SCHOLARSHIPS

Second class honors, Khon Kaen University,

Khon Kaen, Thailand, 2005

The Royal Golden Jubilee Ph.D. Program

scholarship, from the Thailand Research Fund

2008-2014

Certificates for poster award, 10th Asia Pacific

Chitin & Chitosan Symposium (Joint with 27th

Japanese Chitin and Chitosan Symposium),

Yonago, Japan, 2013